Development of an Alternative Method and Design for Setting Wood Utility Poles on Rock

By

Heather Bilesky

A Thesis submitted to the Faculty of Graduate Studies of

The University of Manitoba

in partial fulfillment of the requirement for the degree of

MASTER OF SCIENCE

Department of Civil Engineering

University of Manitoba

Winnipeg, Manitoba

ABSTRACT

Manitoba Hydro's current practice for setting wood poles onto exposed rock has been generating safety concerns for nearly two decades. Manitoba Hydro's current Distribution Standard for the installation of rock-set wood poles entails fusing rebar into holes drilled in the rock with molten sulphur. Unfortunately, accidental overheating of the sulphur causes it to lose its strength properties, and has lead to the premature failure of a number of these rock sets. Even if the grout is heated precisely and sets adequately, full-scale testing by Manitoba Hydro in 1980 revealed that these grouted anchor rods performed poorly in bending at the ground line while the wood poles remained in good condition, indicating that the full bending capacity of the wood poles is not developed. A more effective design would promote the wood pole to fail first, such that the anchors could be re-used.

A research program was conducted at the University of Manitoba's McQuade Structural Laboratory in an attempt to remedy the aforementioned shortcomings associated with Manitoba Hydro's current practice for setting wood utility poles on rock. The research focused on developing an alternative method and design for setting wood poles on rock – namely, a prefabricated steel base mount detail that itself is anchored to the rock – and experimentation with different annulus backfill materials to use in conjunction with the mount. Nine tests were conducted using the 6.1 m (20-foot) long bottom halves of 12.2 m (40-foot) long Lodgepole Pine specimens. All specimens were tested as cantilevers under static loading. One test was conducted with mechanical fasteners, while eight tests were conducted with backfill materials (four with crushed limestone and four with sand). The experimental results showed that the base mount detail, with either compacted crushed limestone or sand as the annulus material, successfully developed the full moment capacity of the wood pole and satisfied limits on deflection for everyday conductor tensions.

ACKNOWLEDGEMENT

I would like to acknowledge the contributions of the following individuals without whom this project would not have been a success:

- My advisors, Dr. Nipon Rattanawangcharoen and Dr. Ehab El-Salakawy, for their support and guidance throughout the duration of this research project;
- Mr. Jon Kell (Manitoba Hydro) for his valuable mentorship, motivation, support, and technical guidance;
- The staff at the McQuade Structures Laboratory, Mr. Chad Klowak and Mr. Brendan Pachal, for their technical assistance during testing;
- Mr. Tyler Epp, undergraduate research assistant, for his assistance with the design of the test set-up and during testing;
- Manitoba Hydro for their financial contribution to the project (Research Project T308);
- The Examining Committee, consisting of Dr. Dimos Polyzois and Dr. Qiang Zhang from the University of Manitoba, for their review of both this document and the oral defense; and
- My husband Alex for his loving support and encouragement.

TABLE OF CONTENTS

LIST OF TABLES

LIST OF FIGURES

CHAPTER 1 – INTRODUCTION

1.1 GENERAL

Manitoba Hydro's current practice for setting wood poles onto exposed rock has been generating safety concerns for nearly two decades. In 1994, Manitoba Hydro's Corporate Safety & Health Division published a safety circular entitled "Power Pole Rock Sets" that outlined the risks associated with climbing and working on sulphur-grouted rock-set poles. In particular, several incidents in Manitoba and Saskatchewan were identified where linemen were either injured or killed due to falling from poles where rock sets failed prematurely (Manitoba Hydro, 1994).

Manitoba Hydro's current Distribution Standard for the installation of rock-set wood poles entails fusing rebar into holes drilled in the rock with molten sulphur (Manitoba Hydro, 2011). The protruding end of the rebar, which is welded to a flat steel bar prior to installation, is fixed to the base of the wood pole with through-bolts. Figures 1.1 and 1.2 illustrate this procedure.

Figure 1.1: Manitoba Hydro's current practice for setting wood poles on exposed rock

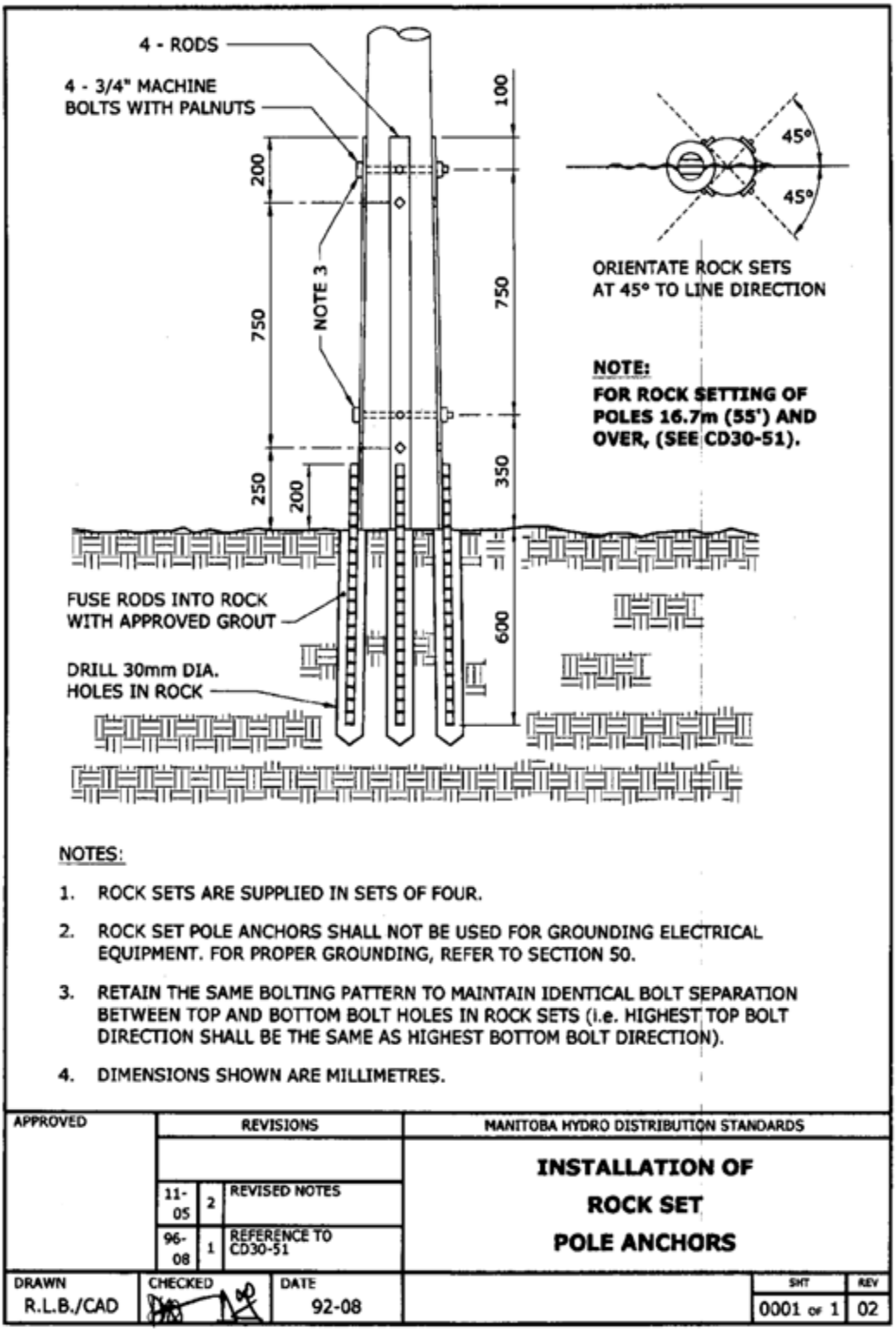

Figure 1.2: Manitoba Hydro's Distribution Standard for setting wood poles on rock (Manitoba Hydro, 2011)

The circumstances leading to the premature failure of these rock sets has been attributed to improper sulphuring. When using sulphur as a grout, temperature and heat application are critical factors that influence its integrity. Specifically, the sulphur must be constantly stirred and gently heated to precisely 112°C (235°F). It is in this state that, when poured, the sulphur will harden to its optimum strength. Even the slightest overheating will cause the sulphur to lose its strength properties. Unfortunately, sulphur cools to a yellow solid whether heated properly or overheated, so it is impossible for the installer to visually determine if the sulphur has melted properly (Manitoba Hydro, 1994). Sulphur that has been overheated during the melting process will degrade quickly over time. This is evidenced in Figure 1.3 below, where the sulphur grout that once secured the anchor rod in the hole has disintegrated.

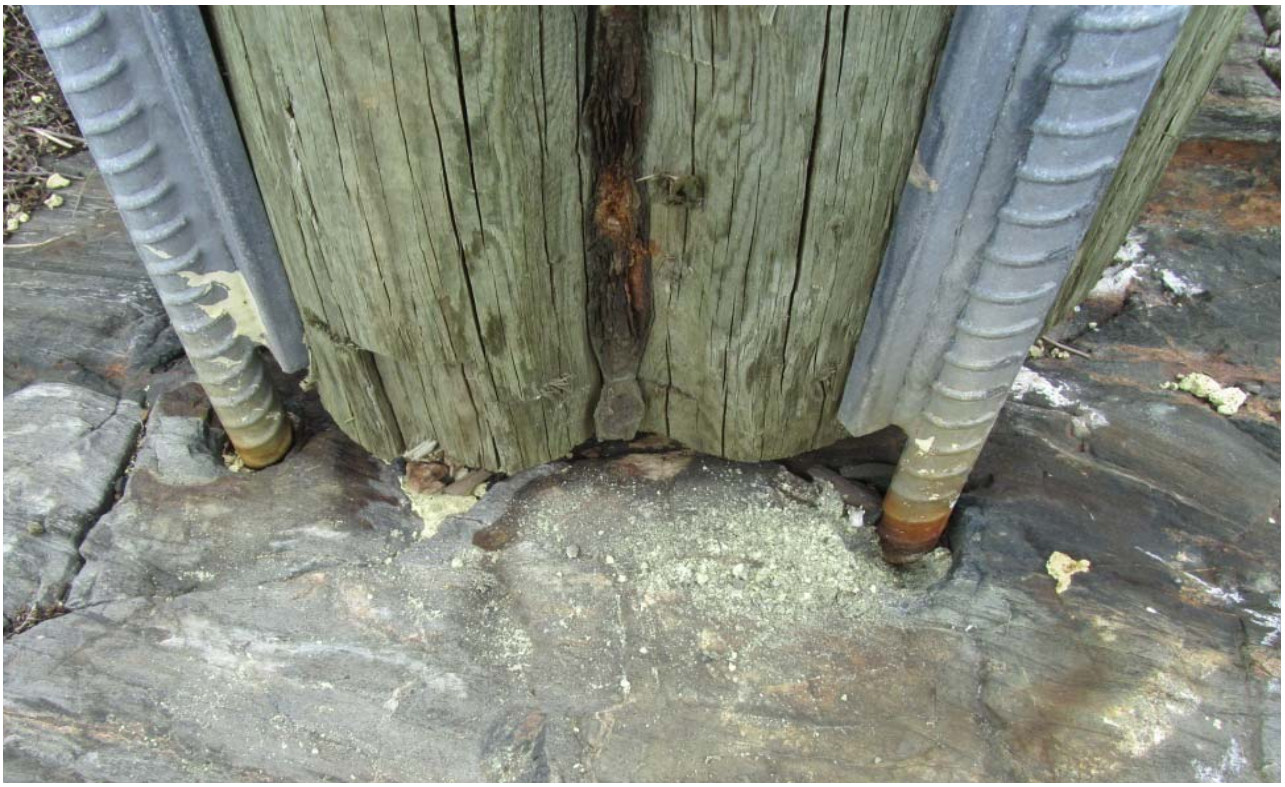

Figure 1.3: Rock set pole anchor with complete sulphur disintegration

In addition to the difficulty associated with achieving sulphur's optimum strength, the use of molten sulphur is extremely dangerous. Toxic gases are created during the melting process if the sulphur is overheated. Furthermore, molten sulphur poured into wet or damp holes can splash back at the installer and cause serious harm.

Even if the grout is heated precisely and sets adequately, full-scale testing by Manitoba Hydro in 1980 revealed that these grouted anchor rods perform poorly in bending at the ground line (Storie, 1980). This bending of the anchor rods is illustrated in Figure 1.4 below. After the test, the wood poles were observed to be in good condition. This would indicate that the full bending capacity of the wood poles was not developed. A more effective design would promote the wood pole to fail first, such that the anchors could be re-used.

Figure 1.4: Bending of grouted anchor rods during full-scale load test (Storie, 1980)

Manitoba Hydro currently uses sulphur-grouted anchors for both transmission and distribution wood pole lines. Based on the aforementioned testing and premature failures observed in the field, the installation procedure for Manitoba Hydro's transmission poles was modified to include guy wires. Although this improved the safety of linemen climbing these poles, the added risk of public users of the right-of-way coming into contact with these guy wires (while travelling on snowmobile or ATV, for example) was introduced. The installation procedure for Manitoba Hydro's distribution poles did not change (i.e. guy wires were not added).

Feedback from Manitoba Hydro's construction personnel has also identified a number of shortcomings related to the installation of these grouted anchors. Variations in pole dimensions makes it difficult to pre-drill holes in the rock that match up with the circumference of the wood pole. Installers can fashion drilling templates for each pole by tracing the protruding rebar pattern onto cardboard (see Figure 1.5 below), but the process is cumbersome and often inaccurate. Installers have also reported that it often takes several attempts to line up the through-bolts that connect and secure the flat bars on opposing faces of the pole.

Figure 1.5: Creating a drilling template for a rock set wood pole installation (Storie, 1980)

1.2 METHODOLOGY AND RESEARCH OBJECTIVES

Manitoba Hydro's current practice for setting wood utility poles on rock has numerous shortcomings: premature failure of the sulphur grout, inadequate bending capacity of the grouted anchor rods, as well as installation difficulties. The research conducted in this project focused on developing an alternative method and design for setting wood poles on rock. Specifically, a prefabricated pole base mount that is easy to install on exposed rock and is capable of developing the full moment capacity of Manitoba Hydro's typical 12.2 m (40-foot) long distribution poles was designed and tested. As shown in Figure 1.6 below, the proposed mount utilized a 12-sided steel sleeve welded to a steel base plate.

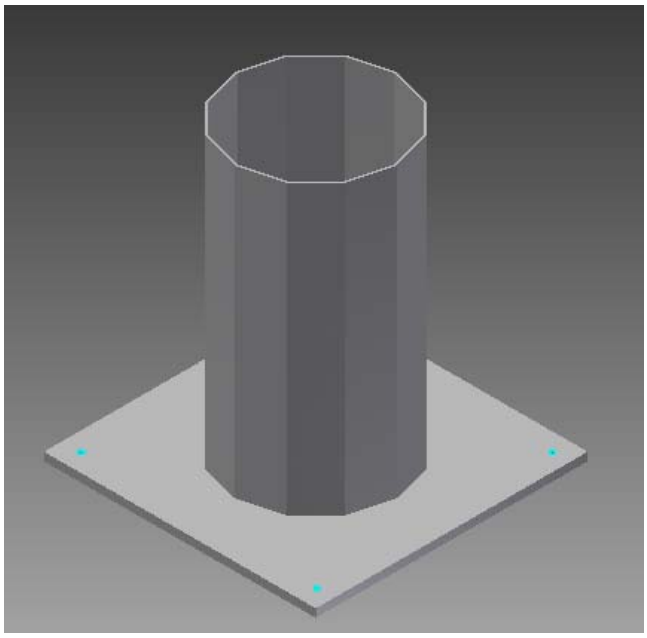

Figure 1.6: Proposed prefabricated pole base mount

Two variations of the aforementioned mount design were fabricated – one with a sleeve height of 1,219 mm (4 feet) and another with a sleeve height of 914 mm (3 feet). The 1,219 mm sleeve height was based on the National Electrical Safety Code's (NESC) embedment depth recommendation for 12.2 m

(40-foot) long utility poles installed in rock. The 914 mm sleeve height was based on analyses performed in MFAD, a software package that more accurately predicts required embedment depths of foundations for single pole structures based on in-situ soil conditions, backfill annulus properties, and wood pole properties (FAD Tools, 2014).

Both variations of the mount were designed to accommodate not only a compacted granular annulus material, but also mechanical fasteners at the top and bottom of the sleeve that would minimize pole movement where there is a gap between the pole and the sleeve. Full-scale testing was performed at the University of Manitoba's McQuade Structural Laboratory. In total, nine tests were conducted using the 6.1 m (20-foot) long bottom halves of 12.2 m (40-foot) long Class 4 Lodgepole Pine specimens. Each specimen was subjected to the transverse loads prescribed by CAN/CSA-015/05, Wood Utility Poles and Reinforcing Stubs (CSA, 2005).

Based on the above, the main objective of this project was to develop an alternative method and design for setting wood utility poles on rock that is easy to install and capable of developing the full moment capacity of Manitoba Hydro's typical 12.2 m (40-foot) long wood distribution poles. This was achieved by:

1. Performing a literature review of relevant wood pole design specifications, the typical failure mode of wood utility poles subject to bending moment, traditional methods for setting wood poles, and wood utility pole deflection criteria and serviceability requirements. Research on embedment depth design that challenges the "rule of thumb" recommendations for embedment depth that have been adopted by most utilities was also investigated;

2. Performing analyses in MFAD, a software package that provides for the design of foundations for single pole structures based on in-situ soil conditions, backfill annulus properties, and wood pole properties, to predict the optimum mount sleeve height;

3. Performing full-scale testing on pole specimens supported by the proposed mount design, as recommended by ASTM Standard D1036 (Cantilever Test Method), that tested the variables of sleeve height and annulus material (ASTM, 2012); and

4. Analyzing the experimental results obtained from laboratory testing, as well as comparing to the results predicted by MFAD, to recommend a sleeve height and an annulus material for use in the field.

1.3 SCOPE

This project only considers the rock-setting of wood poles on distribution-type lines (up to 69 kV) utilizing 12.2 m (40-foot) long, Class 4 Lodgepole Pine poles (i.e. no guy wires are used to support the pole). Furthermore, the alternative method and design for setting wood poles on rock developed in this project assumes that forces at the base of the mount are transmitted below-grade by means of the bond developed between steel anchors (i.e. Dywidag bars), a well-defined methacrylate grout body, and the surrounding rock. The detailed design of the mount's anchorage to rock is outside the scope of this project.

1.4 THESIS OUTLINE

This thesis consists of six chapters. Chapter 1 identifies the shortcomings associated with Manitoba Hydro's current method for setting wood poles on rock, and hence the reasons why this study was initiated. The methodology, research objectives, and scope of the project are also presented.

Chapter 2 contains a literature review of relevant wood pole design specifications, the typical failure mode of wood utility poles subject to bending, traditional methods for setting wood poles, as well as other commercially available techniques for setting wood poles in or on rock. Research related to wood pole embedment depths and serviceability requirements is also reviewed, as well as literature on recommended backfill material types and compaction.

Chapter 3 presents the design and fabrication details of the base mounts, including a discussion of the different variables that will be tested. The test method adopted is also outlined, as well as the preparation required before testing can commence.

The results of the experimental program are presented in Chapter 4. Specifically, the structural performance of the base mount designs and annulus material types tested are evaluated.

In Chapter 5, the analytical model used to predict the optimum mount sleeve height is detailed. A comparison of the analytical results to the full-scale results obtained in this study is also presented.

Finally, a summary of the research findings is presented in Chapter 6, along with conclusions and recommendations for future work.

CHAPTER 2 – LITERATURE REVIEW

2.1 POLE DESIGN SPECIFICATIONS AND STANDARDS

It is common practice to design power line components such that failure of these components is in a precise sequential order. Specifically, the structures themselves should fail prior to their foundations and hardware. As a result, the limiting factor for localized failure in a wood pole power line is the strength of the wood pole itself. Deflection limits for wood utility poles do not typically govern over strength limits (Lu, 2012). The following national standards and design specifications are available to aid in the design of wood pole structures for the purpose of supporting power lines.

2.1.1 CANADIAN STANDARDS ASSOCIATION (CSA)

The most recent edition of the Canadian Standards Association's published Standard CAN/CSA-015/05, "Wood Utility Poles and Reinforcing Stubs", summarizes material, manufacturing, and class dimensional requirements for seasoned wood poles and reinforcing stubs that are primarily intended for the support of electrical power or communication lines (CSA, 2005). The class dimensional requirements of particular importance for each species are length and minimum circumferential measurements.

The minimum circumferences specified in CAN/CSA-015/05 have been determined for various pole lengths of each species in a given strength class such that the ground-line stresses developed when a given horizontal load is applied 610 mm (2 feet) from the top of the pole are approximately equal to the average bending strength of the species. The horizontal loads used in the calculations for separating the 13 classes of poles are given in Table 2.1. The minimum circumferences specified in CAN/CSA-015/05

have been determined assuming that the pole acts as a simple cantilever and that the maximum fibre stress in the pole subjected to the bending moment applied will occur at the ground line. This assumption is valid provided that the circumference at the ground line is less than 1.5 times the circumference at the point of loading (CSA, 2005). The minimum required circumferences at 1,829 mm (6 feet) from the pole butt are also specified in CAN/CSA-015/05 and have been determined for each species in a given strength class using a calculated taper per foot of length between the ground line and a point 1,829 mm (6 feet) from the pole butt. Since all lengths of pole in a given strength class are rated for the same horizontal load, this implies that a longer pole must have a larger circumference at 1,829 mm (6 feet) from the pole butt as compared to a shorter pole of the same species.

Table 2.1: Unfactored transverse load capacity of wood poles by Class (CSA, 2005)

Class of Pole	Horizontal Load (N)
H6	50,700
H5	44,500
H4	38,700
H3	33,400
H2	28,500
H1	24,000
1	20,000
2	16,500
3	13,300
4	10,700
5	8,500
6	6,700
7	5,300
8	4,300

In this study, the 6.1 m (20-foot) long bottom halves of 12.2 m (40-foot) long, Class 4 Lodgepole Pine (species code "LP") poles, the most commonly stocked pole for distribution in Manitoba, were used for full-scale testing. The bending strengths and corresponding minimum and maximum circumferences of LP poles, as specified by CAN/CSA 015-05, are given in Table 2.2. The Canadian standard CAN/CSA

015-05 requires that the maximum circumference at 1,829 mm (6 feet) from the pole butt shall be no more than 178 mm (7 inches) or 20% larger than the specified minimum, whichever is greater.

Table 2.2: Required fibre stress value & circumference for 12.2 m long, Class 4 LP poles (CSA, 2005)

Pole Species (Species Code)	**Fibre Stress, MPa**	**Min. Required Circumference (1,829 mm from pole butt), mm**	**Max. Required Circumference (1,829 mm from pole butt), mm**
Lodgepole Pine (LP)	45.5	901.7	1,082.0

The CAN/CSA 015-05 standard also specifies minimum top circumferences for wood poles. Unlike at 1,829 mm (6 feet) from the pole butt, however, these minimum circumferences do not change with pole length for individual pole classes within a given species. For example, all lengths of LP poles in a given strength class have the same minimum required circumference at the top of the pole (CSA, 2005).

2.1.2 AMERICAN NATIONAL STANDARDS INSTITUTE (ANSI)

The American National Standards Institute has a published standard for wood poles, ANSI 05.1.2008: Wood Poles – Specifications & Dimensions, which is largely similar to the CSA standard. Poles of a given class and length are designed to have approximately the same load-carrying capacity, regardless of species (ANSI, 2008). In other words, a pole made from a wood species with low fibre strength requires larger dimensions to be considered the same class of pole as one made from a wood species with high fibre strength. The fibre stresses and corresponding minimum required circumferences of LP poles, as specified by ANSI 05.1.2008, are identical to those prescribed by CAN/CSA 015-05 in Table 2.2 above.

2.1.3 INSTITUTE OF ELECTRICAL AND ELECTRONICS ENGINEERS (IEEE)

In 1991, the Institute of Electrical and Electronics Engineers (IEEE) published a guide titled "Trial-Use Design Guide for Wood Transmission Structures" that provides guidelines for the design of wood utility pole structures that support overhead power lines. The design strengths recommended within the guide are taken from ANSI Standard 05.1. The main objective of the IEEE design guide is to provide a structure with resistance greater than the maximum load expected during its design lifetime, with levels of safety and reliability that are within acceptable economic parameters (Kell, 2001). Equation 2.1 below summarizes this objective.

$$\phi R \geq \gamma Q \qquad \text{Equation 2.1}$$

Where

R = resistance

ϕ = strength factor (typically ≤ 1, which limits resistance to account for variability of the property)

Q = load or load effect

γ = load factor (typically ≥ 1, which compensates for uncertainty in the definition of loads)

For wood pole structures, the "resistance" of particular importance is the bending moment resistance. In the design of wood utility pole structures, it must be assured that the applied loads do not exceed the designated fibre stress. Equation 2.2 summarizes this objective.

$$\phi f_b \geq \gamma(M/S) \qquad \text{Equation 2.2}$$

Where

f_b = wood bending strength

M = applied bending moment

S = section modulus of pole at critical bending section

Although shear failure is rarely observed in wood utility poles that are undamaged, the IEEE design guide recommends that it also be considered as a possible failure mode as per Equation 2.3 below.

$$\phi f_v \geq \gamma V(Q/I) \qquad \text{Equation 2.3}$$

Where

f_v = wood shear strength

V = applied shear force

Q = first moment of area above or below the neutral axis

I = moment of inertia of the critical section

Q/I = $1.7D^{-2}$ for an undamaged cross-section

D = diameter of the critical section

2.1.4 AMERICAN SOCIETY FOR TESTING AND MATERIALS (ASTM)

The design and economical use of poles for the support of overhead power lines relies on an accurate determination of the maximum fiber stress for the different species of timber used for poles. Furthermore, the values of maximum fiber stress obtained from testing need to be comparable across the

industry. It is for this reason that the American Society for Testing and Materials (ASTM) has developed and published ASTM Standard D1036, "Standard Test Methods of Static Tests of Wood Poles". The test methods contained in this standard cover testing procedures in sufficient detail so that the results of tests made in accordance with the test methods defined will be comparable (ASTM, 2012). The standard does, however, permit the use of other test methods that may be better suited to a particular investigation.

The cantilever test method outlined in ASTM Standard D1036 requires the pole to be supported from the butt to the ground line in a horizontal position with load applied at a point 610 mm (2 feet) from the pole tip at a constant rate of speed. Equation 2.4 below is proposed by ASTM Standard D1036 to determine the maximum fibre stress at the ground line (modulus of rupture).

$$MOR = \frac{32\pi^3 P_{ult}(L - \Delta_L)}{C^3} \qquad \text{Equation 2.4}$$

Where

MOR = Modulus of Rupture, the maximum fibre stress at ground line

P_{ult} = load at failure

L = distance from ground line to point of load

Δ_L = longitudinal deflection of the load point at the maximum load, and

C = circumference at ground line

2.2 FAILURE MODE OF WOOD UTILITY POLES SUBJECT TO BENDING

According to the Canadian Standards Association's published Standard CAN/CSA 22.3 No. 1-10, "Overhead Systems", the bending strength of wood is governed by the tensile strength of its wood fibres. This definition of failure assumes that bending effects are dominant and neglects the effects of shear (CSA 2010).

As a cantilevered pole bends, tensile stresses develop on the convex side of the pole while compressive stresses develop on the concave side of the pole. The compressive strength of wood parallel to the grain is significantly less than its corresponding tensile strength (Mortensen, 2007). As a result, initial material yielding occurs on the compression side of the pole once the compressive stress exceeds the pole's compressive strength. As the compressive failure zone increases, the neutral axis shifts toward and redistributes the increasing load to the tension side of the pole. Tensile stresses continue to increase until the load exceeds the pole's tensile strength.

2.3 TRADITIONAL WOOD POLE INSTALLATION

Due to its simplicity, direct embedment is the preferred method for wood utility pole installation in most ground conditions. The direct embedment technique involves excavating a hole in the ground, directly inserting the wood pole into the hole, and then backfilling the space between the pole and the edges of the excavated hole with an annulus material (either the native soil or a selected material), as shown in Figure 2.1 below. The Rural Utilities Service (RUS, 1999) recommends placing the backfill in layers not exceeding 150 mm (6 inches) in depth, with each layer mechanically tamped before the next layer is added. The industry standard followed for wood poles embedded in soil is to embed the pole to a depth equal to 10% of its length plus two additional feet (Gajan & McNames, 2010). Some of the benefits of

direct embedment include low cost (compared to a separate foundation), structural continuity between the pole and its foundation, quick installation, and a clean, neat appearance (Sky Cast Canada, 2013).

Figure 2.1: Directly embedded wood pole backfilled with compacted sand

Unfortunately, direct embedment becomes more challenging when the transmission or distribution line right-of-way traverses rocky terrain. If direct embedment is to be used in these conditions, a truck-mounted drilling system capable of drilling sockets into solid rock is required, as shown in Figure 2.2 below. Although effective, rock-socket drilling is time-consuming and expensive. The most sophisticated heavy-duty rock augers on the market take about 25 minutes to auger a hole measuring 6 feet deep by 16 inches in diameter (Whiteshell, 2008), while less expensive augers presumably take even longer. Rocky terrain also makes it difficult for the heavy equipment required for the job to gain

easy access. The National Electrical Safety Code's (NESC) recommendation for utility pole embedment depths in rock, regardless of the properties of the rock or of the pole (other than length), is given in Table 2.3 below.

Figure 2.2: Utility pole hole drilling in solid rock (America West Drilling Supply, 2012)

Table 2.3: NESC Recommended Pole Setting Depths in Rock (Pansini, 2004)

Length of Pole	**Recommended Setting Depth in Rock**	
feet	feet	mm
20	3	914
25	3.5	1,067
30	3.5	1,067
35	4	1,219
40	4	1,219
45	4.5	1,372
50	4.5	1,372
55	5	1,524
60	5	1,524
65	6	1,829
70	6	1,829
75	6	1,829
80	6.5	1,981

2.4 EMBEDMENT DEPTH DESIGN

As mentioned above, the standard of practice employed by most utilities when specifying embedment depths for wood pole foundations subject to lateral loading is to adopt a rule of thumb that is a function of pole length only. This is in stark contrast to the typically detailed design of the pole itself. As observed by Keshavarzian (2002), "The setting depth of a pole is at least as important as the wood fibre strength. It is the supporting part of a pole structure that transmits the forces from the pole to the earth. It is a structural connection that needs to be properly designed, and whose properties are influenced by soil type (properties), pole diameter, and forces at groundline. It should not be strictly a function of pole length" (p. 148).

By using a generalized approach to determine the required embedment depth of a self-supported pole, one runs the risk of specifying a depth that is either (1) not adequate for the combination of applied loads and in-situ soil properties or (2) over-conservative and therefore uneconomical. For instance, Keshavarzian (2002) found that a 21.3 m (70 foot) long class H-4 pole embedded 2,743 mm (9 feet) in a granular soil (62.8 kPa/m lateral bearing strength) developed less than 50% of its capacity under extreme wind loading before the surrounding soil failed. On the other hand, he found that the capacity of an 25.9 m (85 foot) long class H-1 pole embedded 3.2 m (10.5 feet) in a stiffer soil (94.3 kPa/m lateral bearing strength) was governed by the wood fibre stress. In fact, the latter pole's embedment depth could be reduced by an additional 457 mm (1.5 feet) and its capacity was still governed by the wood fibre stress.

2.5 SERVICEABILITY REQUIREMENTS

In addition to designing wood poles to withstand extreme loads, care must also be taken to ensure that they perform satisfactorily under normal everyday service conditions. This is accomplished by

specifying a deflection limit, or the maximum allowable deflection of pole top under an everyday condition of annual mean temperature without ice and wind (Lu, 2012). Deflection limits not only ensure that the power line remains in normal operation under everyday loads, but also promote aesthetically acceptable deflections from the public's perspective and stability for linemen who climb these poles. As observed by Lu, however, there are currently neither code provisions nor a generally accepted standard for serviceability across all utilities in North America.

A single pole structure subjected to normal everyday load conditions will not experience excessive longitudinal deflection, provided the spans on either side are approximately equal (Lu, 2012). If the pole is subject to a small line angle (say up to 3 degrees, as is common for tangent single pole suspension structures), however, the transverse component of the conductor tension will cause some transverse deflection. Also, Lu (2012) noted that a properly designed wood pole structure should behave fairly linearly under everyday loading conditions. More specifically, he observed that pole deflection is almost linearly proportional to transverse load, which in turn is almost linearly proportional to line angle.

In his research, Lu (2012) analyzed a number of scenarios in an attempt to determine maximum deflections resulting from conductor tensions under everyday loading conditions. An annual mean temperature of 0^{o}C (with no wind or ice) and a maximum line angle of 3 degrees were assumed, in addition to three ruling spans (50 m, 100 m, and 150 m) and a variety of commonly used conductors and pole sizes for 69 kV distribution lines within BC Hydro's system. The resulting conductor tensions that were found are summarized in Table 2.4 below.

Table 2.4: Representative conductor tensions under everyday loading conditions (Lu, 2012)

Conductor Designation	Conductor Tension under Everyday Loading Conditions (N)
ACSR Raven	2,159
ACSR Partridge	4,686
ACSR Hawk	5,083
ACSR Drake	6,139
ASC Orchid	4,524
ASC Arbutus	4,985
ASC Magnolia	5,393
ASC Narcissus	6,050

Based on the conductor tensions given above, Lu (2012) recommends a 2% deflection limit for 69 kV single circuit, single pole structures. He found that the single pole structures currently used by BC Hydro can achieve this limit fairly easily, and that the methodology adopted in the study is applicable to other utilities.

2.6 BACKFILLING REQUIREMENTS

2.6.1 ANNULUS MATERIAL

In selecting a backfill material to fill the space between a directly embedded pole and the edges of the excavated hole, it is desirable that the backfill material possess certain characteristics – the material should be inexpensive and readily available, transportation of the material to the site should be easy, little or no preparation of the material in the field should be necessary before placing the material in the

annulus, placement procedures should be simple, the backfill material should develop strength quickly so that the pole can be left standing without external support immediately after backfill placement, the in-place strength and deformation characteristics of the material should be predictable, and the material should maintain its strength and stiffness properties for the expected life of the foundation (DiGioia et al., 1998). Materials that are able to achieve good compaction, and are well-drained, non-frost susceptible and non-expansive, are also essential (US Departments of the Army and the Air Force, 1983). Backfill materials that meet these criteria include crushed rock (such as limestone or basalt) and sand. It is possible that the in-situ soil may also meet these criteria.

The particular backfill material to use for a given direct embedded pole installation depends on the in-situ soil conditions. The backfill recommendations presented in Table 2.5 below have been adopted by most utilities (Whatley Inc., 2013).

Table 2.5: Recommended backfill material for direct embedded pole installations (Whatley, Inc., 2013)

In-situ soil type	**In-situ soil characteristics**	**Recommended Backfill Material**
Good Soil	Well-drained, non-expansive soils of the silt, compacted sand, or selected clay types. These soils will result in a smooth side wall in a dug hole, and the excavated material will be of an even consistency. A minimum hole diameter that will allow a compaction tool to reach the bottom of the hole is all that will be required in good soil.	Existing fill
Average Soil	Less well-drained soils of the heavy silt, expansive clay and/or moderately organic types, with the possibility of standing water during wet season. Natural bearing capacity will be adequate to support the lateral loads of the pole base. These soils will result in a smooth side wall in a dug hole except during wet periods. The excavated material usually is not acceptable for backfilling.	Clean, washed sand or 19 mm (or smaller) crushed rock
Poor Soil	Highly organic soils, loose rock or gravel, or any other soil type or site condition that precludes the creation of a sound structural base and therefore requires special consideration.	Consult with a soil expert with knowledge of local conditions to determine an appropriate backfill material

2.6.2 BACKFILL COMPACTION

Research has also been conducted to determine the importance of backfill compaction in direct embedded pole installations. In 1998, researchers DiGioia et al. performed full-scale load tests on such installations in which the backfill material was loose in one test and well-compacted in another. In both tests, a crushed stone backfill material was used. Interestingly, both tests developed nearly identical maximum applied ground moments (2,041 kN-m in the loose backfill test, 2,126 kN-m in the well-compacted backfill test). The two tests, however, did not develop similar groundline pole deflections, with the loose backfill test exhibiting nearly 3 times the groundline pole deflection as the well-compacted backfill test. DiGioia et al. (1998) concluded that although minimal compaction of a granular backfill may achieve adequate foundation strength, a well-compacted backfill will minimize pole deflections.

2.7 COMMERCIALLY AVAILABLE METHODS FOR INSTALLING WOOD POLES ON ROCK

2.7.1 TRI-ANCHOR SYSTEM

Several of the largest Canadian utility companies, including Hydro-Quebec and Ontario Hydro, have adopted the Tri-Anchor system for setting wood utility poles on rock (as shown in Figure 2.3). It has been reported that these utilities alone have erected over 50,000 wood poles using the Tri-Anchor system over the past two decades (Tri-Steel Industries Inc., 2012).

The Tri-Anchor system for setting wood utility poles on rock is straightforward and, in principle, similar to the method currently employed by Manitoba Hydro. Both the Tri-Anchor system and Manitoba Hydro's current Distribution Standard rely on anchors secured in holes drilled into the rock, with their protruding ends fastened to the pole. Several features of the Tri-Anchor system, however, set it apart from Manitoba Hydro's method.

Figure 2.3: Typical Tri-Anchor installation on exposed rock (On Target Utility Services, 2012)

The universal design of the Tri-Anchor system can accommodate pole butts from 203 to 508 mm (8 to 20 inches) in diameter, and connects to the pole with lag screws and a collar versus hard-to-install through-bolts. The system comes with a drilling template, taking the guess work out of hole placement, and the anchor rods achieve their holding power by way of expansion shells rather than hazardous molten sulphur (although grouting the holes is optional). As a result, the molten sulphur that currently prevents Manitoba Hydro's method from being installed in wet areas is a non-issue for the Tri-Anchor system.

A detailed installation procedure for the Tri-Anchor system is illustrated in Figures 2.4 to 2.9. First, the drilling template is adjusted to fit the pole butt (Figure 2.4). Once sized, the template is removed from the pole butt and then used to drill holes in the rock (Figure 2.5). The anchor module is then placed into the drilled holes (Figure 2.6), after which the pole is lowered through the loose module (Figure 2.7). Studs are used to join individual pole band sections into tight collars (Figure 2.8). Finally, the anchor bolts are tightened to engage their expansion shells in the rock (Figure 2.9).

Figure 2.4: Adjust the drilling template to fit the pole butt (Tri-Steel Industries Inc., 2012)

Figure 2.5: Use the template to drill holes in the rock (Tri-Steel Industries Inc., 2012)

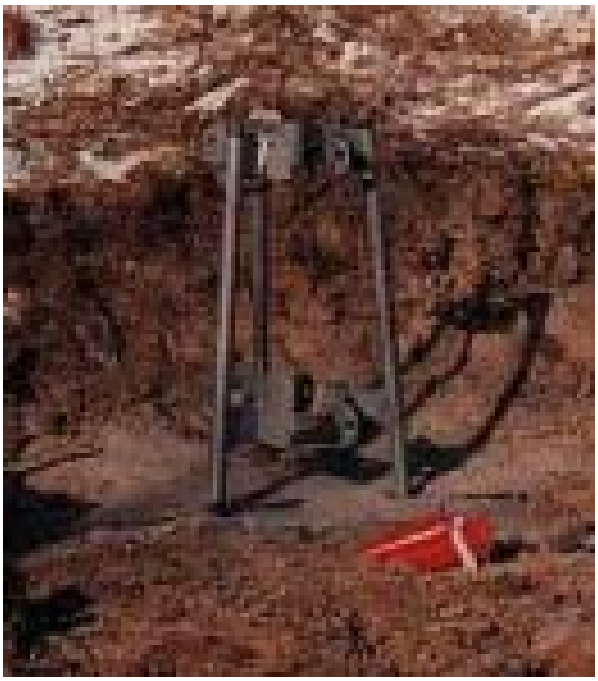

Figure 2.6: Place the anchor module into the drilled holes (Tri-Steel Industries Inc., 2012)

Figure 2.7: Lower the pole through the loose anchor module (Tri-Steel Industries Inc., 2012)

Figure 2.8: Insert studs and tighten to join pole bands into tight collars (Tri-Steel Industries Inc., 2012)

Figure 2.9: Tighten the anchor bolts to engage their expansion shells (Tri-Steel Industries Inc., 2012)

2.7.2 MANITOBA HYDRO'S PAST EXPERIENCE WITH THE TRI-ANCHOR SYSTEM

In the 1980s, Manitoba Hydro considered the Tri-Anchor system for their wood pole installations on rock (Storie, 1980). Full-scale testing of both Manitoba Hydro's conventional grouted anchor system and Tri-Anchor's Product No. 10-28-38 (see Figure 2.10 below) was conducted at a limestone quarry in Garson, Manitoba. 12.2 m (40 foot) long, Class 1 Western Red Cedar poles were used with each anchor system. The purpose of the test was to determine the installation costs, ultimate capacities, and application of each system.

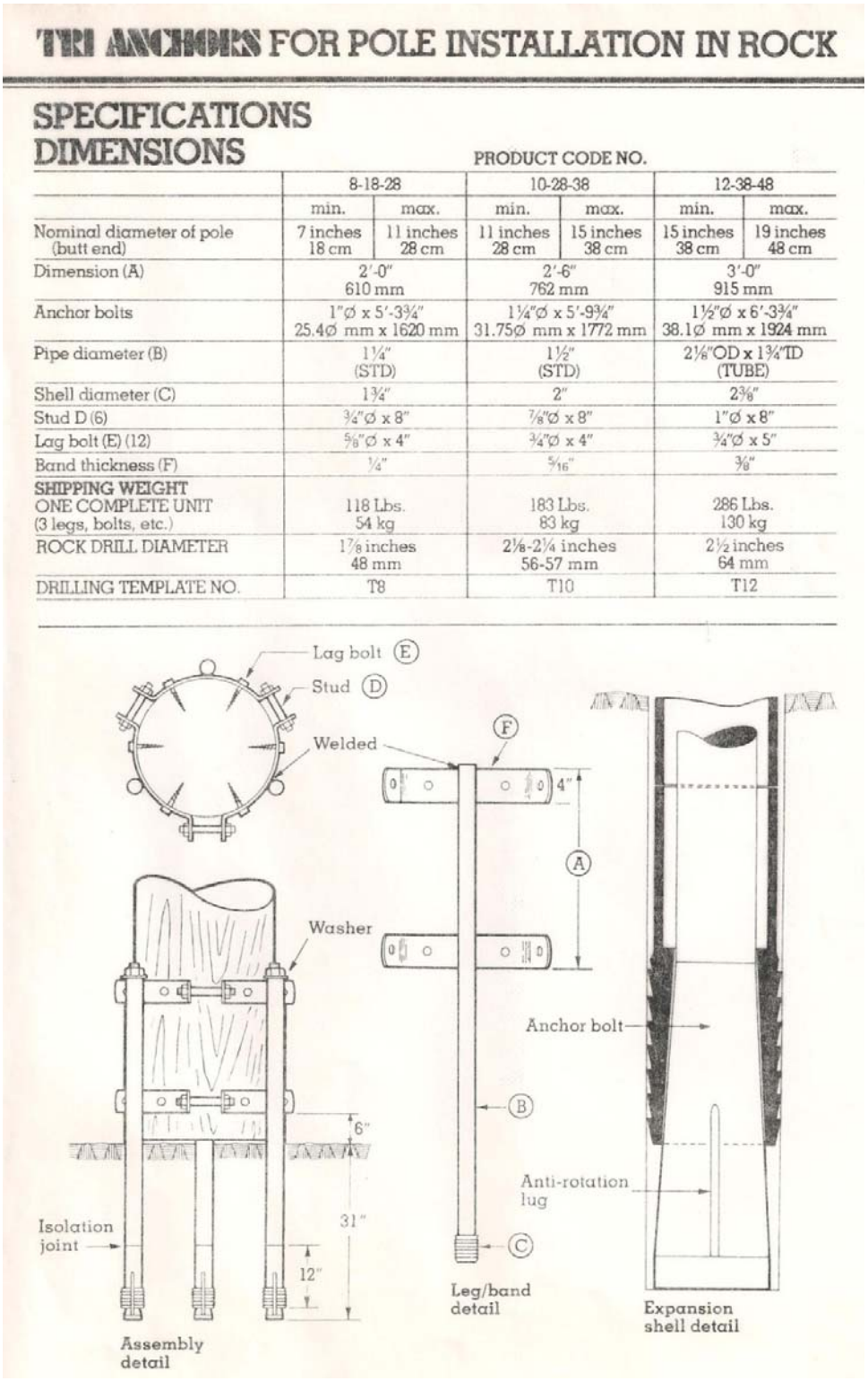

TRI ANCHORS FOR POLE INSTALLATION IN ROCK

SPECIFICATIONS
DIMENSIONS

	PRODUCT CODE NO.					
	8-18-28		10-28-38		12-38-48	
	min.	max.	min.	max.	min.	max.
Nominal diameter of pole (butt end)	7 inches 18 cm	11 inches 28 cm	11 inches 28 cm	15 inches 38 cm	15 inches 38 cm	19 inches 48 cm
Dimension (A)	2'-0" 610 mm		2'-6" 762 mm		3'-0" 915 mm	
Anchor bolts	1"Ø x 5'-3¾" 25.4Ø mm x 1620 mm		1¼"Ø x 5'-9¾" 31.75Ø mm x 1772 mm		1½"Ø x 6'-3¾" 38.1Ø mm x 1924 mm	
Pipe diameter (B)	1¼" (STD)		1½" (STD)		2⅛"OD x 1¾"ID (TUBE)	
Shell diameter (C)	1¾"		2"		2⅜"	
Stud D (6)	¾"Ø x 8"		⅞"Ø x 8"		1"Ø x 8"	
Lag bolt (E) (12)	⅝"Ø x 4"		¾"Ø x 4"		¾"Ø x 5"	
Band thickness (F)	¼"		5/16"		⅜"	
SHIPPING WEIGHT ONE COMPLETE UNIT (3 legs, bolts, etc.)	118 Lbs. 54 kg		183 Lbs. 83 kg		286 Lbs. 130 kg	
ROCK DRILL DIAMETER	1⅞ inches 48 mm		2⅛-2¼ inches 56-57 mm		2½ inches 64 mm	
DRILLING TEMPLATE NO.	T8		T10		T12	

Figure 2.10: Details of Tri-Anchor Product No. 10-28-38 tested by Manitoba Hydro (Tri-Steel Fabricators Ltd., 1980)

Manitoba Hydro's conventional anchor system, of which the installation crew were very familiar with, took 55 minutes to install. This included 8 minutes required to drill four 35 mm (1-3/8 inch) diameter holes in the rock. The Tri-Anchor system, on the other hand, took 50 minutes to install. Since this was the installation crew's first time working with the Tri-Anchor system, it was predicted that the installation time could be reduced further by 10 to 15 minutes with practice. Of the total installation time, 18 minutes were required to drill three 57 mm (2-1/4 inch) diameter holes in the rock.

Based on the above, the installation costs for each system (compared in 1980 dollars) were considered to be equal. The total cost to supply each system, as shown in Table 2.6, varied somewhat.

Table 2.6: Comparison of supply & install costs for the two anchor systems tested (Storie, 1980)

Cost Item	**Tri-Anchor System**	**Manitoba Hydro System**
Crew & Equipment	$95.57	$95.57
Material	$275	$81
TOTAL	$370.57	$176.57

For the test, each anchor system was loaded by applying load to a cable attached 3.0 m (10 feet) from the top of the 12.2 m (40 foot) pole. The load was applied slowly to 4 kN (900 lb.), after which the load was applied in 2.2 kN (500 lb.) increments. After each 2.2 kN (500 lb.) increment, the pole tip deflection was measured with a transit and measuring tape. Both anchor systems were observed to fail in bending at the ground line at approximately the same applied load. Both poles were also observed to be in good condition after the test, which would indicate that neither anchor system developed the full moment-capacity of the pole. The results of the test are presented graphically in Figure 2.11 and pictorially in Figure 2.12.

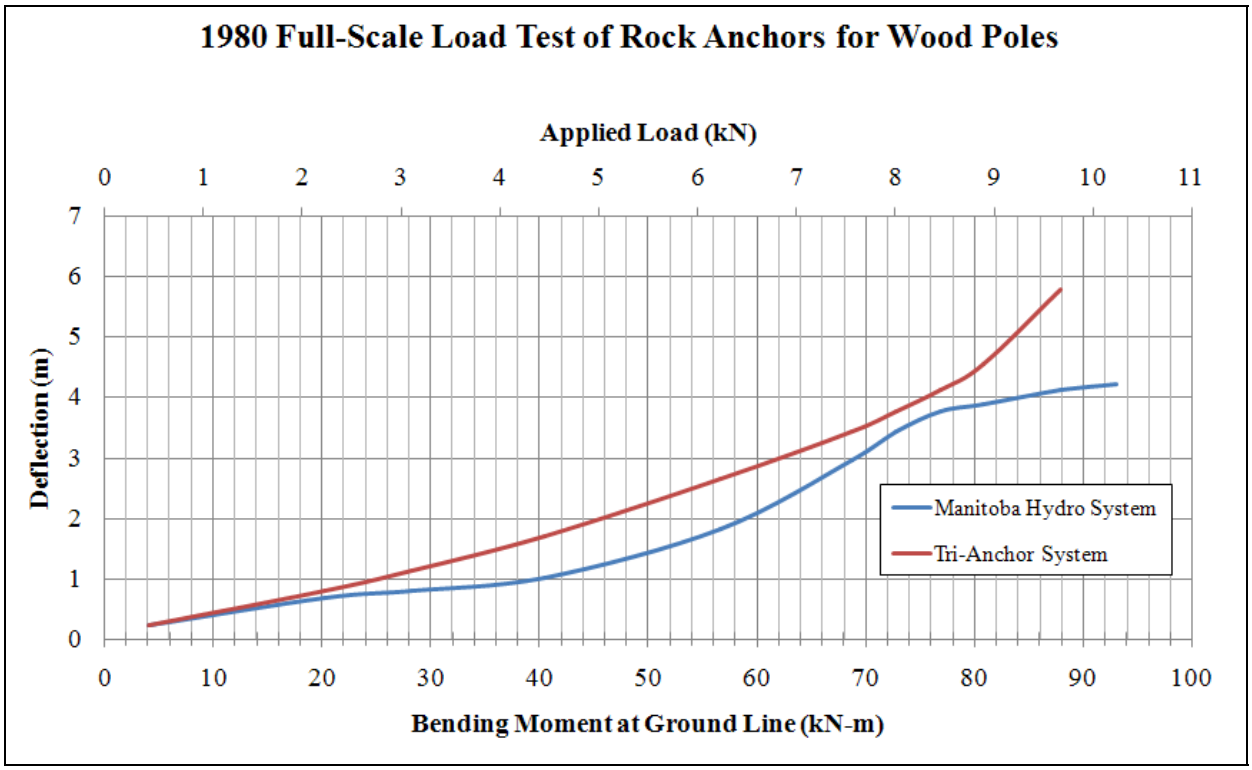

Figure 2.11: Full-Scale load test results of rock anchors for wood poles (Storie, 1980)

Figure 2.12: Full-scale testing of Tri-Steel's Tri-Anchor and Manitoba Hydro's grouted anchor (Storie, 1980)

A review of Tri-Anchor's current products that would be suitable to replace Manitoba Hydro's Distribution Standard indicates that the Tri-Anchor system is not designed to develop the full bending capacity of the pole. For example, based on Tables 2.1 and 2.3 above, a 12.2 m (40-foot) long, Class 4 pole with 1,219 mm (4 feet) of embedment in rock should develop a minimum bending moment of 111 kN-m (i.e. 10,700 N x [12.2 m - .61 m - 1.219 m]). Yet from Table 2.7 below, a summary of the modules available from Tri-Anchor, the module that could accommodate this size of pole is only rated for 95 kN-m at most.

Table 2.7: Ground line moment range for universal Tri-Anchor Model No. 9

(Tri-Steel Fabricators Ltd., 2011)

Pole Butt		**No. of Anchors Per Pole**	**Ground Line Moment Range @ 5° Rotation**	
Min.	**Max.**		**(kN-m)**	**(ft-lbs)**
203 mm (8")	305 mm (12")	3	35 – 53	26,000 – 39,000
279 mm (11")	406 mm (16")	4	47 – 95	35,000 – 70,000
356 mm (14")	508 mm (20")	5	104 – 150	77,000 – 110,000

CHAPTER 3 – EXPERIMENTAL PROGRAM

3.1 INTRODUCTION

The main objective of this experimental program is to evaluate the ability of a prefabricated fixed-end base mount connection detail, which itself is anchored to an exposed rock surface, to develop the full moment capacity of a 12.2 m (40-foot) long, Class 4 Lodgepole Pine (abbreviated "LP") wood pole under different annulus backfill conditions. Due to laboratory height constraints, the 6.1 m (20-foot) long bottom halves of 12.2 m (40-foot) long pole specimens were tested according to the requirements of ANSI/ASTM D1036-99, Standard Methods of Static Tests of Wood Poles (Cantilever Test Method). The transverse load applied to these shortened poles was such that they were subjected to the same applied base moment that a 12.2 m long, Class 4 LP pole is required to withstand. The base mount is expected to develop the bending capacity of the pole prescribed by CAN/CSA-015-05.

3.2 OVERVIEW OF THE BASE MOUNT

The base mount utilizes a 12-sided steel sleeve fabricated from 7.9 mm (5/16 inch) thick plate welded to a 35 mm (1-3/8 inch) thick base plate. As detailed below, the section properties of both the steel sleeve and base plate are adequate to resist the moment generated by the load rating of a 12.2 m (40-foot) long, Class 4 pole. Furthermore, the thickness of the sleeve satisfies the width-to-thickness ratios recommended by the American Association of State Highway and Transportation Officials (AASHTO) for multisided tubular sections to prevent premature buckling. The inside diameter of the steel sleeve is also large enough to accommodate not only the range of permissible butt diameters of the LP poles tested, but also an extra 150 mm (6 inch) annulus around the pole to permit the compaction of a backfill material, as shown in Figure 3.1 below.

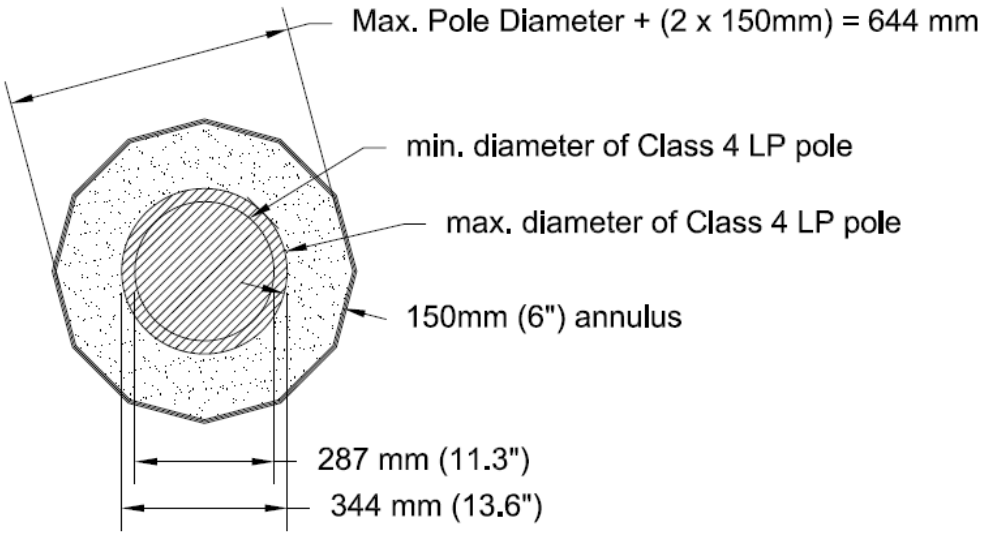

Figure 3.1: Sizing the mount sleeve to permit a 150 mm (6 inch) compacted annulus material

A multi-sided section was used because the largest diameter of commercially available round hollow structural section (HSS) is typically 406 mm (CSA, 2014). An added benefit of using a multi-sided section is that, for equal diameters and wall thicknesses, a multi-sided section has a larger moment of inertia and subsequent resistance to bending than the corresponding round section (Northwest Signal, 2011).

Holes in the base plate have been provided to accommodate threadbar that will be used to anchor the mount to an exposed rock surface. For this study, the spacing of these threadbars was dictated by the 500 mm x 500 mm grid of existing holes in the laboratory strong floor. This would not be a constraint in practice.

Two variations of the aforementioned mount design were fabricated – one with a sleeve height of 1,219 mm (4 feet) and another with a sleeve height of 914 mm (3 feet). The former is consistent with NESC's embedment depth recommendation for 12.2 m (40-foot) long utility poles installed in rock, as discussed in Section 2.3. The latter was selected based on analyses conducted in MFAD, a software package that provides for the design of foundations for single pole structures subject to high overturning moments. MFAD uses a multi-spring, nonlinear subgrade modulus approach to predict the load-deflection response and ultimate capacity of direct embedment foundations placed in multi-layered soil subsurface profiles with either uniform or multi-layered annulus backfills (Rojas-Gonzales et al., 1991). The software was verified by comparing the results of numerous full-scale single pole lateral load tests in rock (as published by Caswell et al. in 1954) with similar analyses produced by the software program A comparison of these results is provided in Appendix A. Additional details pertaining to the software, as well as the results of the optimum sleeve height analysis, are presented in Chapter 5.

3.3 STRUCTURAL DESIGN OF THE SLEEVE

The Canadian Standards Association's published Standard CAN/CSA S16-14, "Design of Steel Structures", specifies maximum width-to-thickness ratios for elements in flexural compression. For circular hollow sections, these maximum width-to-thickness ratios are given by Equations 3.1 to 3.3 below.

A circular hollow section is considered a Class 1 section in flexural compression when Equation 3.1 is satisfied:

$$\frac{D}{t} < \frac{13{,}000}{F_y} \qquad \text{Equation 3.1}$$

A circular hollow section is considered a Class 2 section in flexural compression when Equation 3.2 is satisfied:

$$\frac{D}{t} < \frac{18{,}000}{F_y} \qquad \text{Equation 3.2}$$

A circular hollow section is considered a Class 3 section in flexural compression when Equation 3.3 is satisfied:

$$\frac{D}{t} < \frac{66{,}000}{F_y} \qquad \text{Equation 3.3}$$

Where

D = outside diameter of the section

t = thickness of the section

F_y = specified minimum yield strength of steel

Multi-sided tubular steel sections of large diameter compared to their relatively small wall thickness are typically Class 3 sections. The factored moment resistance of a Class 3 section, as specified by CAN/CSA S16-14, is given by Equation 3.4 below:

$$M_r = \phi S F_y \qquad \text{Equation 3.4}$$

Where

M_r = moment resistance of the section

ϕ = steel resistance factor

S = elastic section modulus

The American Association of State Highway and Transportation Officials (AASHTO) "Standard Specifications for Structural Supports for Highway Signs, Luminaires, and Traffic Signals" provides Equation 3.5 below to approximate the section modulus of a 12-sided dodecagonal section:

$$S = 3.29R^2t \qquad \text{Equation 3.5}$$

Where

S = elastic section modulus

R = radius measured to the mid-thickness of the wall

t = wall thickness

In our case, we want to minimize the diameter of the sleeve (and therefore weight), but still accommodate the range of permissible butt sizes plus an extra 150 mm annulus around the pole. Therefore, the only unknown becomes "t". By setting M_r to the anticipated maximum factored moment (which is equal to 1.5 times the anticipated maximum unfactored moment) and substituting Equation 3.5 into Equation 3.4, the minimum required wall (or sleeve) thickness, t, can be determined.

The detailed calculations that were used in the structural design of the sleeve can be found in Appendix B.

3.4 STRUCTURAL DESIGN OF THE THREADBAR

The structural design of the threadbars used in this project entails using the same procedure that one would use to determine the bolt forces in an ungrouted base plate application. Assuming that the base plate behaves as an infinitely rigid body, the load in bolt 'i' (BL_i) can be determined by Equation 3.6 below, as per the American Society of Civil Engineers' Manual of Practice No. 113, "Substation Structure Design Guide".

$$BL_i = \left(\frac{P}{A_{BC}} + \frac{M_x y_i}{I_{BC_x}} + \frac{M_y x_i}{I_{BC_y}}\right) A_i \qquad \text{Equation 3.6}$$

Where

P = vertical load supported by all bolts

M_x = base moment about the x-axis

M_y = base moment about the y-axis

x_i, y_i = x and y distances of bolt 'i' from reference axes

A_i = net area of bolt 'i'

A_{BC} = total bolt cage area = $\sum_{i=1}^{n} A_i$

I_{BCx} = bolt cage inertia about the x-axis = $\sum_{i=1}^{n} (A_i y_i^2 + I_i)$

I_{BCy} = bolt cage inertia about the y-axis = $\sum_{i=1}^{n} (A_i x_i^2 + I_i)$

n = total number of bolts

I_i = moment of inertia of bolt 'i', which is often a very small value and therefore typically omitted when calculating I_{BCx} and I_{BCy}

When the base plate is solid (or in other words, it does not have a central hole), the plate is assumed to be sufficiently rigid that it distributes the shear load to all of the threadbars equally. This is summarized by Equation 3.7 below:

$$F_v = V / n \qquad \text{Equation 3.7}$$

Where

F_v = shear load per threadbar

V = total shear load

n = number of threadbars

When the clear distance between the bottom of the base plate and the top of the concrete (or exposed rock surface) exceeds 2 times the diameter of the threadbar, as may be the case when the base plate is installed on leveling nuts, shear loads can create a significant bending moment in the threadbars. The shear is assumed to act on a rigid frame consisting of the base plate as the beam and the anchor bolts as the columns. As per the American Society of Civil Engineers (ASCE)' Manual of Practice No. 113 "Substation Structure Design Guide" (ASCE, 2008), a moment distribution with typical relative stiffness ratios for columns to beams shall be assumed. As shown in Figure 3.2 below, this yields a conservative point of inflection at a point approximately 0.625 times the distance from the top of the concrete to the bottom of the base plate. The bending in the threadbars resulting from shear load, F_v, is therefore given by Equation 3.8 below:

$$M_b = \left(\frac{5}{8}\right)(h)(F_v) \qquad \text{Equation 3.8}$$

Where

M_b = bending moment per threadbar

h = distance from the top of concrete (or exposed rock surface) to the bottom of the base plate

F_v = shear load per threadbar

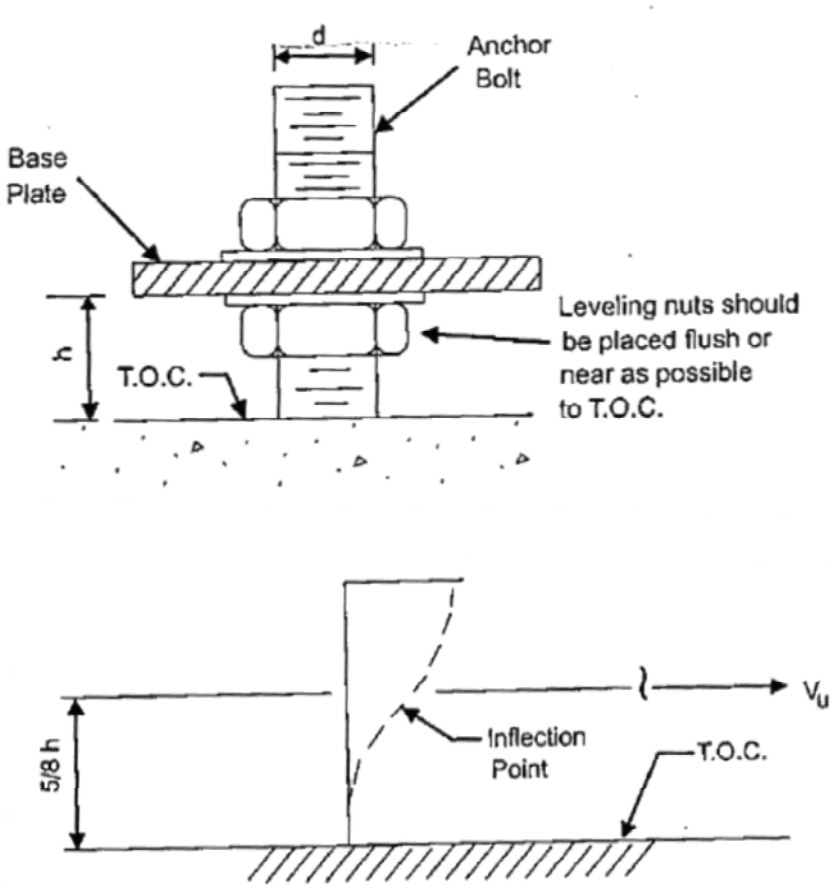

Figure 3.2: Leveling nut arrangement and inflection point in threadbar due to shear load (ASCE, 2008)

The tensile area of threadbar, A_s, required to resist combined axial load, shear, and bending are additive, as given by Equation 3.9 below (ASCE, 2008):

$$A_s = A_a + A_v + A_b \qquad \text{Equation 3.9}$$

Where

A_a = area required to resist axial load in tension = BL_i / min($0.9F_y$, $0.8F_u$)

A_v = area required to resist shear load = $\frac{F_v}{\phi F_y}$

A_b = area required to resist bending = $\left\{\pi \left[\frac{5hF_v}{2\phi F_y}\right]^2\right\}^{1/3}$

h = distance from top of concrete (or exposed rock) to bottom of base plate

F_v = shear load per threadbar

F_y = specified minimum yield strength of steel

F_u = specified minimum tensile strength of steel

For threadbars that are loaded in compression, however, axial compressive resistance can be determined using Equation 3.10 below. A value of 1.2 is assumed for the effective length factor, K, as recommended by CAN/CSA S16-14 for fixed-fixed connections where rotation is restrained at both ends but translation is fixed at one end only.

$$C_r = \phi A F_y (1+\lambda^{2n})^{-1/n} \qquad \text{Equation 3.10}$$

Where

C_r = axial compressive resistance

ϕ = steel resistance factor

A = compressive area of the threadbar

F_y = specified minimum yield strength of steel

λ = non-dimensional slenderness parameter = $\frac{KL}{r}\sqrt{\frac{F_y}{\pi^2 E}}$

n = 1.34

K = effective length factor

L = length of compression member

r = slenderness ratio

E = modulus of elasticity of steel

The detailed calculations that were used in the structural design of the threadbars can be found in Appendix C.

3.5 STRUCTURAL DESIGN OF THE BASE PLATE

There are currently no available standards that provide specific requirements for the analysis of base plates for tubular pole structures that are supported on levelling nuts. The ASCE Manual of Practice No. 72 "Design of Steel Transmission Pole Structures" (ASCE, 2006), however, presents basic guidelines that should be considered when designing such base plates. These considerations are detailed below.

The resultant loads of each individual anchor bolt are required to calculate the stresses in the base plate. An assumption is normally made that these anchor bolt loads will produce a uniform bending stress

along the effective portion of the bend line analyzed, and that the entire width of plate along the bend line is effective in resisting bending moment.

It is common to check several bend line configurations in the analysis of a single base plate. Two of the possible bend lines that are typically considered for symmetrical, square base plates supporting multisided tubular structures are illustrated in Figure 3.3 below. The first bend line (Line 1-1) is taken tangential to the column face in a plane parallel to the edge of the base plate. Bending about this line represents the scenario where wind is applied at 90 degrees, or perpendicular, to the power line. A second bend line (Line 2-2) is taken tangential to the column face in a plane that is inclined at 45 degrees to the edge of the base plate. Bending about this line represents the scenario where wind is applied at 45 degrees to the power line.

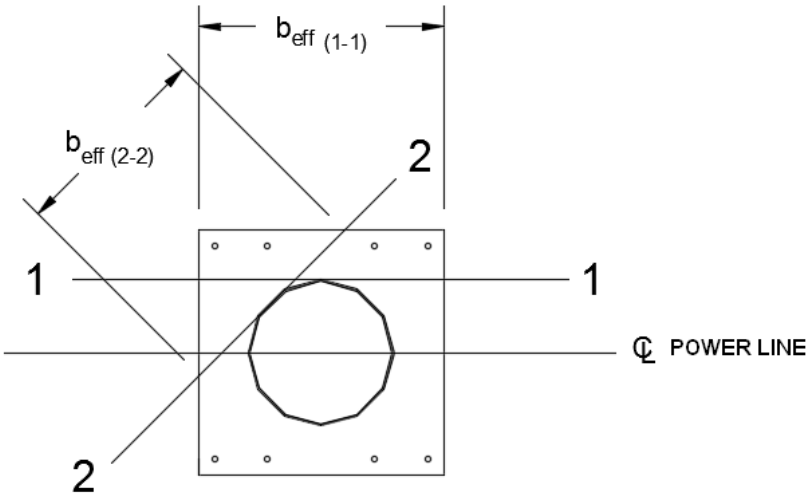

Figure 3.3: Bend lines used in the design of the base plate

For each bend line considered, the minimum thickness of the base plate required to keep the bending stress in the plate below the yield stress of steel, F_y, can be determined by using Equation 3.11 below (ASCE, 2006):

$$t_{min} = \left[\left(\frac{6}{b_{eff} F_y}\right)(BL_1c_1 + BL_2c_2 + \ldots + BL_ic_i)\right]^{1/2} \qquad \text{Equation 3.11}$$

Where

t_{min} = minimum base plate thickness required

b_{eff} = width of base plate that is effective in resisting moment (assumed to equal the entire width of base plate along the bend line)

F_y = specified minimum yield strength of steel

BL_i = individual anchor bolt load

i = number of anchor bolt load values contributing moment along the bend line

c_i = shortest distance from anchor bolt (that contributes moment along the bend line) to the bend line

Of the two bend lines considered, Line 2-2 is most critical and governed the thickness of the base plate. Based on the 500 mm x 500 mm grid of existing holes in the laboratory strong floor with respect to the location of the strong wall and laboratory crane, however, it was not feasible to test the mount in an orientation that would create bending about Line 2-2. Therefore, although the mount was designed to resist bending about Line 2-2, it was tested such that the bending resulted about Line 1-1.

The detailed calculations that were used in the structural design of the base plate can be found in Appendix D.

3.6 ANNULUS BACKFILL MATERIAL

With the cross-sectional properties of the mount remaining constant, another variable that was tested in addition to sleeve height was annulus backfill material. As mentioned in the previous chapter, the most common backfill materials (other than native soil) are 19 mm (3/4 inch) or smaller well-graded crushed rock or sand. However, holes in the sleeve have also been provided to accommodate mechanical fasteners as an alternative annulus material.

3.6.1 MECHANICAL FASTENERS

The function of the mechanical fasteners is to minimize pole movement where there is a gap between the pole and the sleeve. An advantage of using mechanical fasteners over a granular backfill material is that mechanical fasteners can be tightened by Line Maintenance personnel as required to accommodate pole shrinkage. As shown in Figure 3.4 below, the ends of 25.4 mm (1") diameter all-thread rod bear on pole gains to help minimize local stress concentrations. Pole gains are a stock item available through Manitoba Hydro's Central Stores, as shown in Figure 3.5 below. Although the use of mechanical fasteners as a backfill annulus material is not a technique that is familiar to Manitoba Hydro construction personnel, the materials required would be easy to store and transport to site.

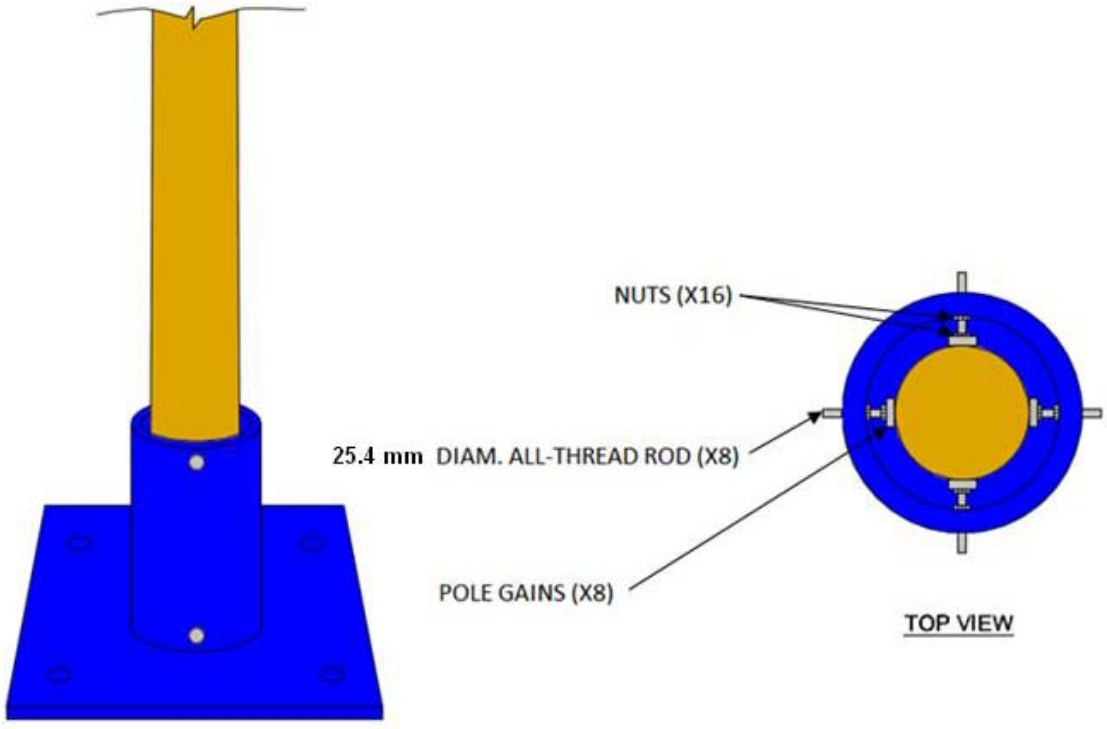

Figure 3.4: Conceptual design of base mount with mechanical fasteners as annulus material

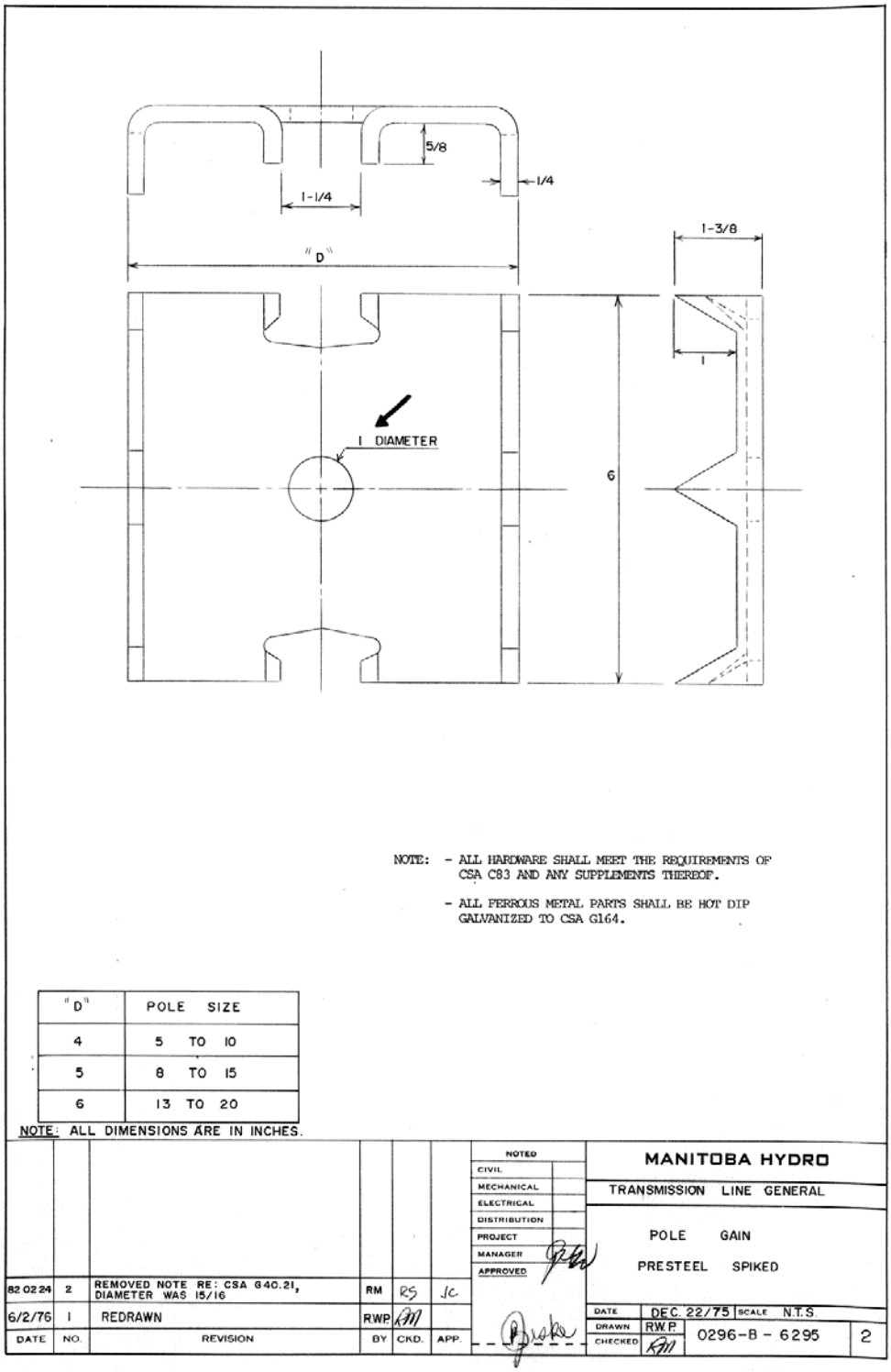

Figure 3.5: Manitoba Hydro Central Stores Item #32-12-15, Pole Gain.

The resultant loads in the upper and lower mechanical fasteners, as given by Equations 3.12 and 3.13 below, can be determined by considering the free body diagram presented in Figure 3.6 below and by summing moments about the resultant load in the lower fasteners or upper fasteners, respectively. It should be noted that the resultant loads in the upper and lower mechanical fasteners are for 2 fasteners, each.

$$P_{upper\ fasteners} = \frac{H(L-610\ mm)}{h_{mount}} \qquad \text{Equation 3.12}$$

$$P_{lower\ fasteners} = \frac{H(L-610mm-h_{mount})}{h_{mount}} \qquad \text{Equation 3.13}$$

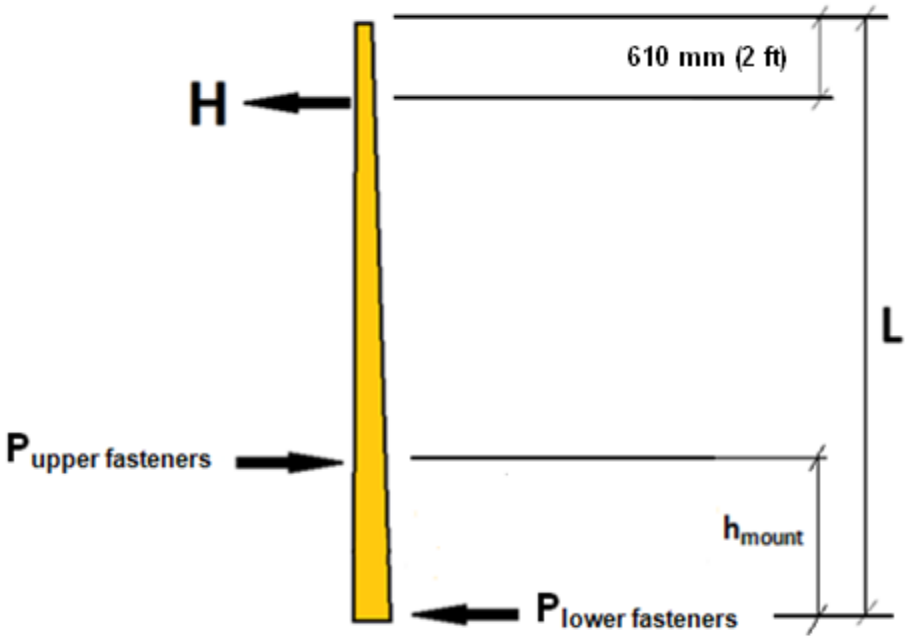

Figure 3.6: Free body diagram for load in upper and lower fasteners

Once the load in the upper and lower fasteners is known, the compressive and shear components acting on each fastener can be determined by Equations 3.14 and 3.15 below. The derivation of these equations is based on Figure 3.7 below, and is specific to the testing orientation described above in Section 3.5 (i.e. moment about Bend Line 1-1 in Figure 3.3).

$$C_U = V_U = \cos 45^\circ \times \frac{P_{upper\ fasteners}}{2} \qquad \text{Equation 3.14}$$

$$C_L = V_L = \cos 45^\circ \times \frac{P_{lower\ fasteners}}{2} \qquad \text{Equation 3.15}$$

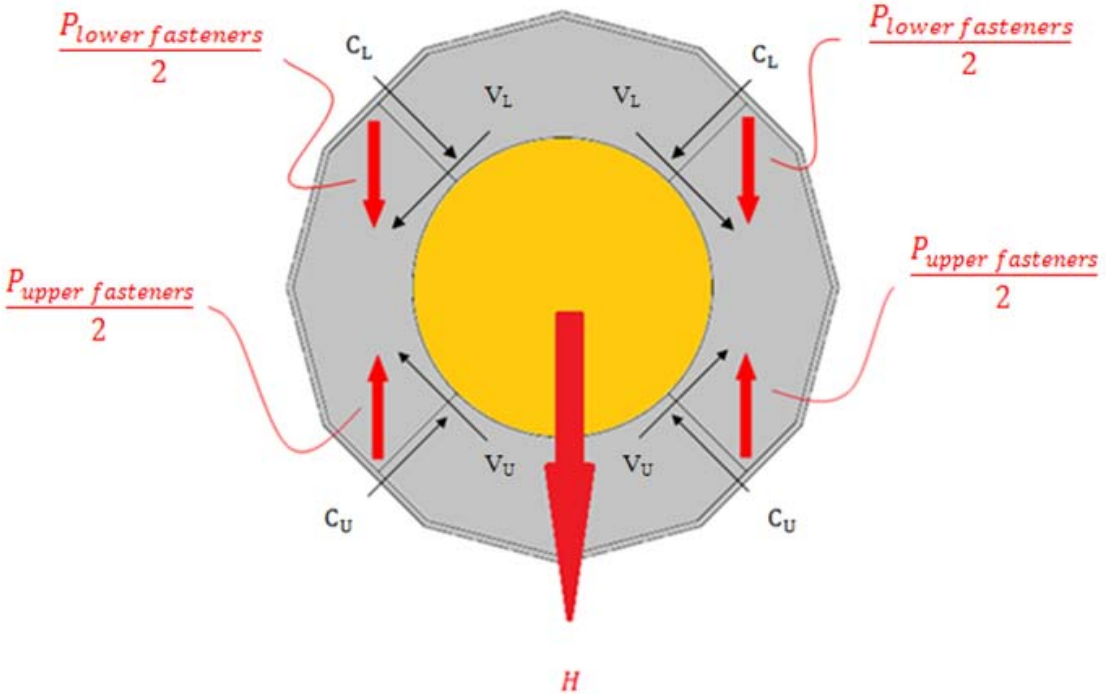

Figure 3.7: Resolving the upper and lower fastener loads into compression and shear

The mechanical fasteners were designed as axially loaded columns, as per CAN/CSA S16-14. The factored axial compressive resistance of the mechanical fasteners, C_r, was determined using Equation 3.13 above (i.e. the same calculations as were used to determine the axial compressive resistance of threadbars loaded in compression). The only exception was that a value of 1 was assumed for the effective length factor, K, as recommended by CAN/CSA S16-14 for pin-pin connections where rotation is unrestrained but translation is fixed.

The factored shear resistance of each mechanical fastener, V_r, was determined using Equation 3.16 below. As recommended by CSA/CAN S16-14, a factor of 0.7 was applied to account for the fact that the bolt threads are intercepted by a shear plane.

$$V_r = (0.7)0.6\phi_b nmA_b F_u \qquad \text{Equation 3.16}$$

Where

ϕ_b = resistance factor for bolts (= 0.8)

n = number of bolts

m = number of shear planes

A_b = cross-sectional area of a bolt based on its nominal diameter

F_u = specified minimum tensile strength of bolt

In addition to designing the mechanical fasteners themselves, deflections of the mount sleeve (due to individual fastener loads acting normally to the face of the sleeve) were checked. As recommended by Carvill (1993), Equation 3.17 below approximates the deflection of a simply supported square plate with

a concentrated load applied at the center. It should be noted that this equation assumes the deflection is small compared to the plate thickness, and that the load acts over a small circular area.

$$y_m = k_1 \frac{Pa^2}{Et^3}$$ Equation 3.17

Where

y_m = deflection at center of plate

k_1 = 0.127 for a square plate

P = applied concentrated load

a = width (or length) of plate

E = modulus of elasticity of steel

t = plate thickness

The detailed calculations that were used in the structural design of the mechanical fasteners can be found in Appendix E.

3.6.2 19 MM WELL-GRADED CRUSHED LIMESTONE OR SAND

As alluded to earlier, the use of a compacted granular annulus material is a technique that is familiar to construction personnel. A compacted granular annulus material such as crushed limestone or sand keeps the pole securely in place, and can accommodate varying dimensions of poles. A conceptual design of this technique is shown in Figure 3.8 below. Grading requirements commonly used by Manitoba Hydro for 19 mm (3/4 inch) crushed rock and sand are provided in Tables 3.1 and 3.2 below, respectively.

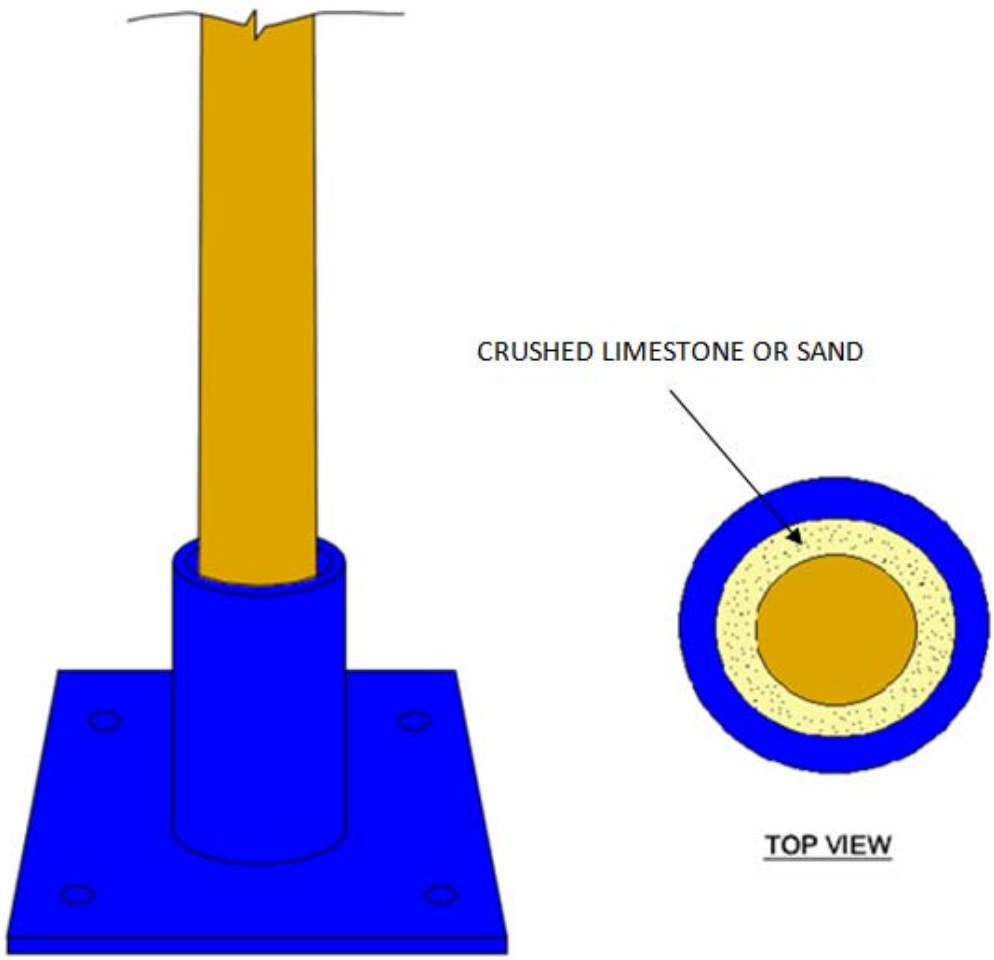

Figure 3.8: Conceptual design of base mount with compacted crushed limestone or sand annulus material

Table 3.1: Typical Grading Requirements used by Manitoba Hydro for 19 mm Crushed Rock

Gradation		**Aggregate Quality Requirements**
Sieve Size	**Percent Passing (by dry mass)**	The aggregate should be crushed and have a minimum California Bearing Ratio (CBR) of 60 percent The coarse fraction of the aggregate should have a maximum Los Angeles abrasion loss of 35% The aggregate should consist of sound, durable crushed stone. It should not contain thin elongated particles, sods, topsoil, roots or plants 100% of the material retained on the 4.75 mm sieve should consist of crushed stone
19 mm	100%	
4.75 mm	35 – 70%	
0.425 mm	15 – 30%	
0.075 mm	6 – 17%	

Table 3.2: Typical Grading Requirements used by Manitoba Hydro for Sand

Gradation	
Sieve Size	**Percent Passing (by dry mass)**
9.5 mm	100%
4.75 mm	90 – 100%
0.595 mm	25 – 60%
0.075 mm	0 – 3%

3.7 PROTOTYPE FABRICATION

A total of four base mounts were fabricated by a local manufacturer in Winnipeg according to the fabrication details shown in Figure 3.9 below – two with a sleeve height of 1,219 mm (4 feet) and two with a sleeve height of 914 mm (3 feet). All four mounts were fabricated in a black (non-galvanized) condition in order to minimize the fabrication time. If adopted for field-use, however, all mounts supplied would be galvanized in order to protect the steel from corrosion. The use of non-galvanized base mounts had no effect on the results of this experimental work.

The base mounts fabricated with a 1,219 mm (4 foot) sleeve weighed 500 kg (1,104 lbs.) and cost $3,215.00 each. The base mounts fabricated with a 914 mm (3 foot) sleeve weighed 460 kg (1,014 lbs.) and cost $2,937.00 each. Galvanizing would add approximately 4% extra weight to each sleeve. The unit costs provided above would likely be reduced with mass fabrication, issue for tender to multiple bidders, and further optimization if warranted by the results of this study.

A prototype inspection was conducted at the manufacturer's facility on May 16, 2013. The purpose of this inspection was to inspect the prototype's welds for conformance to the fabrication details provided to the fabricator (as per Figure 3.9 below), as well as with the shop drawings submitted by the fabricator (as per Figure 3.10 below). More specifically, the inspection aimed to confirm that the complete joint penetration weld connecting the base plate to the sleeve was made with a backing bar as requested, and that the longitudinal seam of the sleeve was made with a groove bevel weld complete with a backing weld of length 250 mm at each end of the sleeve. These weld requirements were performed acceptably, as shown in Figures 3.11 and 3.12 below.

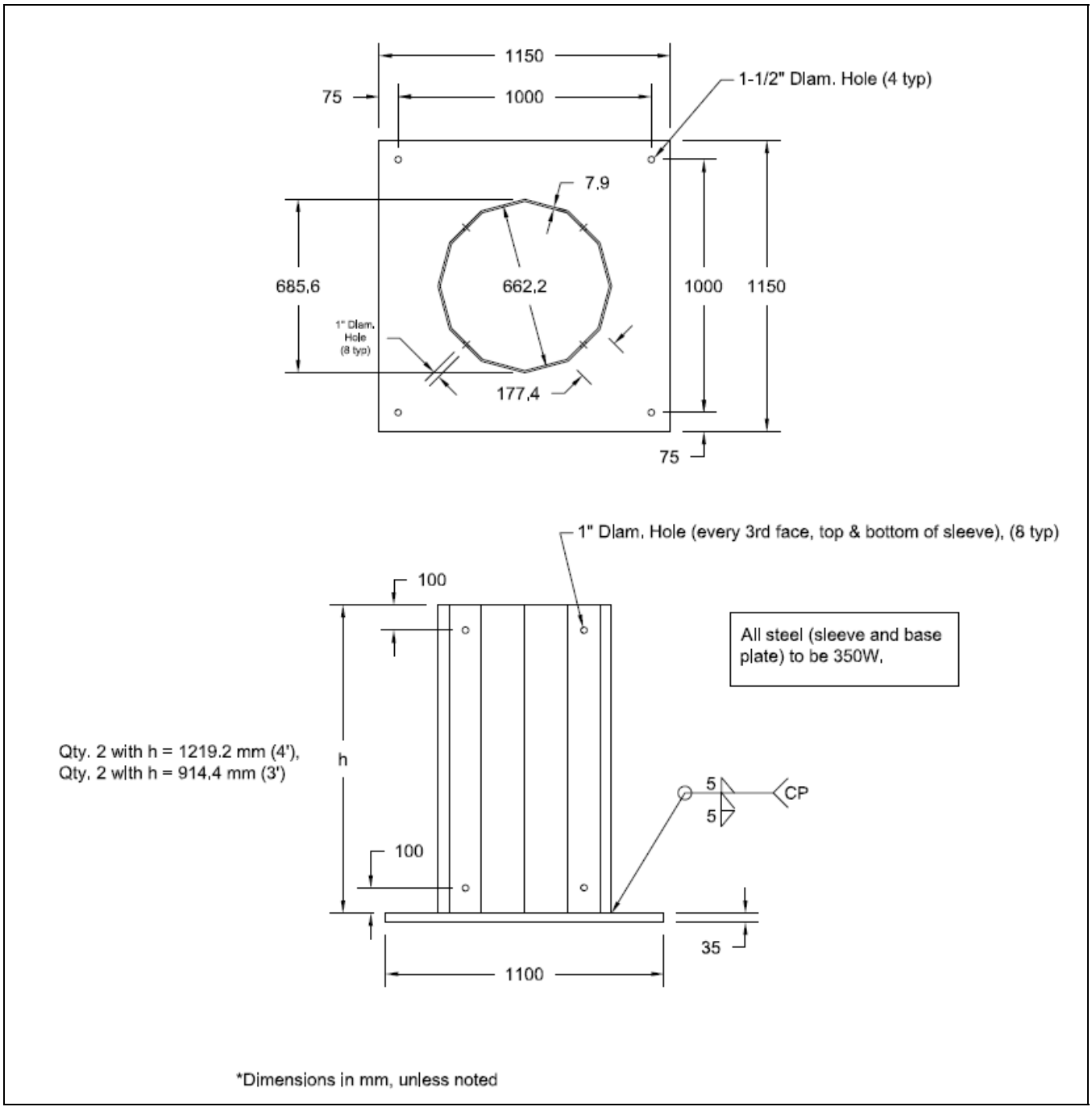

Figure 3.9: Fabrication details provided to the fabricator

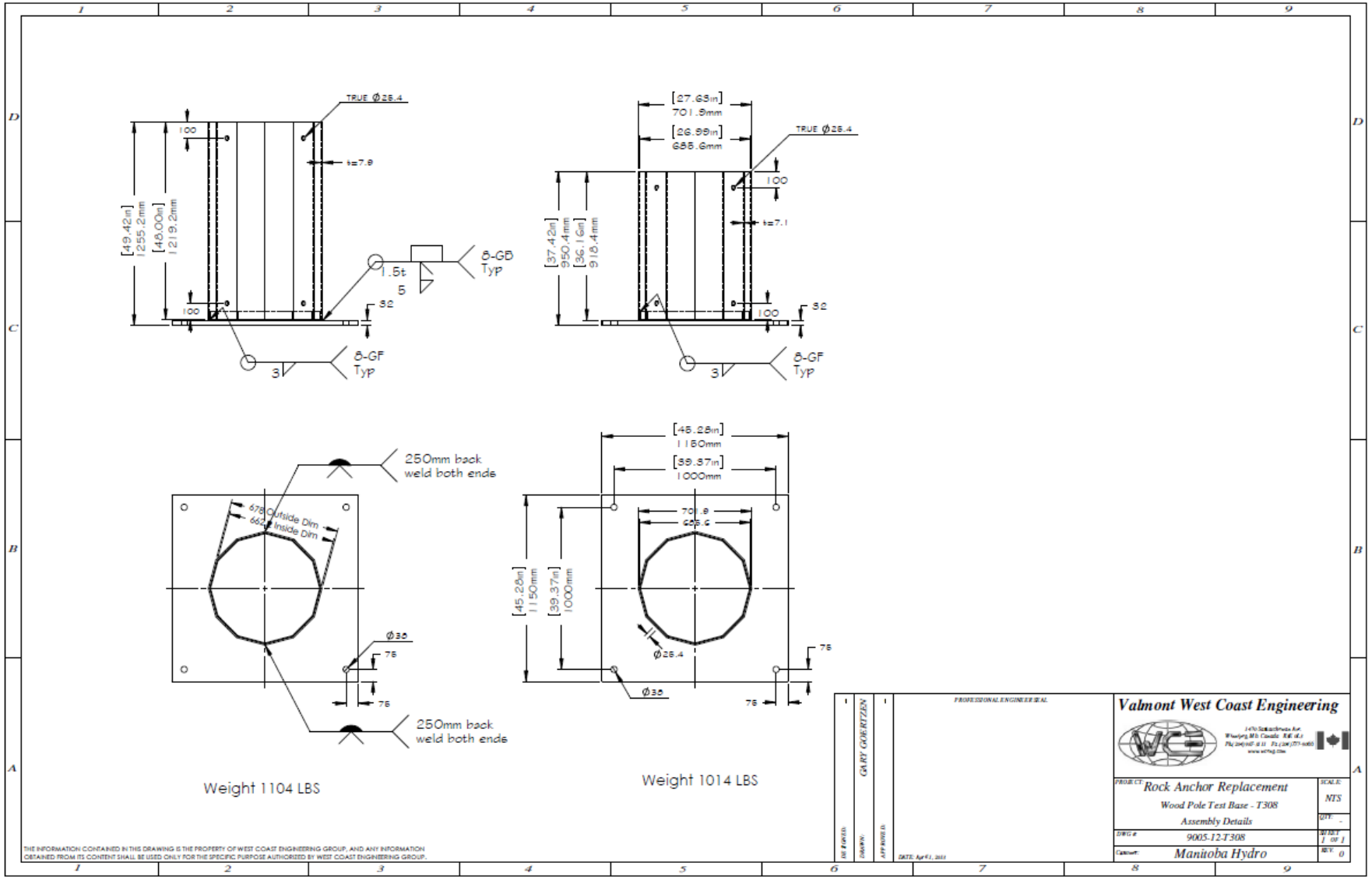

Figure 3.10: Shop drawing provided by the fabricator

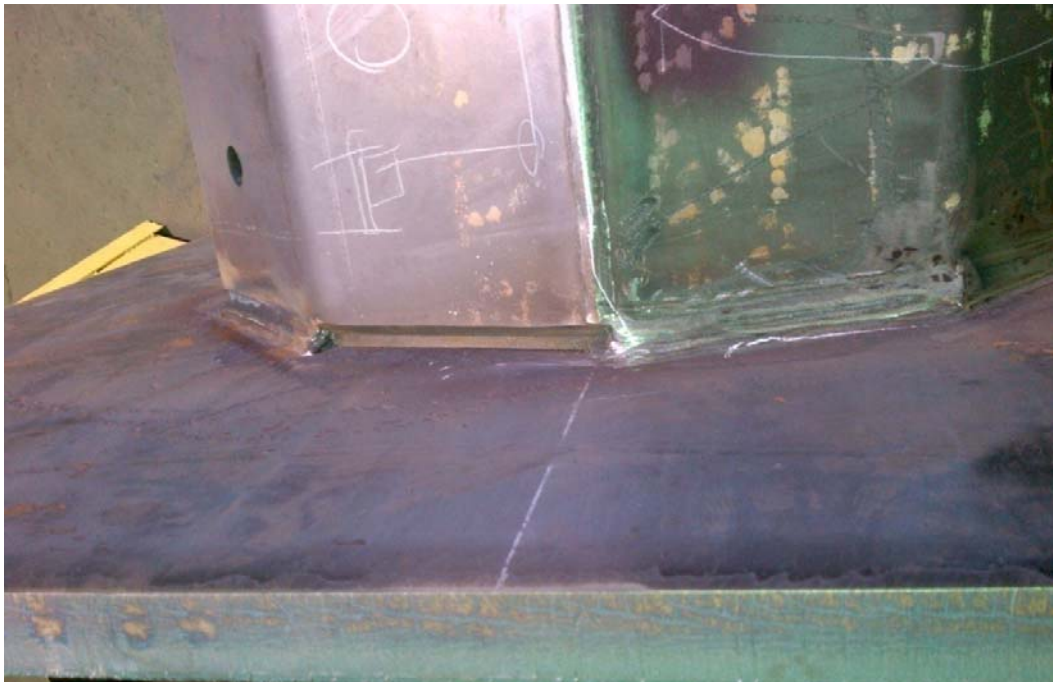

Figure 3.11: Inspection of the complete joint penetration weld (sleeve-to-base plate connection)

Figure 3.12: Inspection of the sleeve's longitudinal seam weld

3.8 TEST METHOD

All poles were tested using a method that was established based on ASTM D1036-99's Cantilever Test Method. Each pole was tested in a vertical orientation, rather than the horizontal orientation recommended by ASTM D1036-99, in order to contend with a shortage of available space in the lab. As shown in Figure 3.13 below, load was applied horizontally at a point 610 mm (2 feet) from the pole tip by the laboratory crane via a cable and a pulley that was mounted to the laboratory strong wall. The maximum load that could be applied by the crane was 10 metric tons (100 kN), with load applied at a rate of approximately 500 N per second. A schematic of the test method used is provided in Figure 3.14 below.

Figure 3.13: Horizontal load applied to the pole by the laboratory crane via a cable and pulley

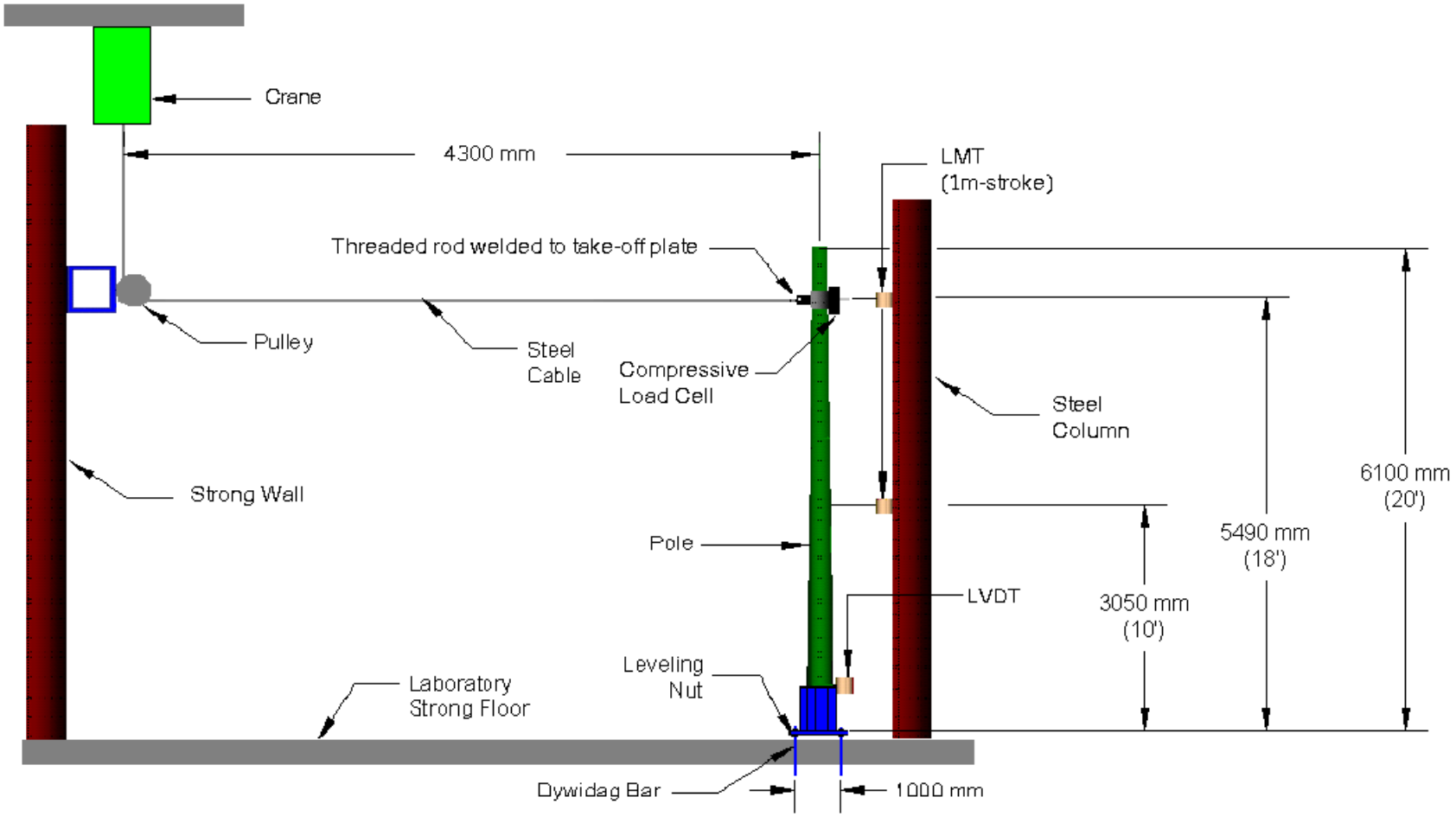

Figure 3.14 Test method schematic

All poles were initially 12.2 m (40 feet) long, but were cut in half to satisfy height constraints imposed by the lab. The bottom half of each pole was used for testing. Cutting the poles in half to 6.1 m (20 feet), versus using 6.1 m (20-foot) long Class 4 poles, maintained the geometric pole butt properties of poles that would be used with these mounts in the field. For example, a 12.2 m (40 foot) long Class 4 LP pole has a minimum circumference of 902 mm (35.5 inches), whereas a 6.1 m (20 foot) long Class 4 LP pole's minimum required circumference is only 673 mm (26.5 inches).

According to CAN/CSA 015-05, a Class 4 pole shall be capable of withstanding an unfactored transverse force of 10,700 N applied 610 mm (2 feet) from the top of the pole. The moment generated at the fixed base of the pole, as given by Equation 3.18 below, can be determined by considering the free body diagram presented in Figure 3.15 below.

$$M = H \times (L - h - 610\ mm) \qquad \text{Equation 3.18}$$

Where

M = maximum moment generated at the fixed end of a pole

H = horizontal load applied at a distance 610 mm (2 feet) from the tip of the pole

L = length of the pole

h = sleeve height

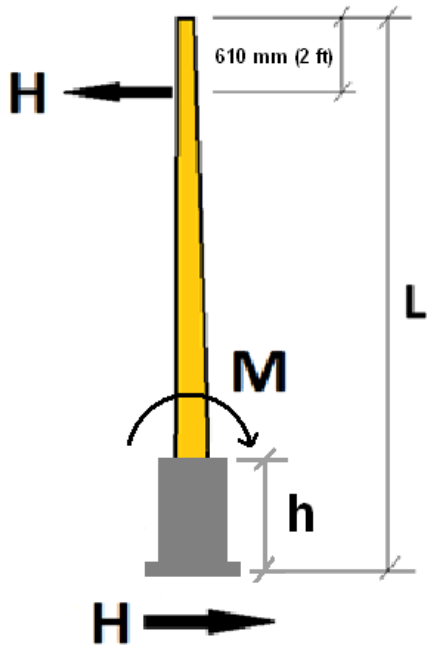

Figure 3.15: Free body diagram for maximum moment generated at the fixed end of a pole

In order to maintain the maximum applied base moment generated for a 12.2 m (40-foot) long pole, CAN/CSA 015-05's transverse load requirement of 10,700 N for Class 4 poles was increased to 26,000 N and 24,250 N for the 6.1 m (20-foot) long poles tested in 1,219 mm and 914 mm mounts, respectively. These increased values of transverse load were determined using Equation 3.19 below.

$$H_{20} = \frac{(10{,}700\ \text{N}) \times (L - h - 610\ \text{mm})}{(\frac{L}{2} - h - 610\ \text{mm})} \qquad \text{Equation 3.19}$$

Where

H_{20} = transverse load requirement for 12.2 m long Class 4 poles cut in half to 6.1 m

L = length of the pole above ground line (prior to being cut in half)

h = sleeve height

As shown in Figure 3.15 above, the shear generated at the fixed end of the pole is equal to the applied transverse load. Therefore, by increasing the transverse load requirement as described above, the corresponding base shear is also more than doubled. It therefore becomes necessary to ensure that the failure mode of the pole does not change from one of bending to one of shear. From Equation 2.3, it can be shown that the increased value of applied transverse load results in a shear stress that is less than 1% of the shear strength of Lodgepole Pine (see detailed calculations in Appendix F). Therefore, the use of 6.1 m (20-foot) long poles with an increased transverse load requirement should provide results analogous to those generated for 12.2 m (40-foot) long poles tested with the transverse load requirement specified by CAN/CSA 015-05.

Although CAN/CSA 015/05 only requires testing the poles to a specified transverse load, all poles were tested to failure. By testing all poles to failure, this would confirm that the full bending capacity of each pole was developed and that the foundation (i.e. base mount) could survive the pole that it supports.

For each test, the base mount was attached to the structural floor of the laboratory. This connection was made using four #10 Dywidag threadbars, each of which was fixed to the underside of the structural floor and prestressed to 60% of its tensile strength. Each mount was installed on leveling nuts, rather than directly to the floor, to simulate the likely field installation of these mounts on unlevel surfaces. The installation of the mount on levelling nuts is shown in Figure 3.16 below.

Although holes had been provided in the base plate at 1000 mm x 1000 mm, additional holes perpendicular to the direction of the applied load had to be added based on where the steel column was situated in the lab, which was used to support some of the testing instrumentation.

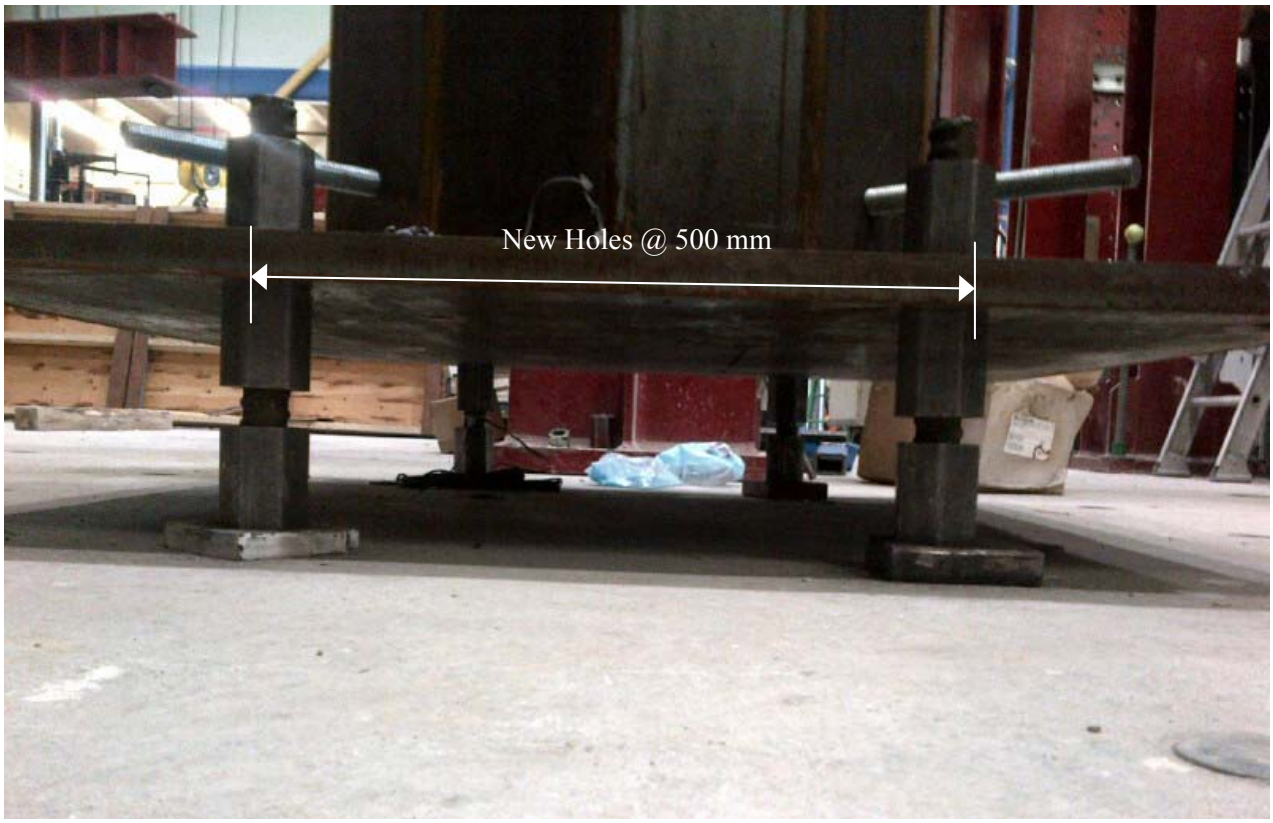

Figure 3.16: Base mount installed on leveling nuts

3.9 POLE PREPARATION

A small amount of pole specimen preparation, in addition to cutting the 12.2 m (40-foot) long poles in half to 6.1 m (20-foot) lengths (such that the bottom halves were tested and the top halves were discarded), was required prior to placing each pole in the base mount. This was necessary in order to attach the cable that applied the horizontal load to the pole tip, as well as the compressive load cell that measured the magnitude of load applied during the test.

As shown in Figure 3.17, a chalked string line was used to indicate the centreline of the pole along its length. Once this was done, the round pole was notched just enough to create a flat bearing surface (Figure 3.18) and a hole was drilled through the pole at 610 mm (2 feet) from the pole tip to accommodate the load take-off plate (Figure 3.19).

Figure 3.17: Marking the centerline of the pole with a chalk line

Figure 3.18: Notching the pole tip to create a flat bearing surface

Figure 3.19: Drilling a hole through the pole at 610 mm (2 feet) from the tip

3.10 TEST PROCEDURE

3.10.1 POLE TESTS WITH MECHANICAL FASTENERS

When mechanical fasteners were used as a backfill annulus material to fill the gap between the pole and the sleeve, the pole was first lowered into the base mount using the laboratory crane and plumbed. The pole remained supported by the crane until all 8 mechanical fasteners were installed.

Starting at the bottom, a 25.4 mm (1 inch) diameter all-thread rod was inserted through the hole in the sleeve and two nuts were turned onto its end that was nearest to the pole. The end of the rod was then passed through the hole in the pole gain until it bore on the pole, and the nut closest to the pole gain was tightened up against it until the teeth of the pole gain bit into the pole. The remaining nut was turned in the opposite direction until it bore against the inside edge of the mount sleeve. The remaining 7 fasteners were installed in a similar manner. A complete installation of all 8 fasteners is shown in Figure 3.20 below. A close-up view of the installed fasteners, as viewed from inside the sleeve, is provided in Figure 3.21 below.

Figure 3.20: Complete installation of all 8 mechanical fasteners

Figure 3.21: Close-up view of the installed fasteners, as viewed from inside the sleeve

3.10.2 POLE TESTS WITH CRUSHED LIMESTONE OR SAND

Before crushed limestone or sand was used as a backfill annulus material to fill the gap between the pole and the sleeve, the pole was first lowered into the base mount using the laboratory crane and plumbed. The pole remained supported by the crane until backfilling was complete. The backfill material was placed in 150 mm (6 inch) lifts, with each layer mechanically tamped before the next lift was added (as shown in Figure 3.22 below).

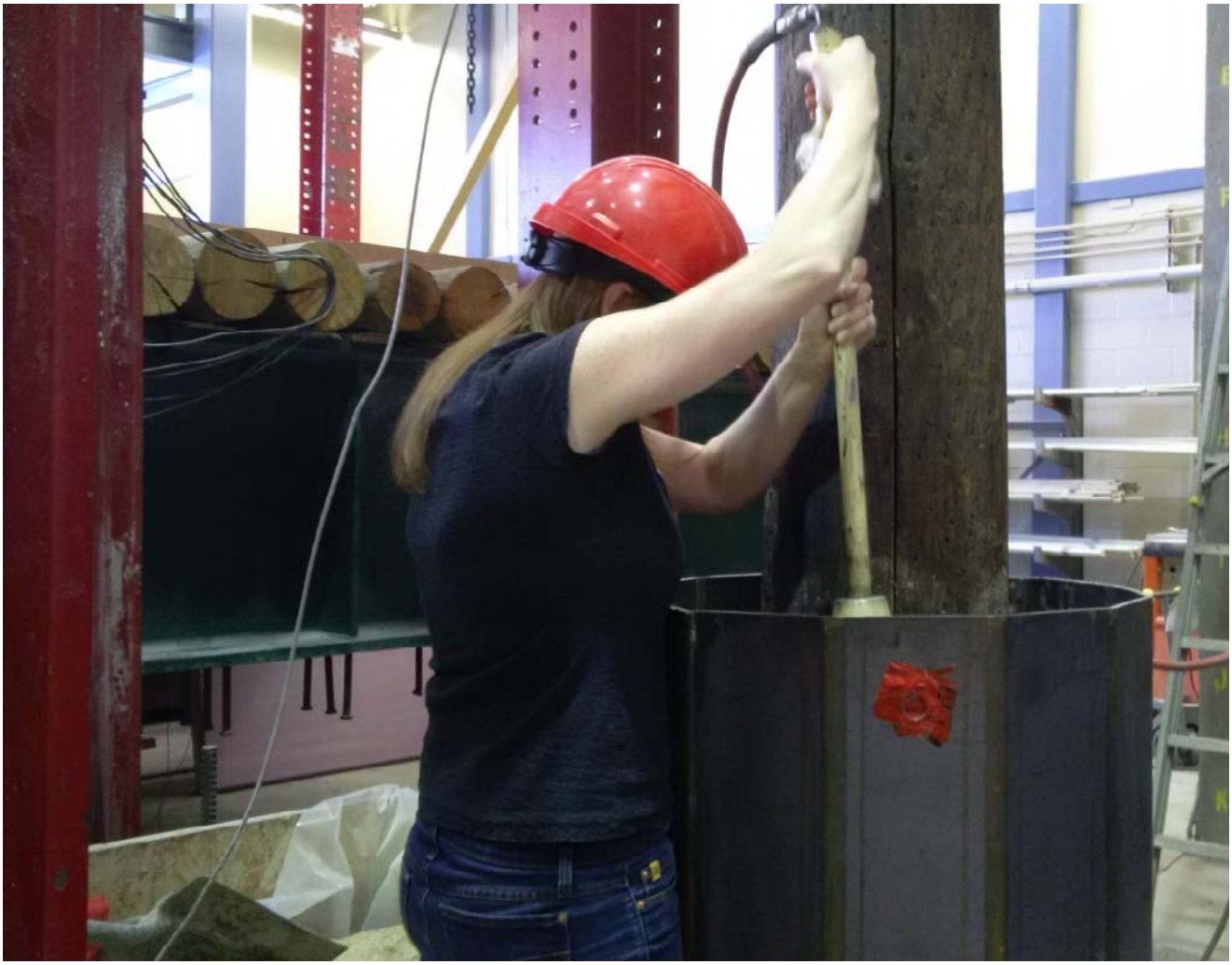

Figure 3.22: Compacting the crushed limestone with a pneumatic tamper

3.11 INSTRUMENTATION

The instrumentation used, regardless of the annulus material tested, was designed to measure:

- the applied load at 610 mm (2 feet) from the tip of the pole;
- the horizontal pole displacement at the load application point, at pole mid-height, and at the top of the base mount (i.e. groundline); and
- strains in the base plate, mount sleeve, and Dywidag threadbars.

3.11.1 APPLIED LOAD MONITORING

With the preparation detailed in Sections 3.9 and 3.10 complete, the pole is ready to accept both the load take-off plate and the compressive load cell used to measure applied load. A 19 mm (3/4 inch) diameter all-thread rod with a 19 mm (3/4 inch) thick take-off plate welded to one of its ends is passed through the hole in the pole. Then a nut, two thin bearing plates, compressive load cell, round adapter, and another thick bearing plate are connected in series at the end of the all-thread rod, as shown in Figure 3.23 below. The capacity of the load cell used was 300.00 kN.

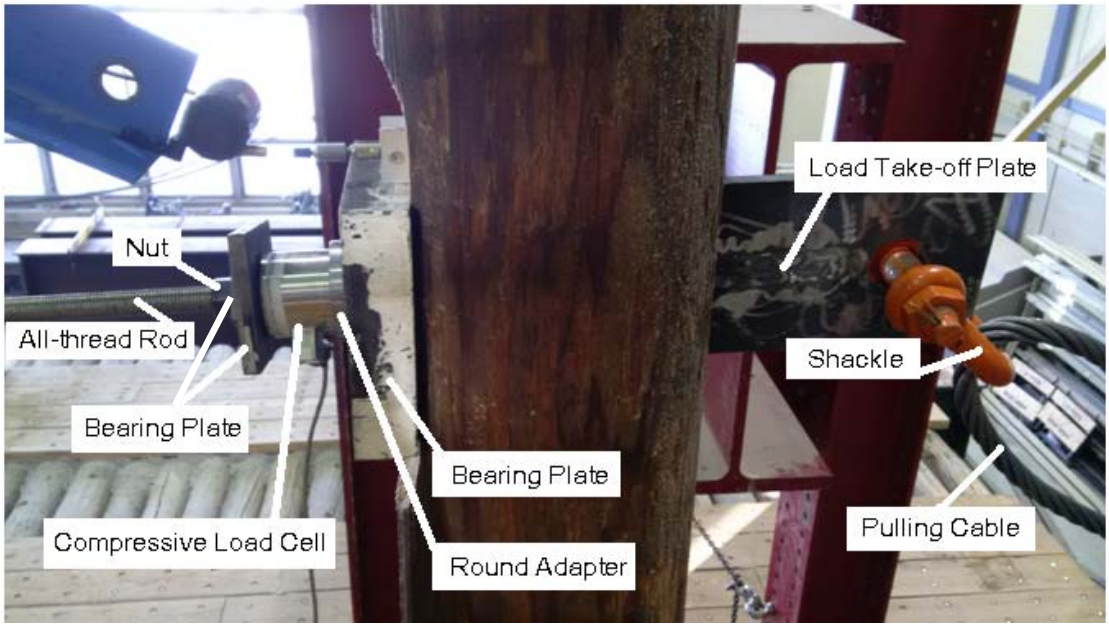

Figure 3.23: Installation of the compressive load cell used to measure applied load

3.11.2 POLE DEFLECTION MONITORING

A lateral deflection profile of the pole under load was monitored by a linear variable displacement transducer (LVDT) mounted to the top of the base mount and two linear measurement transducers (LMTs) mounted on extenders that were fixed to a steel column located behind the pole. The LVDT, with a maximum stroke of 300.00 mm, was suitable to record small displacements such as at the top of the sleeve (see Figure 3.24). The two additional LMTs, each with a stroke of 1,000.00 mm, were used to record the larger anticipated displacements at 3,050 mm (10 feet) and 5,490 mm (18 feet) above the pole butt (see Figures 3.25 and 3.26, respectively).

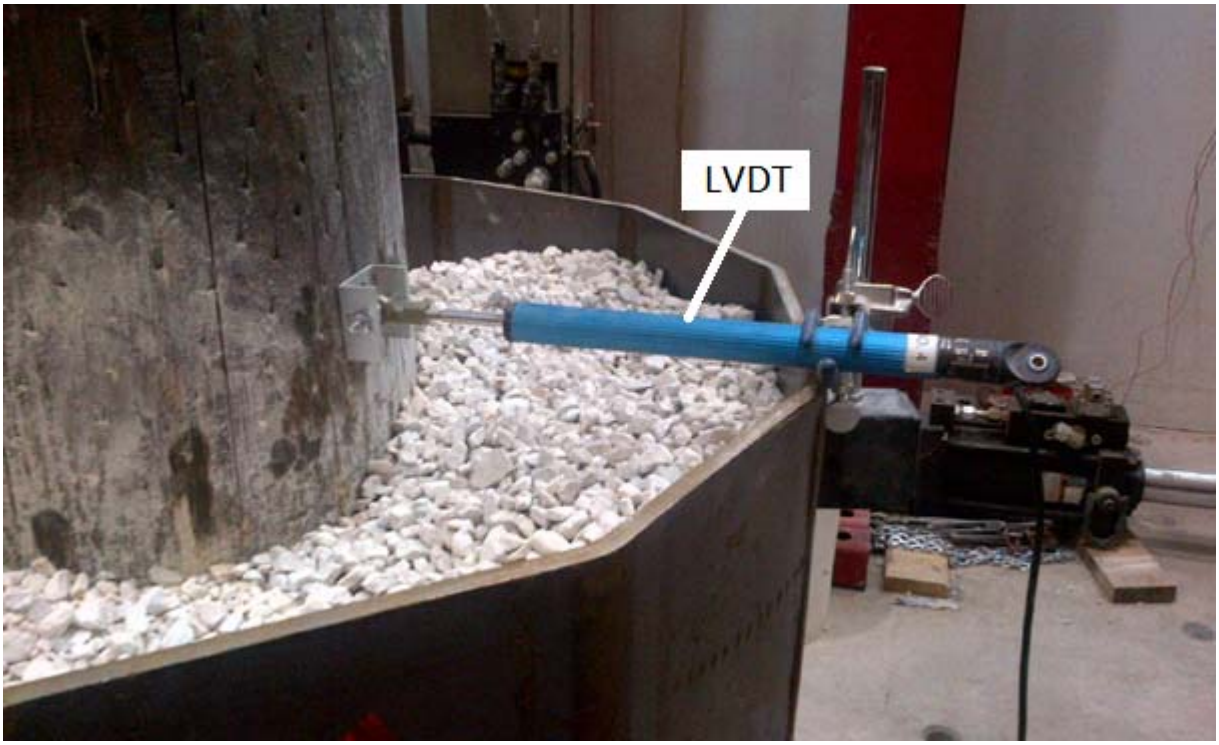

Figure 3.24: LVDT installed at top of sleeve

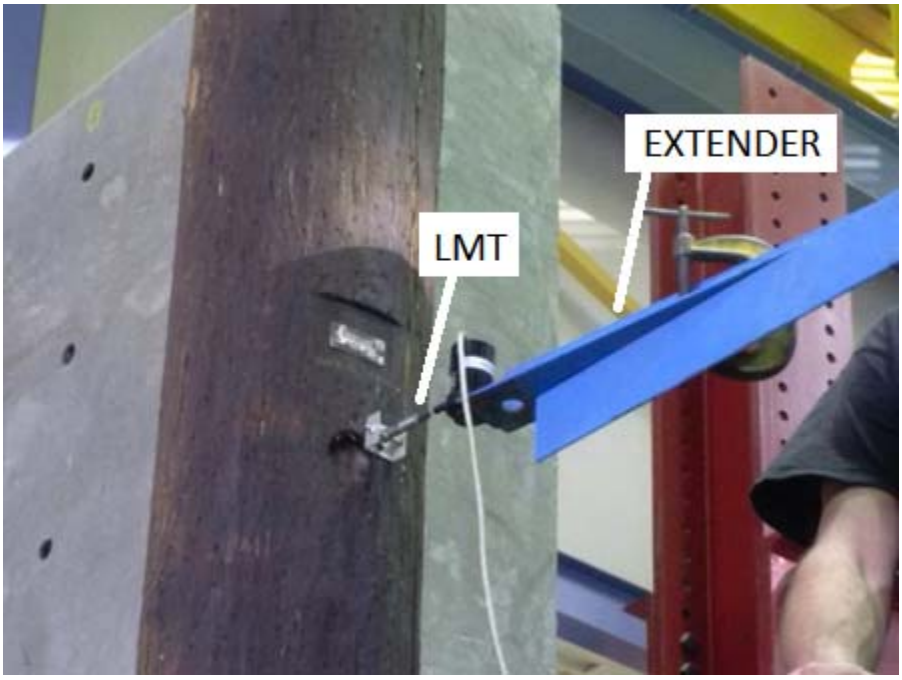

Figure 3.25: LMT installed at 3,050 mm (10 feet) above the pole butt

Figure 3.26: LMT installed at 5,490 mm (18 feet) above the pole butt

3.11.3 STRAIN MONITORING

Strains in the mount sleeve, base plate, and Dywidag threadbars that anchored the mount to the structural laboratory floor were recorded using electronic strain gauges, each with a 6 mm gauge length. As shown in Figure 3.27, a total of 8 strain gauges were positioned at the critical bending sections of the base plate and mount sleeve, as well as on one of the Dywidag threadbars. The critical bending sections of the base plate were established as recommended by The American Society of Civil Engineers' Manual of Practice No. 72 (Design of Steel Transmission Pole Structures) and as detailed in Section 3.5 above. The critical bending sections of the mount sleeve were established as recommended by The Canadian Standards Association's published Standard CAN/CSA S16-14, "Design of Steel Structures" for cantilever beams subjected to a point load at their free end.

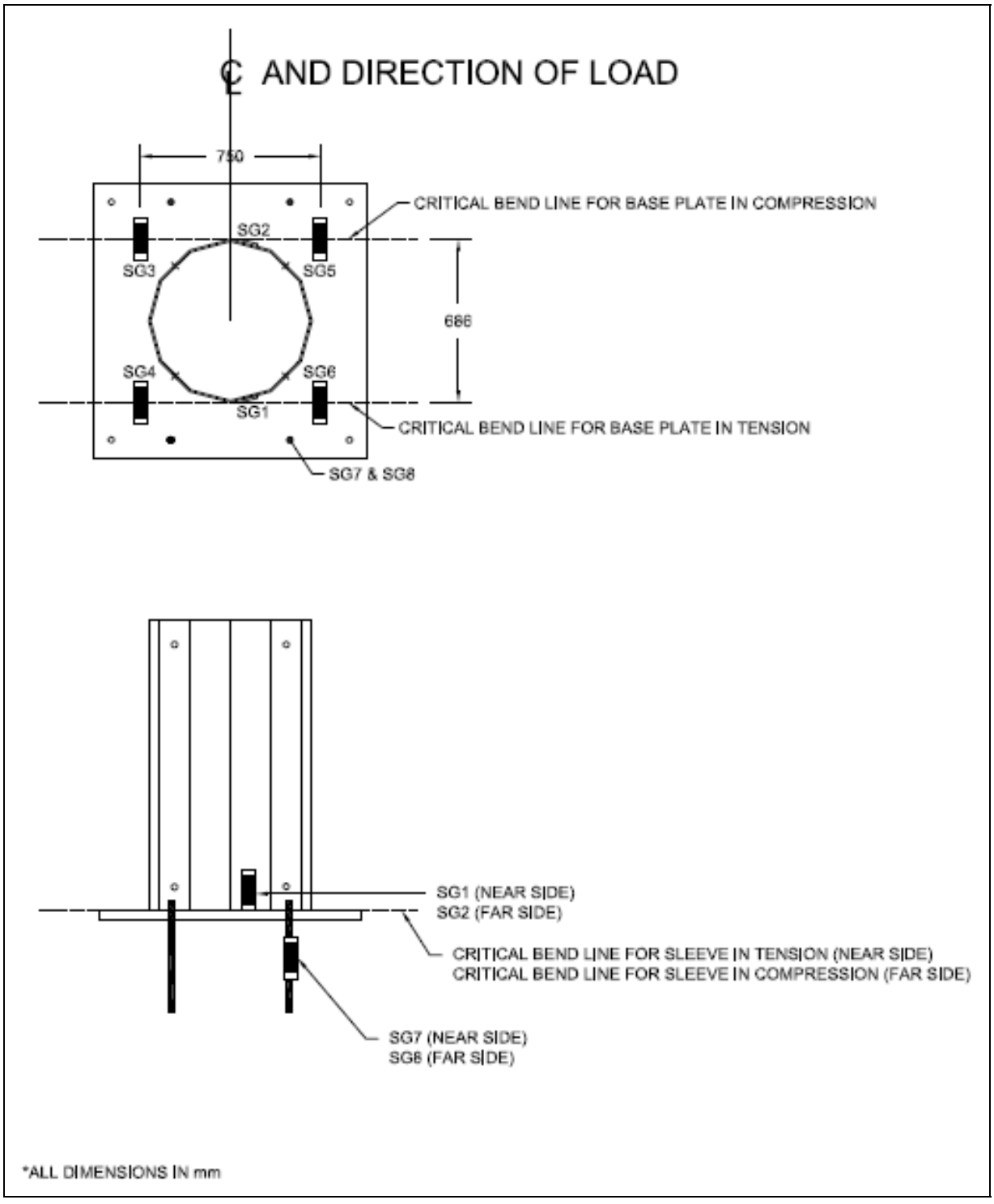

Figure 3.27: Strain gauge and critical bend line locations

3.11.4 DATA ACQUISITION SYSTEM

A data acquisition system (DAQ) was used to acquire and process the signals obtained by the compressive load cell, LVDTs, LMT, and all 8 strain gauges. The DAQ stores this data as converted values in a memory efficient binary format, which can then be exported into comma or tab-delimited format for further manipulation in Microsoft Excel. Approximately 4 readings per second were obtained with the DAQ.

3.12 POLE SPECIMENS

Table 3.3 below lists the test specimens of the experimental program. The circumference of each pole at the top of the sleeve, at the top of the pole, and at a point 1,829 mm (6 feet) from the pole butt were noted to verify conformance to required CAN/CSA 015-05 dimensions, as well as to confirm the actual MOR of each specimen afterward. In total, 8 LP poles were tested.

Table 3.3: Test Specimens

Pole Specimen	Height of Sleeve (mm)	Backfill Material	Circumference at Butt (mm)	Circumference at 1829 mm from butt (mm)	Circumference at Top of Sleeve (mm)
P1*	1,219	Fasteners	1107	960	975
	1,219	Limestone			
P2	1,219	Limestone	1095	1039	1059
P3	914	Limestone	1026	988	1006
P4	914	Limestone	1049	998	1014
P5	914	Sand	1125	1054	1105
P6	914	Sand	1001	947	988
P7	1,219	Sand	1014	940	983
P8	1,219	Sand	1019	998	1003

*Pole specimen P1 was used for 2 tests

As shown in Table 3.3, each of the poles tested had a circumference at 1,829 mm from their butt of at least 940 mm but no more than 1,054 mm, which is within the permissible range of dimensions specified by CAN/CSA 015-05 of 902 to 1,082 mm.

CHAPTER 4 – EXPERIMENTAL RESULTS AND ANALYSIS

4.1 INTRODUCTION

The results of the pole testing conducted are presented and discussed in this chapter. The data is presented in the form of Load versus Deflection graphs, tables and figures. The results for each annulus material are presented separately.

4.2 TESTS WITH MECHANICAL FASTENERS

Although four tests with mechanical fasteners as the annulus material were planned, only one test in a 1,219 mm mount was conducted. The decision not to follow the original test plan was based on the results of this test, which are outlined below. The ultimate load and the deflections at ultimate load are presented in Table 4.1. The load-deflection (610 mm from tip) curve for this test is shown in Figure 4.1.

Table 4.1: Ultimate load and deflections at ultimate load for test with mechanical fasteners

			Deflection at Ultimate Load (mm)		
Pole Specimen	**Sleeve Height (mm)**	**Ultimate Load (kN)**	**At Load Application Point**	**At Pole Mid-Height**	**At Top of Sleeve**
P1	1,219	16.37	586.26	262.88	70.20

As indicated by Table 4.1 and Figure 4.1, this pole test was not able to withstand the required transverse loading of 26 kN for the 1,219 mm sleeve height. The pole was only able to withstand 63% of the required load before one of the upper mechanical fasteners that was in compression failed. The pole visibly appeared to be in good condition after the test.

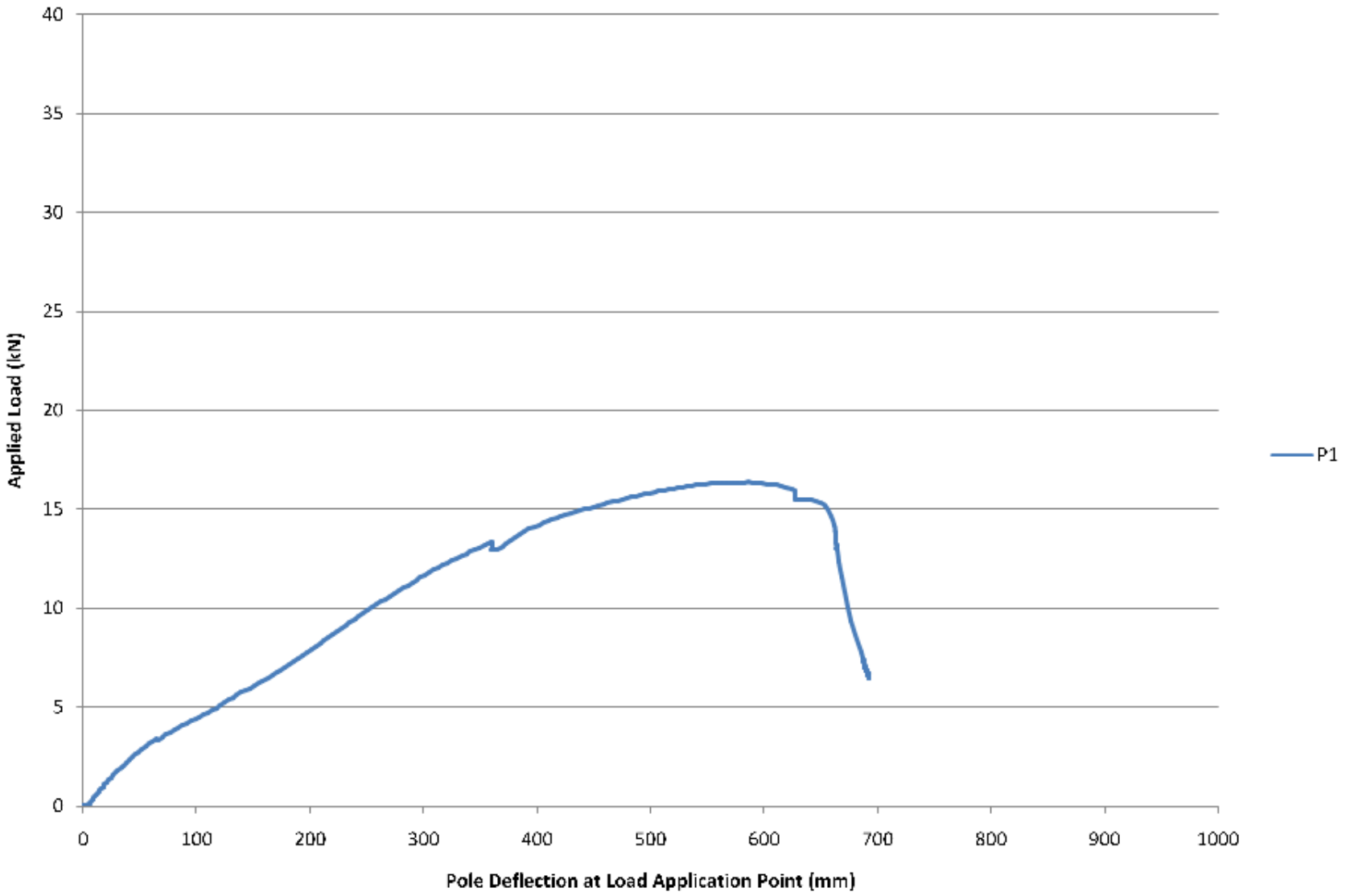

Figure 4.1: Load-deflection (610 mm from tip) curve for mechanical fasteners test

Figure 4.2 below depicts the failure mode of one of the upper mechanical fasteners that was in compression. Although it appeared at first to be a purely compressive failure, the fact that the load take-off plate was off-centre with respect to the longitudinal axis of the pole (as shown in Figure 4.3 below) led to the presumption that the failure was actually due to a combination of compression as well as bending due to translation. It was reasoned that the degree to which the gains bit deeper into the pole varied among the fasteners in compression as the load in each increased, and likely caused the pole to twist. Furthermore, this likely led to an unequal distribution of load among the compressive fasteners, which is why only one of the upper gains in compression failed.

When designing the threaded rod component of the mechanical fasteners, an assumption was made that the fasteners would hold the pole securely in place and could be treated as pin-pin connections with no translation at either end. The resulting bending due to translation, estimated at a minimum of 4.6 kN-m (i.e equally distributed shear component acting on one upper fastener in compression at failure load x cantilever length of fastener), had not been taken into account in the design. The factored moment resistance of each threaded rod, however, is approximately only 0.3 kN-m. Seeing as the mechanical fasteners were able to resist a fairly large applied crane load prior to failure, it is speculated that the bulk of the translation occurred around the same time as the maximum applied load.

Figure 4.2: Failure mode of one of the upper fasteners

Figure 4.3: Twisting of the pole under applied load

Significant local buckling of the sleeve was also observed at the connection to the fastener that failed, as shown in Figure 4.4 below. This was unexpected, as the deflection due to the point loads imparted by the upper mechanical fasteners was estimated at approximately only 1 mm (as detailed in Appendix E). This indicates that Equation 3.17 should not be used to estimate deflection for the mechanical fastener tests.

Figure 4.4: Local buckling of the mount sleeve

After this unsuccessful test, contemplation was spent on how to remedy the premature failure. One solution was to limit pole twisting by adding through bolts. This technique, however, does not guarantee a uniform distribution of forces in the gains due to the anisotropic characteristics of the pole. Furthermore, it also defeats the purpose of utilizing mechanical fasteners based on their portability and simplicity. Therefore, the test plan was revised to abandon the use of mechanical fasteners in this study.

4.3 TESTS WITH CRUSHED LIMESTONE

Four tests with crushed limestone annulus material were conducted – two with 1,219 mm (4 foot) mounts and two with 914 mm (3 foot) mounts. Since no visual damage of the pole from the previous mechanical fastener test was observed, it was re-used for the first test with crushed limestone. The ultimate loads and the deflections at ultimate loads are presented in Table 4.2, while the load-deflection (610 mm from tip) curves for all four tests are shown in Figure 4.5.

Table 4.2: Ultimate loads and deflections at ultimate loads for tests with crushed limestone

			Deflection at Ultimate Load (mm)			
Pole Specimen	**Sleeve Height (mm)**	**Ultimate Load (kN)**	**At Load Application Point**	**At Pole Mid-Height**	**At Top of Sleeve**	**MOR (MPa)**
P1*	1,219	24.82	395.98	142.14	14.89	36.09
P2	1,219	35.46	537.51	195.98	28.55	40.24
P3	914	29.95	466.87	190.02	28.38	42.48
P4	914	27.86	754.89	329.44	60.56	38.59

*Pole Specimen P1 re-used from mechanical fasteners test

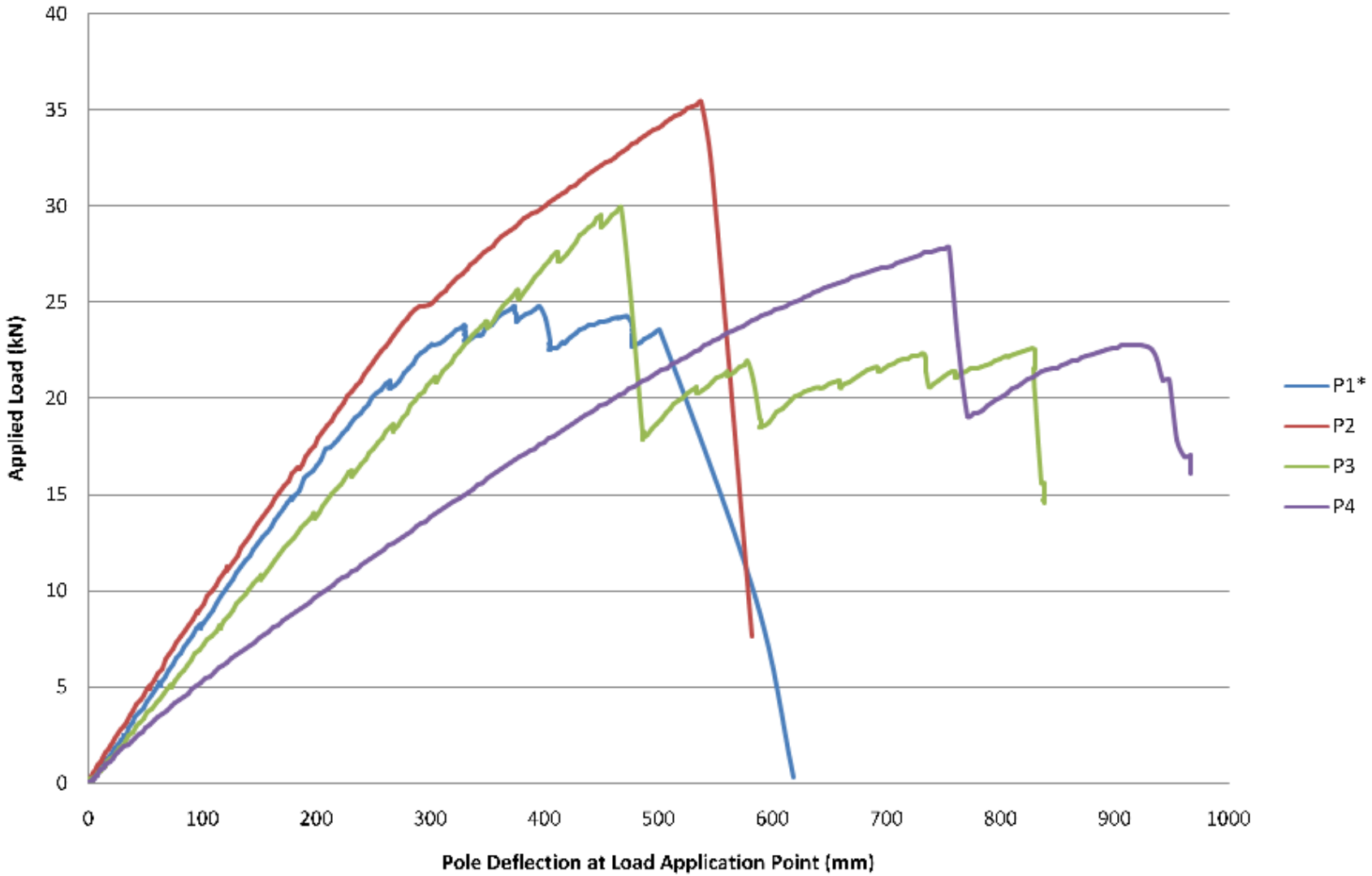

Figure 4.5: Ultimate load-deflection (610 mm from tip) curve for tests with crushed limestone

As indicated by Table 4.2 and Figure 4.5, three of the four pole tests were able to withstand the required transverse loadings of 26 kN and 24.25 kN for 1,219 mm and 914 mm mounts, respectively. The low ultimate load for test P1* (1,219 mm Limestone Test 1) was presumably due to the fact that the pole had been damaged in compression in the previous test (as explained in Appendix G). The results also indicate that the shorter 914 mm (3 foot) sleeve height leads to increased pole deflection values at lower ultimate loads.

Table 4.2 also reveals that the Lodgepole Pine poles tested did not achieve the MOR of 45.5 MPa specified by CAN/CSA-015/05 and ANSI 05.1.2008 for Lodgepole Pine poles. This is likely due to the fact that each pole tested had a circumference at 1,829 mm from the pole butt that was larger than the corresponding minimum value specified by CAN/CSA-015/05 and ANSI 05.1.2008, and that a modified pole was tested to satisfy laboratory constraints (i.e. the bottom halves of 12.2 m long poles were tested).

Each of the pole specimens failed visibly in tension at or near the top of the sleeve, as illustrated in Figure 4.6 below. It is noted, however, that the tensile strength of wood parallel to the grain is much greater than its corresponding compressive strength. Therefore, the poles would have failed in compression before the tension failures were observed, even though this failure mechanism was not visibly apparent. As the wood fibres on the compression side failed, the neutral axis would have shifted toward and redistributed the increasing load to the tension (convex) side of the pole until the load exceeded the pole's tensile strength. With this in mind, the pole used in the mechanical fasteners test likely *had* failed already, leading to a low ultimate load in the first crushed limestone test in which it was re-used.

Figure 4.6: Visible tension failure for tests with crushed limestone (Pole Speciman P1*)

In order to determine compacted crushed limestone's effectiveness in satisfying the serviceability limits recommended in Section 2.5, pole deflections within the limit of everyday tensions identified by Lu (2012) for 69kV distribution lines are presented in Figure 4.7 below. As indicated by the plotted results, all four tests with compacted crushed limestone were able to satisfy the 2% deflection limit proposed by Lu (2012) under the largest everyday conductor tension (6,139 N) presented in Table 2.5.

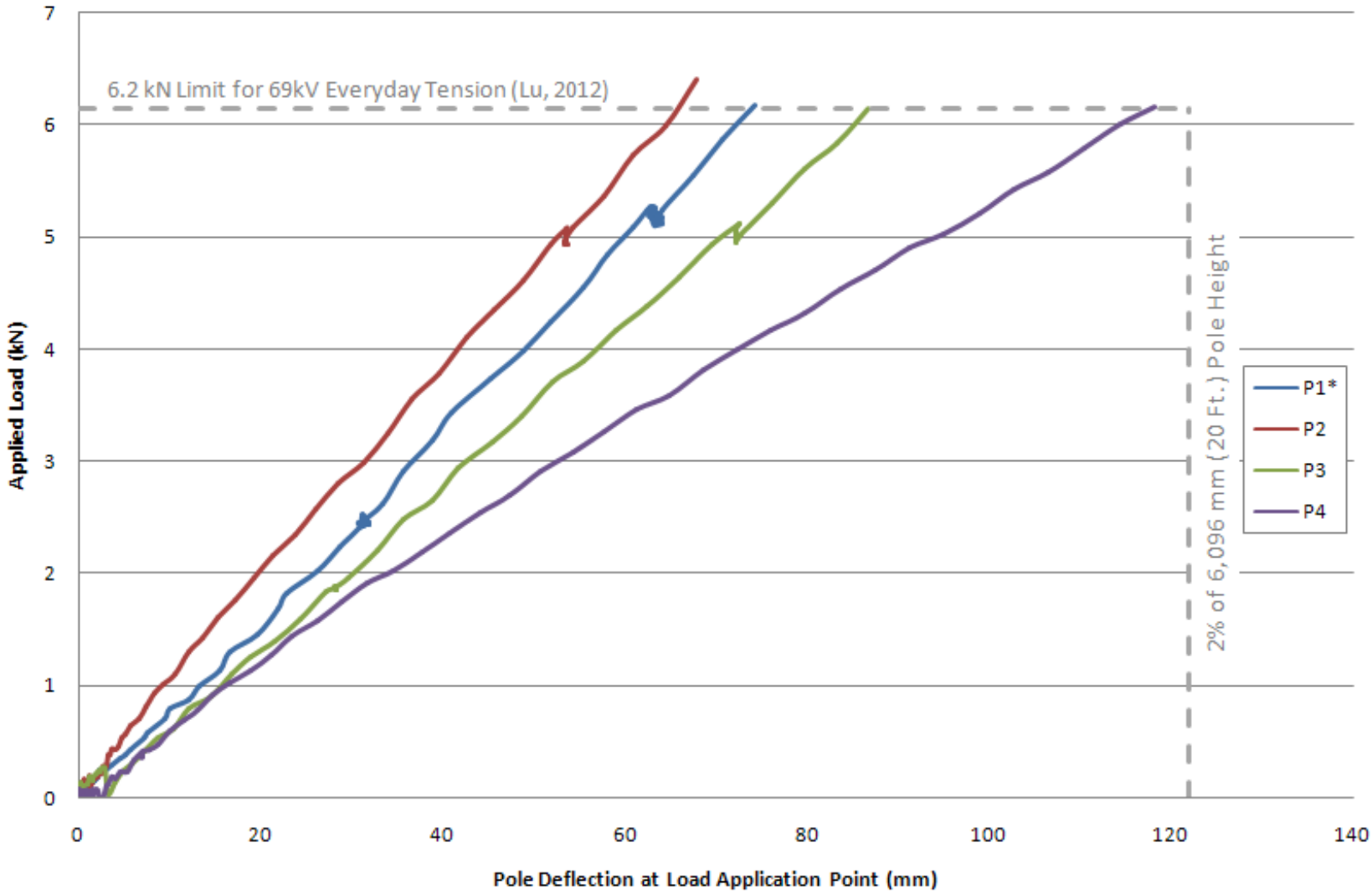

Figure 4.7: Load-deflection (610 mm from tip) curve within limit of everyday conductor tensions for tests with crushed limestone

The strains recorded by each of the 8 strain gauges at ultimate load are presented below in Table 4.3. As indicated by the results, the strains experienced in the sleeve and baseplate in each of the four pole tests with crushed limestone were below the elastic yield strain limit of 1750με for 350W steel (where the elastic yield strain is taken to be the yield stress of 350W steel divided by the modulus of elasticity of steel, or $\varepsilon_y = \frac{F_y}{E} = \frac{350\ MPa}{200{,}000\ MPa}$). The strains recorded in the Dywidag threadbar were also much less than the elastic yield strain limit of 2585με for 517 MPa (75 ksi) steel (again, where $\varepsilon_y = \frac{F_y}{E} = \frac{517\ MPa}{200{,}000\ MPa}$). The largest strains were recorded in the sleeve.

Table 4.3: Strains in the base mount at ultimate load for tests with crushed limestone

		Strain at Ultimate Load (με or 10^{-6}ε)							
		Sleeve		**Base Plate**				**Threadbar**	
Pole Specimen	**Sleeve Height (mm)**	**SG1**	**SG2**	**SG3**	**SG4**	**SG5**	**SG6**	**SG7**	**SG8**
P1*	1,219	830.25	-788.48	-212.89	258.41	-266.27	243.71	654.02	45.69
P2	1,219	1298.02	-1355.91	-360.50	410.09	-411.58	413.58	841.25	200.04
P3	914	424.38	-1454.20	-375.55	451.66	-362.95	438.95	642.68	372.80
P4	914	-21.86	-1382.59	-272.66	414.30	-270.22	407.09	566.54	244.05

4.4 TESTS WITH SAND

Four tests with sand annulus material were conducted – two with 1,219 mm (4 foot) mounts and two with 914 mm (3 foot) mounts. The ultimate loads and the deflections at ultimate loads are presented in Table 4.4, while the load-deflection curves (610 mm from tip) for all four tests are shown in Figure 4.8.

Table 4.4: Ultimate loads and deflections at ultimate loads for tests with sand

			Deflection at Ultimate Load (mm)			
Pole Specimen	**Sleeve Height (mm)**	**Ultimate Load (kN)**	**At Load Application Point**	**At Pole Mid-Height**	**At Top of Sleeve**	**MOR (MPa)**
P5	914	28.12	645.75	279.46	43.05	30.09
P6	914	24.90	525.03	223.00	33.81	37.28
P7	1,219	31.03	463.16	174.31	33.41	44.03
P8	1,219	28.32	546.37	174.22	9.90	37.83

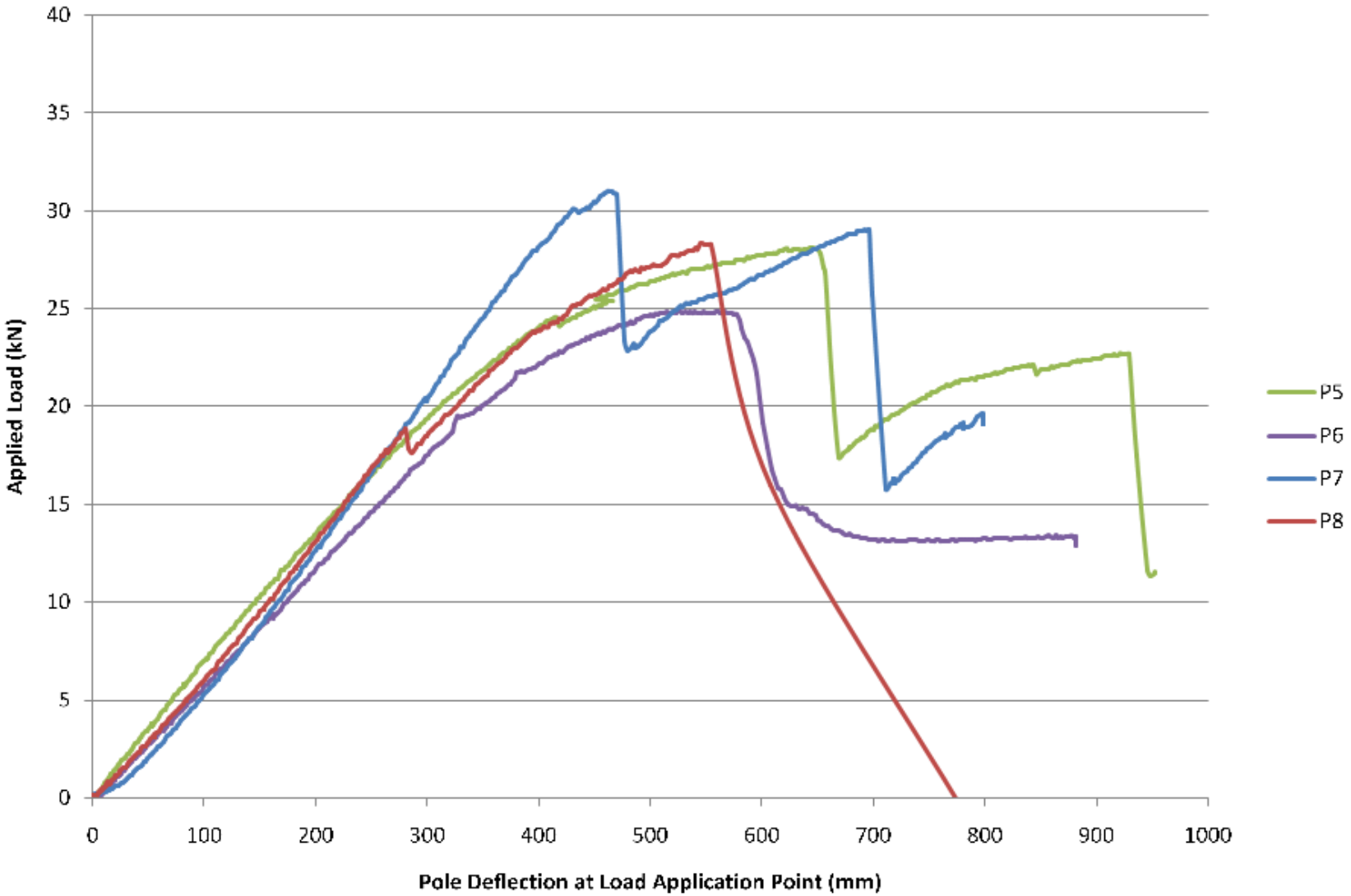

Figure 4.8: Ultimate load-deflection (610 mm from tip) curve for sand tests

As indicated by Table 4.4 and Figure 4.8 above, all four pole tests were able to withstand the required transverse loadings of 26 kN and 24.25 kN for 1,219 mm and 914 mm mounts, respectively. The results also indicate that the shorter 914 mm (3 foot) sleeve height leads to increased pole deflection values at lower ultimate loads.

Table 4.4 also reveals that the Lodgepole Pine poles tested did not achieve the MOR of 45.5 MPa specified by CAN/CSA 015-05 and ANSI 05.1.2008 for Lodgepole Pine poles. Again, this is likely due to the fact that each pole tested had a circumference at 1,829 mm from the pole butt that was larger than the corresponding minimum value specified by CAN/CSA-015/05 and ANSI 05.1.2008, and that a modified pole was tested to satisfy laboratory constraints (i.e. the bottom halves of 12.2 m long poles were tested).

Similar to the crushed limestone tests, each of the pole specimens tested with sand failed visibly in tension at or near the top of the sleeve, as shown in Figure 4.9 below. Again, as the tensile strength of wood parallel to the grain is much greater than its corresponding compressive strength, it is reasonable to assume that the poles actually failed in crushing on the compression side before the tension failures were observed (even though this failure mechanism was not visibly apparent).

Figure 4.9: Visible tension failure for tests with sand (Pole Specimen P5)

In order to determine compacted sand's effectiveness in satisfying the serviceability limits recommended in Section 2.5, pole deflections within the limit of everyday tensions identified by Lu (2012) for 69kV distribution lines are presented in Figure 4.10 below. As indicated by the plotted results, all four tests with compacted sand were able to satisfy the 2% deflection limit proposed under the largest everyday conductor tension (6,139 N) presented in Table 2.5. Comparison of Figure 4.7 with Figure 4.10, however, reveals that pole tip deflections with compacted sand were approximately 19% larger than those with compacted crushed limestone within the limit of everyday tensions for 69kV distribution lines.

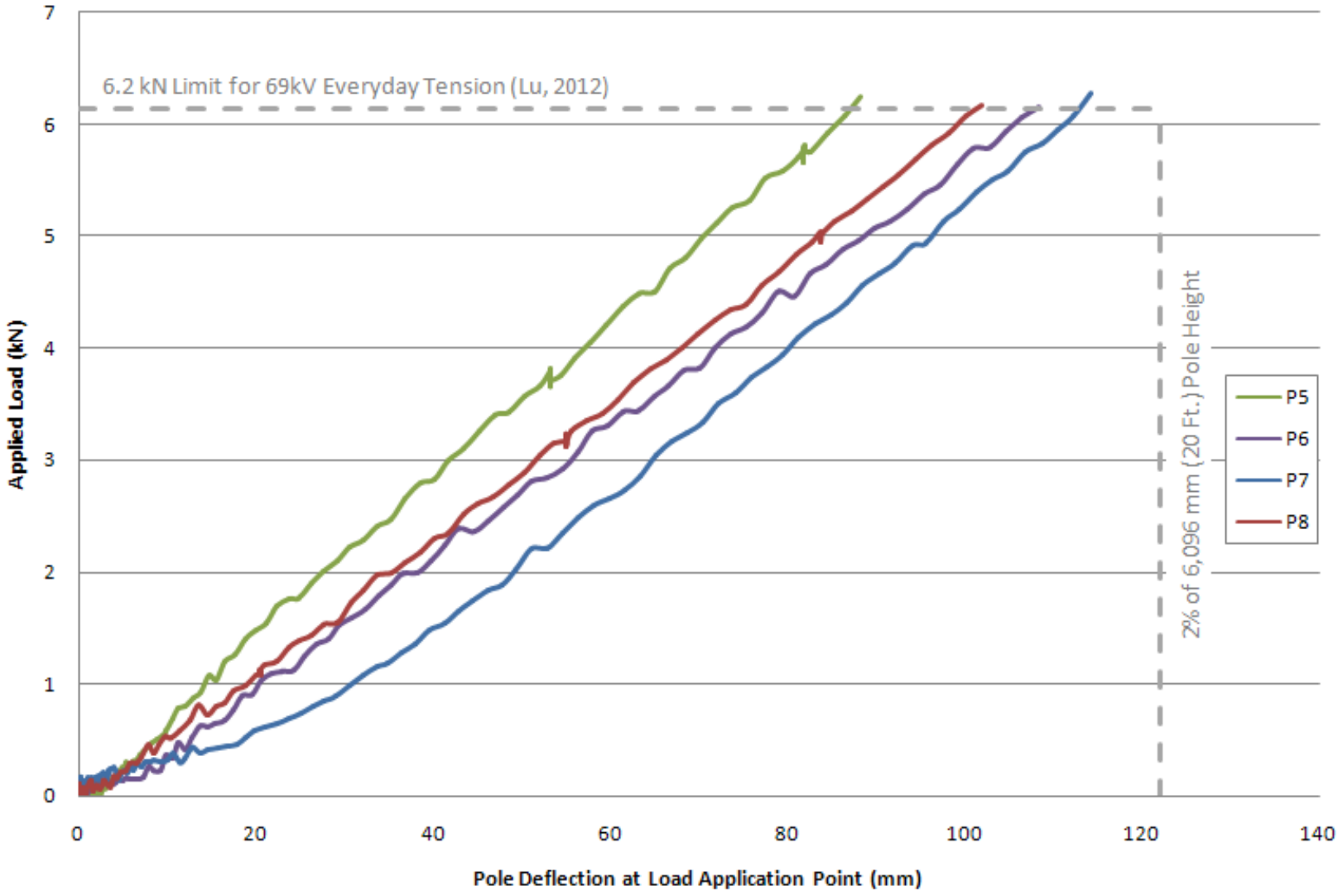

Figure 4.10: Load-deflection (610 mm from tip) curve within limit of everyday conductor tensions for tests with sand

The strains recorded by each of the 8 strain gauges at ultimate load are presented below in Table 4.5. As indicated by the results, the strains experienced in all four pole tests with sand were below the elastic yield strain limit of 1750με for 350W steel (where the elastic yield strain is taken to be the yield stress of 350W steel divided by the modulus of elasticity of steel, or $\varepsilon_y = \frac{F_y}{E} = \frac{350\ MPa}{200,000\ MPa}$). The strains recorded in the Dywidag threadbar were also much less than the elastic yield strain limit of 2585με for 517 MPa (75 ksi) steel (again, where $\varepsilon_y = \frac{F_y}{E} = \frac{517\ MPa}{200,000\ MPa}$). The largest strains were recorded in the sleeve.

Table 4.5: Strains in the base mount at ultimate load for tests with sand

		Strain at Ultimate Load (με or 10^{-6}ε)							
		Sleeve		**Base Plate**				**Threadbar**	
Pole Specimen	**Sleeve Height (mm)**	**SG1**	**SG2**	**SG3**	**SG4**	**SG5**	**SG6**	**SG7**	**SG8**
P7	1,219	518.55	-1286.88	-297.72	341.39	-333.33	223.20	722.26	189.87
P8	1,219	800.40	-885.52	-242.20	255.51	-274.44	326.08	644.30	77.577
P5	914	218.67	-1255.84	-303.67	389.68	-308.57	376.65	836.87	33.86
P6	914	60.83	-1121.71	-233.22	338.46	-252.19	281.69	695.27	-63.33

CHAPTER 5 – NUMERICAL MODELLING

5.1 ANALYTICAL MODEL

The software module Moment Foundation Analysis and Design (MFAD), part of the commercially available software package FAD Tools (2014), aids in the design of foundations for single pole structures subject to high overturning moments. MFAD uses a multi-spring, nonlinear subgrade modulus approach to predict the load-deflection response and ultimate capacity of direct embedment foundations placed in multi-layered soil subsurface profiles with either uniform or multi-layered annulus backfills. In this study, MFAD was used not only to predict the minimum sleeve height that would permit the 6.1 m long bottom half of a 12.2 m long Class 4 LP pole to develop the full moment capacity of Manitoba Hydro's typical 12.2 m (40-foot) long distribution poles, but also to serve as a comparison to the results obtained from full-scale load testing.

The software program MFAD characterizes soil-foundation interaction through the use of four discrete sets of springs: lateral springs characterize the lateral force-displacement response of both the in-situ soil and the annulus material; vertical side shear moment springs characterize the vertical shear stress-vertical displacement response, again, of both the in-situ soil and the annulus material around the shaft perimeter; a base shear spring characterizes the horizontal shearing force-base displacement response, and a base moment spring characterizes the shaft normal base force-rotation response (Rojas-Gonzales et al., 1991). The lateral springs are modeled as finite element beams, while all other spring types are modelled as elastic-perfectly plastic springs. These four sets of springs, as shown in Figure 5.1 below, take into account all the forces acting around the shaft.

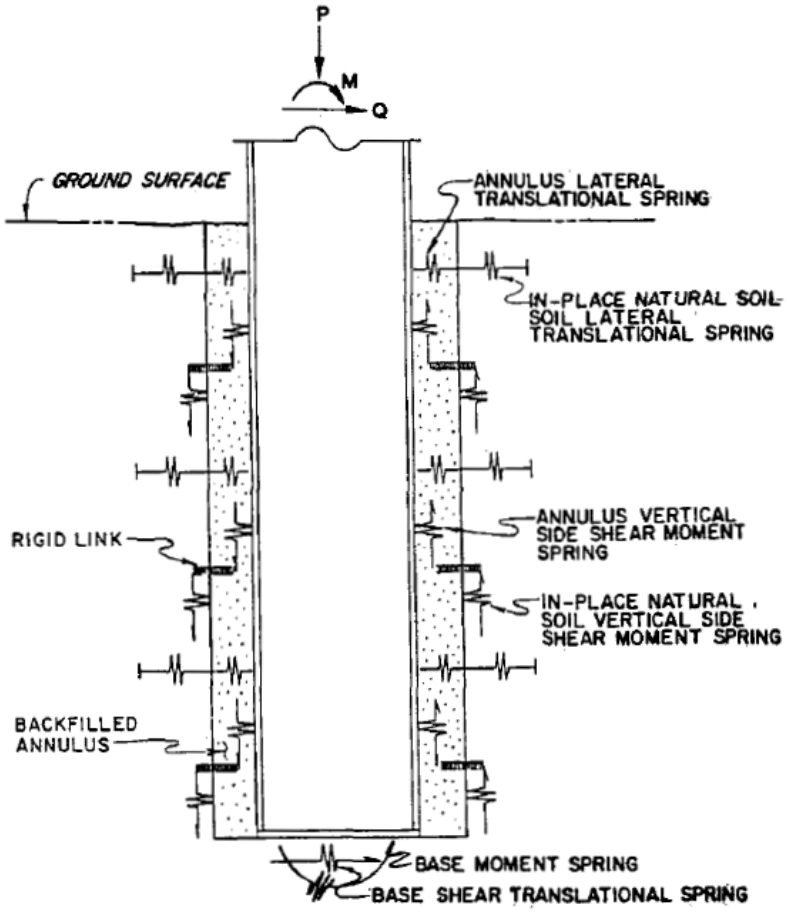

Figure 5.1: Direct embedment foundation model used by MFAD (Rojas-Gonzales et al., 1991)

In MFAD analyses conducted for this study, the strength and deformation properties assumed for a crushed limestone annulus material were adopted from research conducted by DiGioia et al. (1998). A slightly larger angle of friction (and therefore a larger value of undrained shear strength) was assumed, however, because the compaction of the crushed limestone was done in a controlled laboratory environment, versus in the field. The assumed annulus material properties are presented in Table 5.1 below. It should be noted that predictions for minimum sleeve height were made in MFAD considering a crushed limestone annulus material only, as published results of full-scale testing conducted with a compacted sand annulus material (for which to validate the model against) could not be found.

Table 5.1: Assumed properties of crushed limestone annulus material for laboratory testing

Unit Weight (N/m^3)	**Deformation Modulus (MPa)**	**Undrained Shear Strength (kPa)**	**Internal Angle of Friction (deg)**
204.1	41.4	114.9	50

Since MFAD does not accommodate a "steel" in-situ geotechnical material, a directly embedded foundation in rock was modelled. Assuming that the deformation modulus of the crushed limestone annulus material is less than the corresponding modulus of the steel sleeve, modeling the foundation as directly-embedded in rock should produce results for ultimate load that are analogous to those obtained in the laboratory (i.e. the deformation modulus of crushed limestone is presumably much less than in-situ rock as well). Modeling the foundation as directly-embedded in rock should also produce results for groundline pole deflection that are analogous to those obtained in the laboratory. Although it is possible that (unlike in-situ rock) the steel sleeve itself may deflect, any deflection of the sleeve would not contribute to net pole deflection due to the placement of the LVDT on the sleeve (versus another fixed point).

The results of the analyses conducted for 1,219 mm, 914 mm, and 610 mm sleeve heights, as predicted by MFAD, are presented in Table 5.2 below. As shown from the results, MFAD predicted that the 6.1 m long bottom half of a 12.2 m long Class 4, LP pole supported in either a 914 mm (3 foot) or 1,219 mm (4 foot) tall sleeve with crushed limestone as an annulus material would be capable of developing the full moment capacity of Manitoba Hydro's typical 12.2 m (40-foot) long Class 4, LP distribution poles. Since MFAD predicted that a 610 mm (2 foot) sleeve would not be capable of withstanding the required load, the decision was made not to test this sleeve height.

Table 5.2: Analyses conducted for various sleeve heights with crushed limestone annulus material

Sleeve Height (mm)	**Pole Species**	**Annulus Material**	**MFAD Horizontal Failure Load Applied at 610 mm From Tip (kN)**	**Failure Load Required by CAN/CSA-015 (N)**	**MFAD Ground-line Moment at Failure (kN-m)**	**Ground-line Moment Required by CAN/CSA-015 (kN-m)**	**MFAD Deflection at Top of Sleeve (mm)**
1,219	Lodgepole Pine	Crushed limestone	55.51	26.00	236.86	92.25	3.05
914	Lodgepole Pine	Crushed limestone	28.56	24.25	130.51	98.84	7.37
610	Lodgepole Pine	Crushed limestone	11.34	22.75	65.15	105.43	N/A*

*MFAD is not able to determine a value of deflection because the pole has failed; this is a limitation of the program.

The results predicted by MFAD are compared to those obtained from full-scale testing with a crushed limestone annulus material in Table 5.3 below. As shown, MFAD overestimated the average ultimate load for the 1,219 mm (4 foot) mount by approximately 84% and underestimated the corresponding average deflection at the top of sleeve by approximately 86%. Had test P1* not reused the pole from the mechanical fasteners test, however, the results for ultimate load would likely have been a lot closer. For the 914 mm (3 foot) mount, MFAD underestimated the average ultimate load by less than 1%, but underestimated the corresponding average deflection at the top of sleeve by approximately 83%.

Table 5.3: Comparison of results from MFAD and full-scale testing with crushed limestone

Sleeve Height (mm)	Annulus Material	Ultimate Load (kN)		Deflection at Top of Sleeve (mm)	
		MFAD	Full-Scale Testing	MFAD	Full-Scale Testing
1,219	Crushed Limestone	55.51	30.14	3.05	21.72
914	Crushed Limestone	28.56	28.91	7.37	44.47

As indicated earlier, the conceptual design for optimum sleeve height using MFAD was based on assumed strength and material properties of the compacted annulus material. Since 100% compaction of any material in a confined space is generally unattainable, it is reasonable to expect increased values of deflection at the top of the sleeve under laboratory conditions compared to the predicted values from MFAD.

CHAPTER 6 – CONCLUSIONS AND RECOMMENDATIONS

6.1 CONCLUSIONS

In this study, the ability of two variations (with respect to sleeve height) of a prefabricated fixed-end base mount connection detail to develop the full moment capacity of a 12.2 m (40–foot) long, Class 4 Lodgepole Pine wood pole under different annulus backfill conditions was evaluated. One test (with a 1,219 mm sleeve) was conducted with mechanical fasteners, and four tests (two with a 1,219 mm sleeve and two with a 914 mm sleeve) were conducted with both crushed limestone and sand. Based on the results of the testing, the following conclusions were made:

1. The poles tested with compacted crushed limestone had an average ultimate capacity of 30.14 kN and 28.91 kN with the 1,219 mm (4 foot) mount and 914 m (3 foot) mount, respectively. These exceeded the required transverse loadings of 26 kN and 24.25 kN for the 1,219 mm and 914 mm mounts, respectively.

2. The poles tested with compacted sand had an average ultimate capacity of 29.68 kN and 26.51 kN with the 1,219 mm (4 foot) mount and 914 mm (3 foot) mount, respectively. Again, these exceeded the required transverse loadings of 26 kN and 24.25 kN for 1,219 mm and 914 mm mounts, respectively.

3. The pole tested with mechanical fasteners in the 1,219 mm (4 foot) mount did not reach failure. At an applied load of only 16.37 kN, one of the upper fasteners failed due to a combination of

compression as well as bending due to translation. The pole gains used in this test did not provide adequate pole fixity at the base, and rather seemed to encourage pole twisting.

4. For pole tests with compacted crushed limestone, the shorter 914 mm (3 foot) sleeve height led to increased ultimate pole deflections (at 610 mm from the pole tip) that were approximately 31% larger than those obtained with the 1,219 mm (4 foot) sleeve. For pole tests with compacted sand, the shorter 914 mm (3 foot) sleeve height led to increased ultimate pole deflections (at 610 mm from the pole tip) that were approximately 16% larger than those obtained with the 1,219 mm (4 foot) sleeve.

5. All tests conducted with either compacted crushed limestone or sand were able to satisfy the 2% deflection limit proposed by Lu (2012) for 69kV distribution lines subject to typical everyday tensions. Pole tip deflections with compacted sand, however, were approximately 19% larger than those obtained with compacted crushed limestone within this range of applied load.

6. All poles tested with compacted crushed limestone and sand failed visibly in tension at or near the top of the sleeve. It is acknowledged that the poles likely failed in crushing on the compression side before the tension failures were observed, however, even though this failure mechanism was not visibly apparent.

7. The mount strains experienced in tests with crushed limestone and sand were all below the elastic yield strain limit of 1750με for 350W steel. The strains recorded in the Dywidag threadbar in tests with crushed limestone and sand were also all much less than the elastic yield

strain limit of 2522με for 517 MPa (75 ksi) steel. Given that the strains in both the mount and threadbar remained in their respective elastic ranges for all tests conducted, it can be concluded that both performed satisfactorily.

8. Based on the above conclusions, a 914 mm (3 foot) sleeve height with compacted crushed limestone annulus backfill material can be recommended for field use.

9. In comparing the results obtained from laboratory testing for poles tested with compacted crushed limestone, it was found that MFAD overestimated the average ultimate load for the 1,219 mm (4 foot) mount by approximately 84% and underestimated the corresponding average deflection at the top of sleeve by approximately 86%. It is acknowledged that the low average ultimate load observed in the laboratory was likely the result of using a damaged pole in test P1*. For the 914 mm (3 foot) mount, MFAD underestimated the average ultimate load by less than 1%, but underestimated the corresponding average deflection at the top of sleeve by approximately 83%. It is acknowledged that the results predicted by MFAD were based on assumed material and strength properties for compacted crushed limestone. Since 100% compaction of any material in a confined space is generally unattainable, it is reasonable to expect increased values of deflection at the top of the sleeve under laboratory conditions compared to the predicted values from MFAD.

6.2 RECOMMENDATIONS FOR FUTURE WORK

In order to fully develop the prefabricated fixed-end base mount connection detail, further research is recommended in the following areas:

Tests with Mechanical Fasteners

1. Additional full-scale testing with mechanical fasteners that are strong enough to resist the applied bending loads that result as the pole twists and a sleeve thickness that is adequate to resist laterally applied concentrated loads from the fasteners in compression shall be performed.

2. Methods that prevent the pole from twisting shall be developed. If the pole is restrained from twisting, it may not be necessary to design the fasteners to resist bending.

Tests with Crushed Limestone and Sand

3. Additional full-scale testing, for both crushed limestone and sand, with more test specimens shall be performed. The ultimate loads and corresponding pole deflections at ultimate load varied considerably between the two tests conducted for each sleeve height. By conducting sufficiently more tests, less variation between the ultimate load and deflection results is expected.

4. Further parametric studies on the design of the mount, particularly with respect to the base plate plan size and thickness, shall be performed to optimize weight.

REFERENCES

American Association of State Highway and Transportation Officials [AASHTO] (2013). *Standard Specifications for Structural Supports for Highway Signs, Luminaires, and Traffic Signals*. Washington, DC: AASHTO. ISBN: 978-1-56051-540-1.

American National Standards Institute [ANSI] (2008). ANSI 05.1.2008. *Wood Poles - Specifications and Dimensions*. Birmingham, AL: American Wood Protection Association.

American Society for Civil Engineers [ASCE] (2006). *ASCE Manuals and Reports on Engineering Practice No. 72. Design of Steel Transmission Pole Structures*. Reston VA: American Society of Civil Engineers.

American Society for Civil Engineers [ASCE] (2008). *ASCE Manuals and Reports on Engineering Practice No. 113. Substation Structure Design Guide*. Reston, VA: American Society of Civil Engineers.

American Society for Testing and Materials [ASTM] (2012). ASTM D1036. *Standard Test Methods of Static Tests of Wooden Poles*. Developed by ASTM Subcommittee D07.04, 2012.

America West Drilling Supply (2012). *Utility Power Pole Drill.* Web. 25 September 2012. http://www.americawestdrillingsupply.com/UtilityPowerPoleDrill.asp

Canadian Institute of Steel Construction (2014). CAN/CSA S16-14. *Design of Steel Structures*. Toronto, ON: Canadian Institute of Steel Construction.

Canadian Standards Association [CSA] (2010). CAN/CSA-C22.3 No. 1-10. *Overhead Systems.* Mississauga, ON: CSA.

Canadian Standards Association [CSA] (2005). CAN/CSA 015-05. *Wood Utility Poles and Reinforcing Stubs*. Mississauga, ON: CSA.

Caswell, R.W., and Andrews, F.E. (1954). *Foundation Stability of Wood-Pole H-Frame Structures for Transmission Lines*. Power Apparatus and Systems, Part III, Transactions of the American Institute of Electrical Engineers, Volume 73, pp. 245-255.

Carvill, J. (1993). *Mechanical Engineer's Data Handbook*. Oxford, UK: Butterworth-Heinemann Ltd.

DiGioia, A., Hirany, A., Newman, F. B., and Rose, A. T. (1998). *Granular Backfill Selection for Direct Embedded Poles*. ESMO '98. Proceedings of the IEEE 8th International Conference on Transmission & Distribution Construction, Operation and Live-Line Maintenance, Orlando, 26-30 April 1998, pp. 56-61.

FAD Tools Version 5.1.17 (2014). Moment Foundation Analysis and Design (MFAD). Electric Power Research Institute, Palo Alto, CA.

Gajan, S. and McNames, C. (2010). *Improved Design of Embedment Depths for Transmission Pole Foundations Subject to Lateral Loading*. ASCE Practice Periodical on Structural Design and Construction, Vol. 15, pp. 73-81.

Hoek, E. and Brown, E. T. (1997). *Practical Estimates of Rock Mass Strength*. International Journal of Rock Mechanics and Mining Sciences, Volume 34, No. 8, pp. 1165-1186.

Horn, D. (2004). *Design of Monopole Bases*. Technical Manual 1.

Institute of Electrical and Electronics Engineers, Inc. [IEEE] (1991). IEEE Std. 751. *IEEE Trial-Use Design Guide for Wood Transmission Structures*. New York, NY: IEEE. ISBN 166937463-7.

Kell, J. (2001). *Repair of Wooden Utility Poles Using Fibre-Reinforced Polymers* (M.Sc Thesis, Department of Civil Engineering). University of Manitoba, Winnipeg, MB.

Keshavarzian, M. (2002). *Self-supported Wood Pole Fixity at ANSI Groundline*. ASCE Practice Periodical on Structural Design and Construction, Vol. 7, pp. 147-155.

Lu, M. (2012). *On the Deflection Limit for Wood Pole Design*. CIGRÉ Canada Conference, Montreal, QC, 24-26 September.

Manitoba Hydro (1994). *Power Pole Rock Sets*. Safe Practice Guide, Corporate Safety & Health Division, Winnipeg, MB.

Manitoba Hydro (2011). *Installation of Rock Set Pole Anchors*. Standard Drawing, Distribution Standards Department, Winnipeg, MB.

Mortensen, A. (2007). *Concise Encyclopedia of Composite Materials.* Oxford, UK: Elsevier Ltd.

Northwest Signal (2011). *NWS Structural Overview*. Web. 16 November 2014. http://www.nwsignal.com/nws_pdf/NWS_Structural%20Div.pdf

On Target Utility Services (2012). *Utility Pole Setting.* Web. 25 September 2012. http://www.ontargetservices.com/utility-construction/utility-pole-setting/

Pansini, A.J. (2004). *Power Transmission and Distribution*. Lilburn, GA: The Fairmont Press, Inc.

Rojas-Gonzalez, L. F., DiGioia, A. M., and Longo, V. J. (1991). *A New Design Approach for Direct Embedment Foundations*. IEEE Transactions on Power Delivery, Vol. 6, No. 3, pp. 1336-1342.

Rural Utilities Service [RUS] (1999). *Electric Transmission Specifications and Drawings, 34.5 kV Through 69 kV*. Bulletin 1728F-810. Washington, DC: U.S. Department of Agriculture.

Sky Cast Canada (2013). *Installation: Simple Direct Embedment.* Web. 22 September 2013. http://www.flyingcamel.com/clients/skycast/installation_direct_embedment.html

Storie, R. (1980). *"Full-Scale Load Tests of Rock Anchors for Wood Poles".* Technical Report, Manitoba Hydro, Winnipeg, MB.

Tri-Steel Fabricators Ltd. (1980). *Tri-Anchor Line Pole Rock Anchor*. Product Brochure. Montreal, QC: Tri-Steel Fabricators Ltd.

Tri-Steel Fabricators Ltd. (2011). *Tri-Anchor Product*. Web. 11 October 2011. http://www.tri-anchor.com/

U.S. Department of Agriculture (1999). *Wood Handbook – Wood as an Engineering Material.* General Technical Report 113. Madison, WI: U.S. Department of Agriculture, Forest Service, Forest Products Laboratory.

U.S. Departments of the Army and the Air Force (1983). *Backfill for Subsurface Structures*. Technical Manual No. 5-818-4. Washington, DC: Departments of the Army and the Air Force.

Whatley Inc. (2013). *Direct Embedded*. Web. 22 September 2013. http://az276019.vo.msecnd.net/valmontstaging/whatley-documents/-here.pdf?sfvrsn=4

Whiteshell, K.L. (2008). *Augering Through Rock for New Pole Installation*. Transmission & Distribution World. Web. 2 January 2013. http://tdworld.com/overhead_transmission/augering_rock_new_pole/

APPENDIX A - Analytical Model (MFAD)

The software program MFAD was used to analytically determine the minimum sleeve height that would permit a 40-foot long Class 4 LP pole (that was cut in half to 20 feet) to develop 100% of its strength in bending. Confidence in the results was gained by comparing the results of similar analyses produced by the software program with the results of full-scale single pole lateral load tests in rock for transmission line structures, as published by Caswell et al. in 1954. The published results are presented below in Table A.1. In each full-scale test, load was applied until the pole broke (Caswell, 1954).

Table A.1: Results of full-scale lateral load tests in rock (Caswell et al., 1954)

Pole Test	**Pole Species**	**Type of Setting and Depth**	**Horizontal Failure Load Applied at 40 Ft. Above Ground*, lbs.**	**Ground-line Moment at Failure Load, ft-lbs.**	**Deflection at Ground-line, inches**
R-1	Douglas Fir	4 feet of aggregate	4,650	186,000	1.375
R-2	Douglas Fir	5 feet of aggregate	6,000	240,000	0.563

*It should be noted that in Caswell's study, load was applied at the pole tip (versus at 2 feet from the tip)

Although the published results indicated the length of the poles tested (65 feet) and the point of load application (40 feet above ground), the class that each of the pole specimens belonged to was not specified. It was therefore assumed that the poles tested were Class 1, a common pole class for 65-foot long poles in a transmission line application. Assumptions also had to be made regarding the annulus

thickness, as well as the unit weight, deformation modulus, undrained shear strength, and internal angle of friction of the aggregate material. The study indicated that holes approximately 3 feet in diameter were augered into limestone rock, and that the annulus material was power tamped in each of the tests. Based on the above, a crushed limestone material was assumed for the annulus material. The assumed annulus thickness (0.83 feet) was determined by subtracting the pole diameter of a 65-foot long, Class 1 Douglas Fir pole (1.35 feet) from one half of the diameter of the hole. The diameter of the pole was input into MFAD as per the screenshot shown in Figure A.1 below.

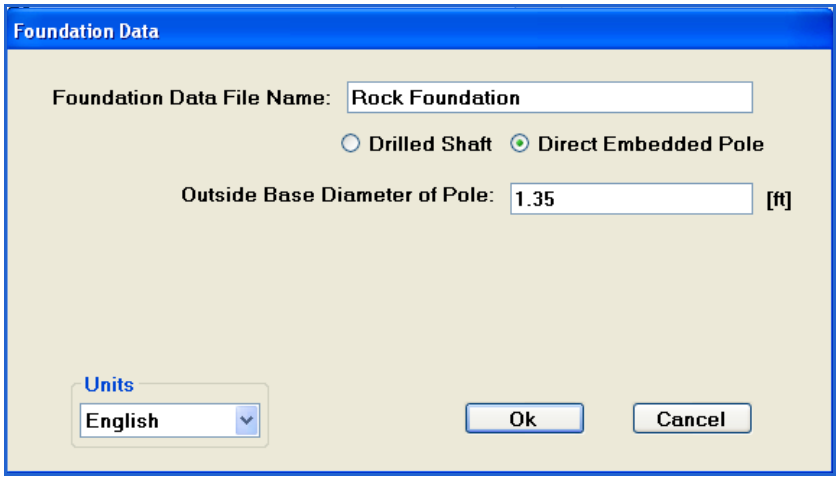

Figure A.1: Pole base diameter specified in MFAD for 65-foot long, Class 1 Douglas Fir poles

The remaining strength and deformation properties of the assumed crushed limestone annulus material were adopted from research conducted by DiGioia et al. (1998) for compacted crushed limestone. These assumed values are provided in Table A.2 below, and were input into MFAD as per the screenshot shown in Figure A.2 below.

Table A.2: Assumed properties of assumed crushed limestone annulus material

Unit Weight (pcf)	Deformation Modulus (ksi)	Undrained Shear Strength (ksf)	Internal Angle of Friction (deg)
125	5.15	1.5	45

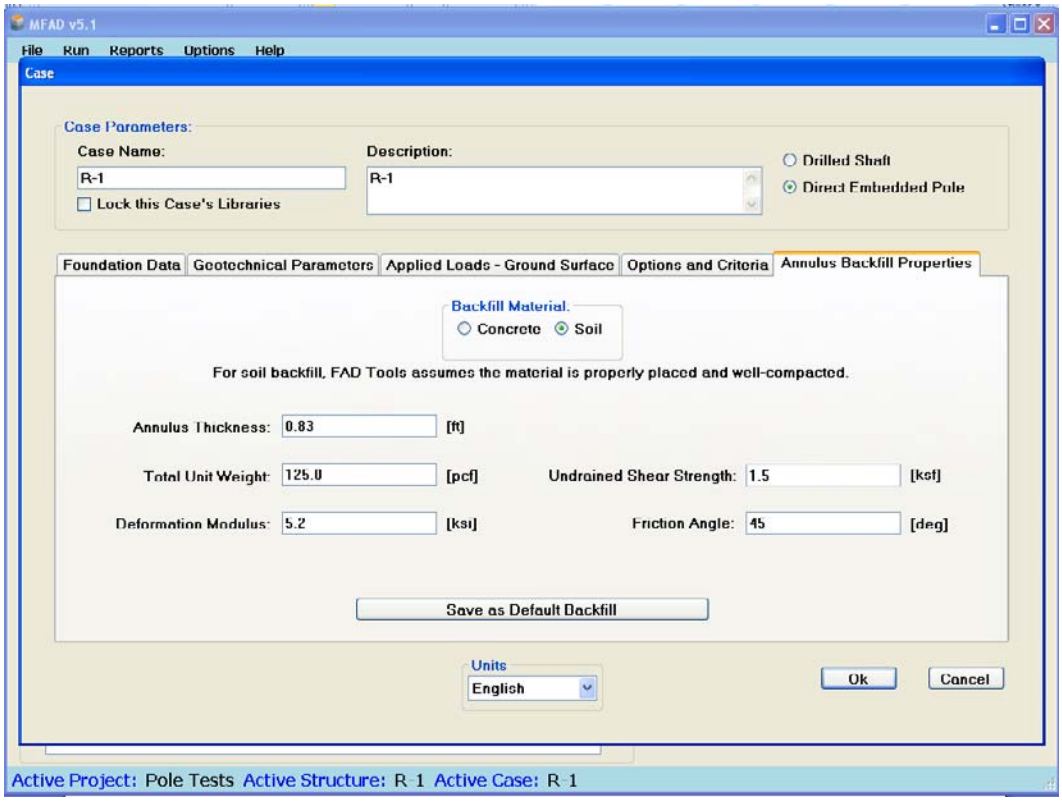

Figure A.2: Assumed annulus properties used in MFAD

The properties of the in-situ limestone were also assumed, this time from research conducted by Hoek and Brown (1997), for a "good" quality rock mass. These assumed values are provided in Table A.3 below, and were input into MFAD as per the screenshot shown in Figure A.3 below.

Table A.3: Assumed properties of in-situ limestone rock mass

Unit Weight (pcf)	Deformation Modulus (ksi)	Rock Cohesion (ksf)
125	1800	6

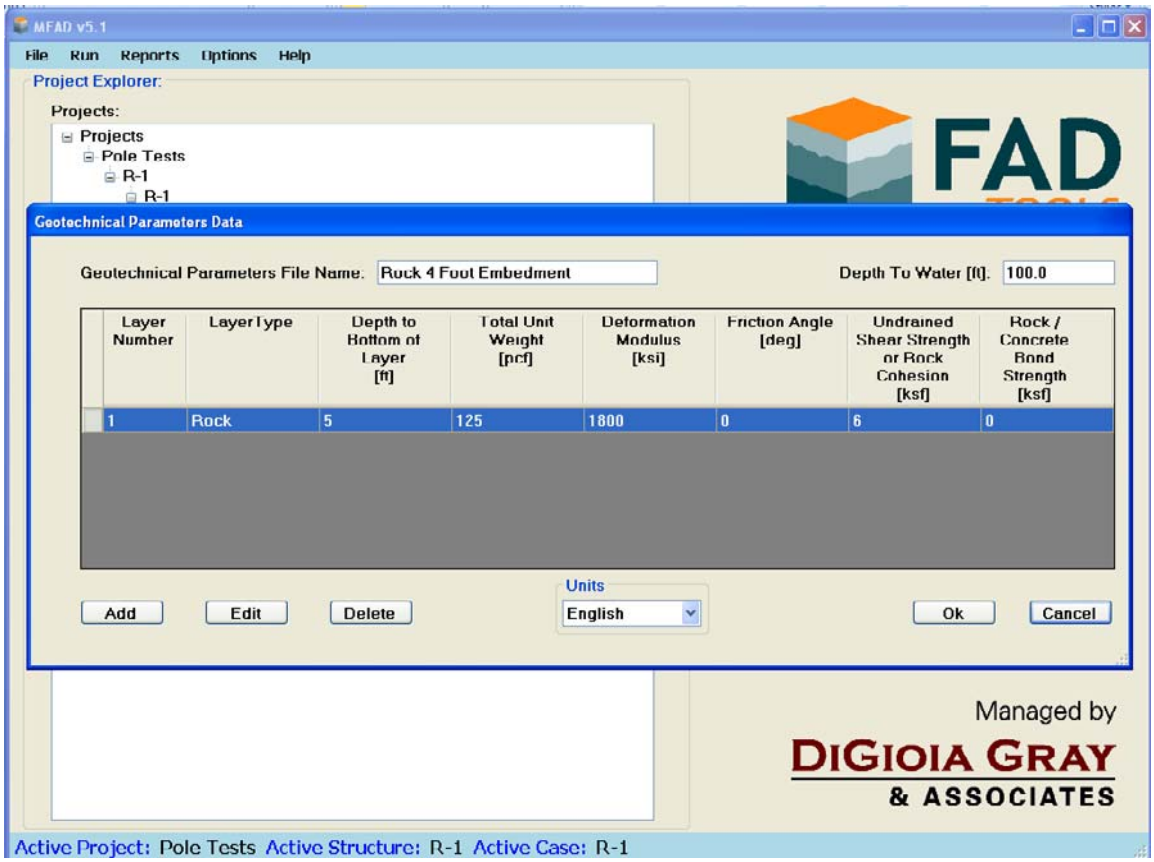

Figure A.3: Assumed in-situ rock mass properties used in MFAD

The results of the full-scale single pole lateral load tests in rock, as predicted by MFAD, are presented in Table A.4 below. The actual and predicted results for Pole Test R-1 are in good agreement, with the

MFAD results only slightly higher by 3.7% for both horizontal failure load and groundline moment at failure. The actual and predicted results are less agreeable for Pole Test R-2, however, with MFAD over-predicting both the horizontal failure load and groundline moment at failure by approximately 30%. For deflection at groundline, MFAD underestimates the published results for Pole Tests R-1 and R-2 by approximately 48% and 56%, respectively. It is not unreasonable to expect some variation in the results, however, as a number of assumptions had to be made.

Table A.4: Results of Caswell et al. pole tests as modelled in MFAD

Pole Test	**Pole Species**	**Type of Setting and Depth**	**Horizontal Failure Load Applied at 40 ft. Above Ground, lbs.**	**Ground-line Moment at Failure Load, ft-lbs.**	**Deflection at Ground-line, inches**
R-1	Douglas Fir	4 feet of aggregate	4,820	192,830	0.71
R-2	Douglas Fir	5 feet of aggregate	7,800	311,860	0.25

APPENDIX B - Structural Design of the Sleeve

As per CAN/CSA S16-14:

Properties of the sleeve:

Diameter across flats, D = 662.2 mm – 7.9 mm = 654.3 mm

Radius, R = D/2 = 327.2 mm

Sleeve Thickness, t = 7.9 mm

S = section modulus of 12-sided sleeve

$= 3.29R^2t = 3.29(327.2\text{ mm})^2(7.9\text{ mm}) = 2781742\text{ mm}^3$

$M_r = \varphi SF_y$ = moment resistance of sleeve ($\varphi = 0.9$, $F_y = 350$ MPa)

$= (0.9)(2781742\text{ mm}^3)(350\text{ MPa})$

$= 876$ kN-m

Factored moment resistance, M, of a 12.2 m long, Class 4 LP pole (as per Equation 3.18)

M = (H)(L – h – 0.61 m) = (10,700 N)(12.2 m – 0 - 0.610 m)(1.5) = 186 kN-m

Where h has conservatively been taken as equal to 0 and a factor of 1.5 has been applied to H

Therefore, $M_r > M$

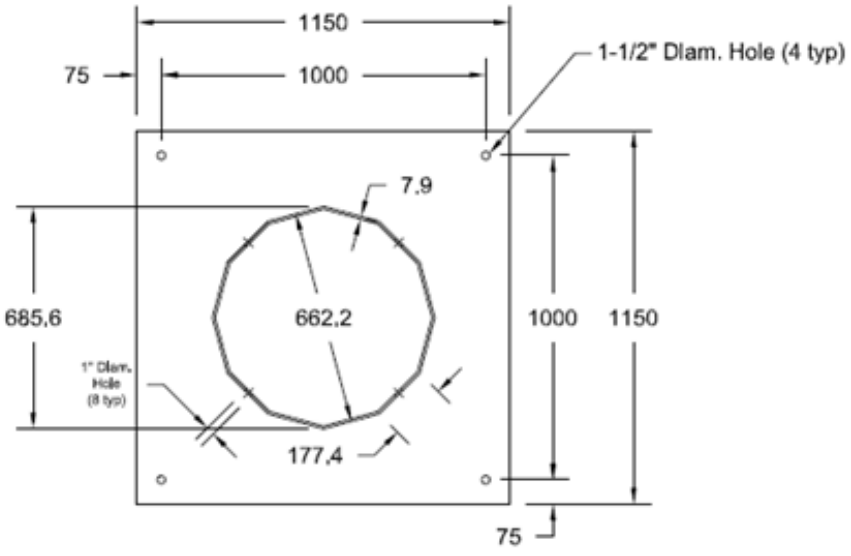

APPENDIX C - Structural Design of the Threadbar

M_f = 186 kN-m (same as for sleeve, see Appendix B)

(1) Assume that moment acts such that 2 threadbars are in tension (T) and 2 threadbars are in compression (C) (shear, V, also acts on each threadbar; combined T + V and C + V will be checked below)

T_f (in 2 threadbars) = C_f (in 2 threadbars) = M_f / (spacing between threadbars in tension & compression)

= 186 kN-m / (1 m) = = 186 kN

Therefore, T_f (in 1 threadbar) = C_f (in 1 threadbar) = 186 kN / 2 = 93 kN

(2) Assume that moment acts such that 1 threadbar is in tension (T) and 1 threadbar is in compression (C)

T_f (in 1 threadbar) = C_f (in 1 threadbar) = M_f / (spacing between threadbars in T & C)

= 186 kN-m / (1.414 m)

= 132 kN (governs)

Required threadbar area (tension) = T_f / min($0.9F_y$, $0.8F_u$)

= 132 kN / min(0.9 x 517 MPa, 0.8 x 690 MPa)

= 283 mm^2

Where F_y = 517 MPa & F_u = 690 MPa

Required threadbar area (shear) = $V_f / 0.9F_y$ = 10,700 N / (0.9 x 517 MPa) = 17 mm^2

Total required threadbar area (tension + shear), as per Equation 3.9 = 283 mm^2 + 17 mm^2 = 300 mm^2

Area of #10 Dywidag Bar = 819 mm^2

Diameter of #10 Dywidage Bar = 32 mm

Unbraced length of #10 threadbar (below base plate) = approximately 50 mm

Since unbraced length (50 mm) < 2x threadbar diameter (64 mm), we do not need to check the threadbar for bending due to shear (as per ASCE Manual of Practice No. 113).

Check compressive resistance of threadbar with unbraced length of 50 mm:

C_f = 132 kN (calculated above)

Assume effective length factor, K, equals 1.2 (as recommended by CAN/CSA S16-14 for fixed-fixed connections where rotation is restrained at both ends but translation is fixed at one end only)

$kL/r = (1.2)(50\ mm) / (32\ mm / 4) = 7.5$

$\lambda = (kL/r)(F_y / E\pi^2)^{1/2} = (7.5)(517\ MPa / 200{,}000\ MPa / \pi^2)^{1/2} = 0.12$

$C_r = \phi A F_y (1+\lambda^{2n})^{-1/n} = 0.9(819\ mm^2)(517\ MPa)(1+0.12^{2.68})^{-1/1.34} = 380\ kN$

Therefore, $C_r > C_f$.

APPENDIX D - Structural Design of the Base Plate

Following the guidelines presented in ASCE Manual of Practice No. 72 for base plate design (and as detailed in Section 3.5 of this thesis document):

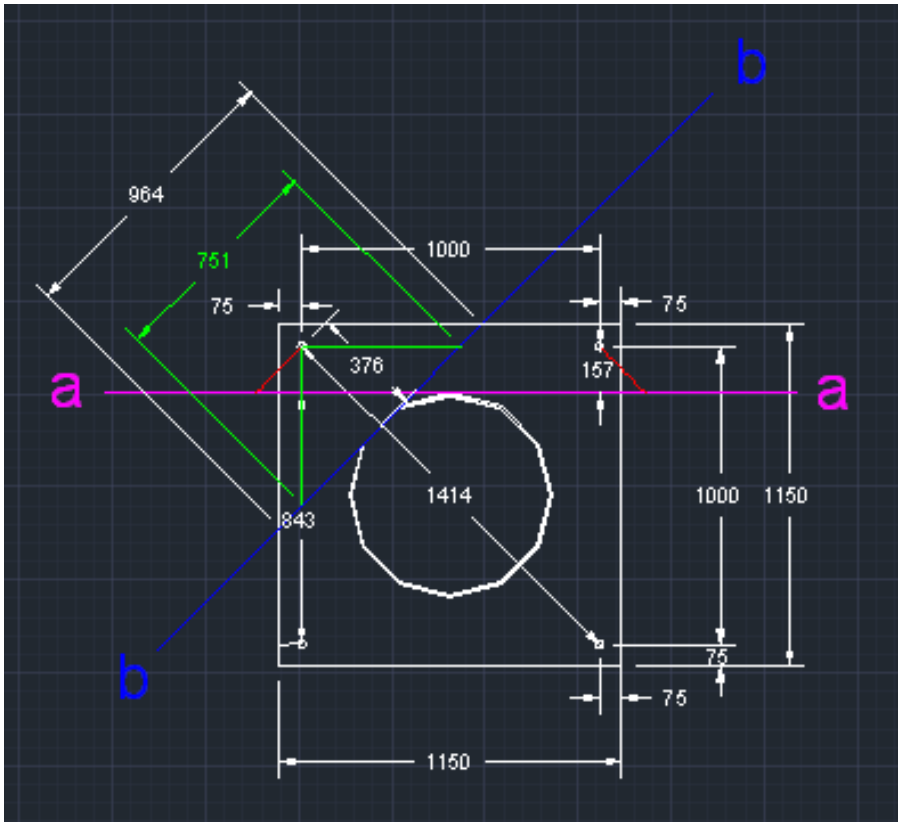

Check bending about a-a:

b_{eff} = 1,150 mm

F_y = 350 MPa

Limit F_y to 90% = 315 MPa

c1 = 157 mm

c2 = 157 mm

$t_{min} = \left[\left(\frac{6}{b_{eff} F_y}\right)(BL_1c_1 + BL_2c_2 + \ldots + BL_ic_i)\right]^{1/2}$

$= [(6 / 1{,}150 \text{ mm} / 315 \text{ MPa})(93 \text{ kN} \times 157 \text{ mm} + 93 \text{ kN} \times 157 \text{ mm})]^{1/2}$

= 22 mm

Check bending about b-b:

b_{eff} = 751 mm

F_y = 350 MPa

Limit F_y to 90% = 315 MPa

c1 = 376 mm

$t_{min} = \left[\left(\frac{6}{b_{eff} F_y}\right)(BL_1c_1 + BL_2c_2 + \ldots + BL_ic_i)\right]^{1/2}$

$= [(6 / 751 \text{ mm} / 315 \text{ MPa})(132 \text{ kN} \times 376 \text{ mm})]^{1/2}$

= 35 mm (governs)

Therefore, use a 35 mm thick baseplate.

APPENDIX E - Structural Design of the Mechanical Fasteners

Size mechanical fasteners based on the loads that they must resist, as detailed in Section 3.6.1 of this thesis document:

As per Equations 3.12 & 3.13 (derived from statics):

$$P_{upper\ fasteners} = \frac{H(L - 610\ mm)}{h_{mount}}$$

$$P_{lower\ fasteners} = \frac{H(L - 610mm - h_{mount})}{h_{mount}}$$

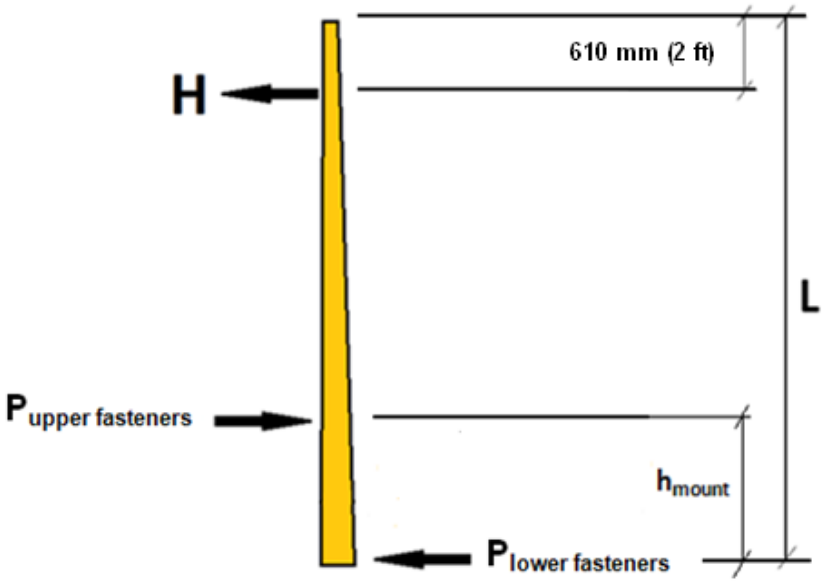

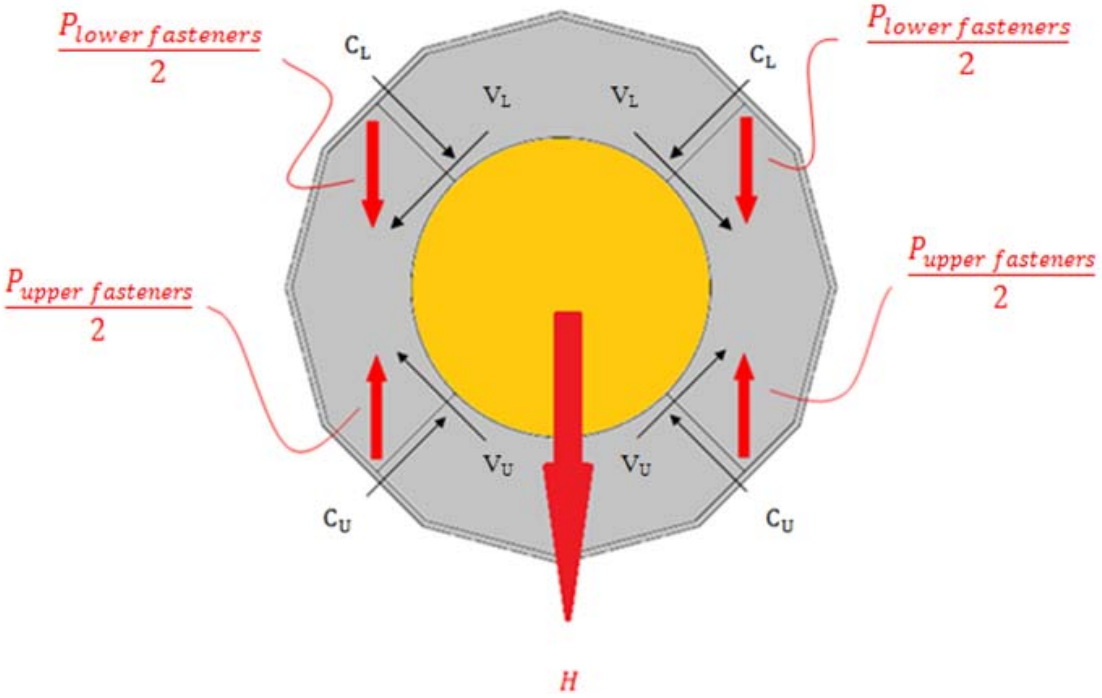

For 1,219 mm sleeve:

$P_{upper\ fasteners}$ = (26 kN)(6,096 mm – 610 mm) / 1,219 mm = 117 kN

$C_u = V_u = \cos 45^o$ x ($P_{upper\ fasteners}$ / 2) = 0.707 x (117 kN / 2) = 41 kN

$P_{lower\ fasteners}$ = (26 kN)(6,096 mm – 610 mm – 1,219 mm) / 1,219 mm = 91 kN

$C_L = V_L = \cos 45^o$ x ($P_{lower\ fasteners}$ / 2) = 0.707 x (91 kN / 2) = 32 kN

For 914 mm sleeve:

$P_{upper\ fasteners}$ = (24.25 kN)(6,096 mm – 610 mm) / 914 mm = 146 kN

$C_u = V_u = \cos45^o \times (P_{\text{upper fasteners}} / 2) = 0.707 \times (150 \text{ kN} / 2) = 51 \text{ kN}$

$P_{\text{lower fasteners}} = (24.25 \text{ kN})(6{,}096 \text{ mm} - 610 \text{ mm} - 914 \text{ mm}) / 914 \text{ mm} = 121 \text{ kN}$

$C_L = V_L = \cos45^o \times (P_{\text{lower fasteners}} / 2) = 0.707 \times (125 \text{ kN} / 2) = 43 \text{ kN}$

Determine compressive resistance of mechanical fasteners as per CAN/CSA S16-14:

Mechanical fasteners are 25 mm diameter all-thread rod ($F_y = 250$ MPa).

Assume k = 1.0 (ends of column have free rotation but fixed translation)

Assume unbraced length of mechanical fastener = 175 mm

$kL/r = (1.0)(175 \text{ mm}) / (25 \text{ mm} / 4) = 28$

$\lambda = (kL/r)(F_y / E\pi^2)^{1/2} = (28)(250 \text{ MPa} / 200{,}000 \text{ MPa} / \pi^2)^{1/2} = 0.32$

$C_r = \phi A F_y (1+\lambda^{2n})^{-1/n} = 0.9(507 \text{ mm}^2)(250 \text{ MPa})(1+0.32^{2.68})^{-1/1.34} = 110 \text{ kN}$

$V_r = (0.7)(0.6)\varphi_b n m A_b F_u = (0.7)(0.6)(0.8)(507 \text{ mm}^2)(400 \text{ MPa}) = 68 \text{ kN}$

Check that $(C_f/C_r)^2 + (V_f/V_r)^2 \leq 1$:

For 1,219 mm sleeve:

Upper Fasteners: $(C_f/C_r)^2 + (V_f/V_r)^2 = (41 \text{ kN} / 110 \text{ kN})^2 + (41 \text{ kN} / 68 \text{ kN})^2 = 0.5 < 1$

Lower Fasteners: $(C_f/C_r)^2 + (V_f/V_r)^2 = (32 \text{ kN} / 110 \text{ kN})^2 + (32 \text{ kN} / 68 \text{ kN})^2 = 0.3 < 1$

For 914 mm sleeve:

Upper Fasteners: $(C_f/C_r)^2 + (V_f/V_r)^2 = (51 \text{ kN} / 110 \text{ kN})^2 + (51 \text{ kN} / 68 \text{ kN})^2 = 0.8 < 1$

Lower Fasteners: $(C_f/C_r)^2 + (V_f/V_r)^2 = (43\text{ kN} / 110\text{ kN})^2 + (43\text{ kN} / 68\text{ kN})^2 = 0.6 < 1$

Check local buckling of sleeve due to governing C_u (i.e. for the 914 mm sleeve)

Assume a 150 mm x 150 mm plate of thickness 7.9 mm

Formula for deflection assumes simply-supported edges, which should produce conservative results since 3 of our edges are fixed.

As per Equation 3.17 (Carvill, 1993)

$$y_m = k_1 \frac{Pa^2}{Et^3}$$

Where $k_1 = 0.127$ for a square plate

P = applied concentrated load (of upper fastener in 914 mm sleeve)

a = width (or length) of plate

E = modulus of elasticity of steel

t = plate thickness

$y_m = (0.127)(51\text{ kN})(0.15\text{ m})^2 / (200{,}000\text{ MPa}) / (0.0079\text{ m})^3 = 1.48\text{ mm}$

A sleeve deflection of 1.48 mm would be hard to detect by the naked eye.

APPENDIX F - Shear Strength of Lodgepole Pine

Ensure that the failure mode of the poles tested does not change from one of bending to one of shear because of the increased transverse load requirement applied when testing the bottom halves of 12.2 m (40-foot) long, Class 4 LP poles. In order to maintain the maximum applied base moment generated for a 12.2 m (40-foot) long pole, CAN/CSA 015-05's transverse load requirement of 10,700 N for Class 4 poles was increased to 26,000 N and 24,250 N for the 6.1 m (20-foot) long poles tested in 1,219 mm and 914 mm mounts, respectively.

From Equation 2.3 (IEEE, 1991):

$\phi f_v \geq \gamma V(Q/I)$

Where

$\phi = 0.9$

$f_v = 5.52$ MPa (U.S. Department of Agriculture, 1999)

$\gamma = 1.5$

V = transverse load requirement (determined using Equation 3.19 in Section 3.8)

= 26 kN (1,219 mm sleeve) or 24.25 kN (914 mm sleeve)

D(min) = 292 mm (1,219 mm sleeve) or 294 mm (914 mm sleeve)

$Q/I = 1.7D^{-2} = 1.7(0.292\ m)^{-2} = 19.9\ m^{-2}$ (1,219 mm sleeve)

$= 1.7(0.294\ m)^{-2} = 19.7\ m^{-2}$ (914 mm sleeve)

Left-hand side of Equation 2.3 (representing factored shear strength of pole)

$\phi f_v = 0.9(5.52\ MPa) = 4.97$ MPa

Right-hand side of Equation 2.3 (representing factored shear stress in pole)

$\gamma V(Q/I) = 1.5(26\text{ kN})(19.9\text{ m}^{-2}) = 0.002$ MPa (1,219 mm sleeve)

$= 1.5(24.25\text{ kN})(19.7\text{ m}^{-2}) = 0.002$ MPa (914 mm sleeve)

Therefore, for both the 1,219 mm and 914 mm sleeves,

$\gamma V(Q/I) \div \phi f_v = (0.002\text{ MPa}) / (4.97\text{ MPa}) = 0.04\%$

In other words, Applied Shear (factored) is 0.04% of Shear Strength (factored).

Therefore, the use of 6.1 m (20-foot) long poles with an increased transverse load requirement should provide results analogous to those generated for 12.2 m (40-foot) long poles tested with the transverse load requirement specified by CAN/CSA 015-05.

APPENDIX G - Failure Analysis of Pole Specimen P1

Confirm that Pole Specimen P1 had indeed failed in compression during the mechanical fasteners test:

From Equation 2.2 (IEEE, 1991):

$\phi f_b \geq \gamma(M/S)$

Where $\phi = 0.9$

$f_b = 45.4$ MPa (tension) and 10.5 MPa (compression)

$\gamma = 1.5$

M = applied moment = (ultimate applied load reached in test) x moment arm

= 16.37 kN x (6.1 m – 0.61 m – 1.219 m) = 69.9 kN-m

$S = \pi D^3/32 = \pi(0.9754 \text{ m} / \pi)^3/32 = 0.003 \text{ m}^3$

ϕf_b (compression) = 0.9 x 10.5 MPa = 9.45 MPa

ϕf_b (tension) = 0.9 x 45.4 MPa = 40.90 MPa

$\gamma(M/S) = 1.5(69.9 \text{ kN-m})/(0.003 \text{ m}^3) = 35.0$ MPa

Therefore, ϕf_b (compression) < $\gamma(M/S)$ < ϕf_b (tension). This confirms that Pole Specimen P1 had failed in compression in the mechanical fasteners test. It also validates why no tensile failure of the pole was observed during this test.